Dynamic Properties of Seawater Surfactants

by

John Thomas Mass

Submitted to the Department of Ocean Engineering in Partial
Fulfillment of the Requirements for the Degree of

Masters of Science in Ocean Engineering
at the
Massachusetts Institute of Technology
February 1996

Signature of Author_____
Department of Ocean Engineering
January 20, 1996

Certified by_____
Jerome Milgram
Professor of Ocean Engineering
Thesis Supervisor

Accepted by_____
A. Douglas Carmichael
Professor of Ocean Engineering
Chairman, Department of Ocean Engineering Graduate Committee

Dynamic Properties of Seawater Surfactants

by
John Thomas Mass

Submitted to the Massachusetts Institute of Technology on January 30, 1995
in partial fulfillment of the requirements for the degree of
Master of Science in Ocean Engineering

Abstract

The relative calm in ship wakes and its persistence for long periods raises questions regarding energy dissipation mechanisms by which surface elevation waves are damped. Wave field disturbances caused by propeller and boundary layer turbulence can readily explain the absence of waves immediately astern but fail to explain their absence many shiplengths astern. A possible mechanism to explain the lack of high frequency surface elevation waves is the presence of surface active agents, surfactants. Surfactant collection into continuous sheets or disturbing previously formed sheets can readily change the decay rates of surface elevation waves through changes in surface tension, elasticity and possibly surface viscosity. In addition to shipwakes, the rheological behavior of a surface film can influence wave growth due to wind.

Elastic properties are typically determined experimentally through quasi-static measurement of the film's pressure-area isotherm but recent discussions have raised the question of whether the quasi-static properties explain the dynamic behavior of naturally occurring ocean surfactants. The objective of this research is to determine if the quasi-static elastic properties (Gibbs' elasticity) of seawater films adequately predict the dynamic behavior of natural sea surface films. Specifically, the dynamics of the films when they undergo distortions from both transverse and longitudinal waves.

The quasi-static elastic properties were found to change with repeated compression resulting in a " work hardening" of the film. However, once determined the quasi-static elasticity predicts the dynamic behavior of natural surface films.

Thesis supervisor: Dr. Jerome Milgram
Title: Professor of Ocean Engineering

ACKNOWLEDGMENTS

Professionally, I would like to thank Professor Jerome Milgram for supervising the work that lead to this thesis. He is everything a MIT professor should be, intelligent and hard working. I would like to thank the Office of Naval Research for providing funds for this project.

During the course of this work I have had the opportunity to work with several people in the MIT community. Dr. Hasan Olmez proved to be a great intellectual big brother when I needed help with computational problems and finding my way around MIT. Noah Eckhouse taught me about high frequency electronic noise at MIT and helped me adjust to the Boston area. Soren Jensen enhanced my knowledge of Denmark and showed me a few tricks on the lathe. When the aforementioned left the LAB to pursue other interests Greg Thomas, Nicole Suoja and Jess Riggle moved in with refreshing zeal and continued to make the place a pleasant working environment. Cindy Dernay deserves credit as a person who can get things done and get almost anything delivered by the next day. Craig Schull spent the summer earning my respect. He is, without a doubt, the best UROP I have ever worked with at MIT.

Personally, I would like to thank my parents and numerous brothers and sisters for somehow helping to make me what I am.. During my stay at MIT I joined another family; James and Diana Brown thank you for your daughter and support in our endeavors.

Finally, I would like to thank my wife Michele, whose love, support and counsel means the world to me.

TABLE OF CONTENTS

LIST OF FIGURES

LIST OF SYMBOLS

SYMBOL	DISCRIPTION
ζ	Vertical Displacement
ξ	Horizontal Displacement
$\bar{k}$	Complex Wavenumber
k	Real Wavenumber
α	Imaginary Wavenumber (Decay Rate)
λ	Wavelength
π	Pi ~ 3.14159265
ρ	Density
g	Gravity
ω	Circular Frequency
m	$m^2 = k^2 - i\omega\rho / \mu$
μ	Dynamic or Absolute Viscosity
υ	Kinematic Viscosity
γ	Surface Tension
$\bar{\varepsilon}$	Complex Elasticity
ε	Gibbs' Elasticity
ε'	Surface Viscosity
$\bar{k}_T^o$	Initial Transverse Wavenumber
$\bar{k}_L^0$	Initial Longitudinal Wavenumber
$\bar{k}_T$	Refined Transverse Wavenumber
$\bar{k}_L$	Refined Longitudinal Wavenumber
γ'	Change in Surface Tension
γ_0	Initial Surface Tension
$phase(\gamma')$	Phase Relationship between Longitudinal Wavemaker and Fluid
x	Distance from longitudinal wavemaker to a Point on the Fluid
d	Distance from Longitudinal Wavemaker to Opposite wall
α_0	Transverse Wave Decay for Clean Water
Π	Film Pressure
F	Force acting on Wilhelmy Plate
L_p	Length of Wilhelmy Plate
V_g	Group Velocity
V_p	Phase Velocity

1. Introduction

The presence of certain compounds on the sea surface alters propagation characteristics of short surface waves. The compounds, generated from phytoplankton by-products and land run-off, can form a monomolecular sheet with elastic properties. The elastic sheet supports the propagation of transverse (gravity-capillary) and longitudinal surface waves. When a transverse wave exists on a film-covered region, the combination of longitudinal and transverse waves that must exist to satisfy the boundary conditions can increase the transverse wave dissipation. This happens because of phase differences in the longitudinal and transverse wave motions which can enhance viscous dissipation in the boundary layer just beneath the surface film. The surface, if wind driven and rough, becomes smoother when a surface film is present.

1.1. Background

Recorded observations of the above phenomenon were noted in ancient Greece and Rome by philosopher-scientists. However, scientific understanding did not begin until late in the 19th century when Italian physicist C. Marangoni documented fluid - fluid interactions at the air-liquid interface. A qualitative understanding was offered by *Aitken* 1883 and summarized by *Adam* 1941. Quantitative analysis by *Dorrestein* 1951 and extensive experimental data on 'oils' followed with work by *Mann and Hansen* 1963, *Lucassen and Hansen* 1966, and *Hansen and Ahmed* 1971.

In 1978 additional interest was focused on the field due to developments in synthetic aperture radar and the use of radar backscatter to measure spectral properties of large areas of the ocean. Shipwakes and oil slicks could now be tracked remotely from air and space. Observed phenomena became measured phenomena. However, understanding the data required evaluation of surface properties. An effort was made to catalogue the elastic properties of a wide variety of surface films taken from the sea to the laboratory [*Barger,* 1984 and *Bock and Frew,* 1993]. Natural Films were shown to have varying composition and quasi-static elastic properties. The films showed an increase in elasticity or " hardening" with repeated compression. Some *in-situ* experiments were carried out on man made slicks composed of a compound with known elastic properties [*Alpers and Huhnerfuss* 1989].

An open question was whether the quasi-static film properties properly describe the film dynamic behavior which influenced seawaves. The result of Hunerfuss, Lange and Walters [1985] suggested that dynamic elasticity and surface viscosity at seawave frequencies may not have quasi-static values, even for pure substance films. This information contributed to stimulating the present study reported here.

1.2. Objective

The objective of this research is to determine if the quasi-static elastic properties (Gibbs' elasticity) of seawater films adequately predict the dynamic behavior of natural sea surface

films. Specifically, the dynamics of the films when they undergo distortions from both transverse and longitudinal waves.

1.3. Approach

We intended to accomplish our objective by:

A. Generating a baseline using a known compound (Oleyl Alcohol) whose quasi-static properties adequately predict its dynamic properties
B. Collecting samples of film covered seawater, transporting it to our laboratory, and spreading the film on wave apparatus in a natural state.
C. Measuring the quasi-static elastic properties of the surface film
D. Measuring dynamic properties of the film for a range of frequencies from 0.4 to 20 Hz

Initial samples were collected from the Little Harbor inlet near Cohasset, Ma (north shore Cape Cod) on the incoming tide. In an effort to prevent the films from changing due to biological growth/decay samples were collected transported and tested within 24 hours. In addition, comparisons were made between samples poisoned with sodium azide and samples not poisoned. The film properties were the same, whether poisoned or not, for films tested within 24 hours.

Near the completion of testing Nelson Frew and Robert Nelson of Woods Hole Oceanographic Institute provided surface film concentrate from a salt pond near Falmouth Ma. (a.k.a. Woods Hole Concentrate). Water samples were collected from the salt pond and concentrated in a centrifuge. The concentrate, eluted with methanol [*Frew and Nelson*, 1992], was spread on tap water and evaluated for quasi-static and dynamic properties. In an effort to establish a baseline for the concentrate evaluations film covered water samples were collected from the salt pond and evaluated in the same manner as the Cohasset samples.

2. Theory

2.1. Dynamic Properties of Transverse and Longitudinal Waves

Two types of surface waves can be supported at the air-water interface. The first, transverse waves, are the general water waves most people are familiar with; the air-water interface oscillates vertically and the vertical motion propagates in the plane of the air-liquid interface. To the observer in the global reference frame, as the wave passes particles trace out a circular pattern in deep water and an elliptical pattern in shallow water.

The second type, longitudinal waves , exist when oscillatory motion is almost completely parallel to the air-water interfacial plane. In this case the horizontal motion is an order of

magnitude greater than the vertical motion of the fluid. To the stationary observer a particle floating on the surface simply moves back and forth as the wave travels parallel to the air-liquid interface. These waves require an elastic surface.

In the case of a film covered surface, the fluid can support both types of waves simultaneously.

For both transverse and longitudinal cases two dimensional wave theory gives us a displacement relationship of the form:

$$\zeta = \zeta_o e^{i(\bar{k}x-\omega t)} \tag{2.1a}$$

in the z direction and

$$\xi = \xi_0 e^{i(\bar{k}x-\omega t)} \tag{2.1b}$$

in the x direction with transverse waves having ξ/ζ O(1) and longitudinal waves having a much smaller ratio of ξ/ζ. The equations relate wavenumber, distance, circular frequency and time to free surface displacement. The complex wavenumber, $\bar{k}$, is equal to $k+i\alpha$. The real portion represents the spatial wavenumber, k, and is related to the wavelength by $\lambda = 2\pi/k$. The imaginary portion, α, represents the spatial decay rate.

The dispersion relationship between $\bar{k}$ and measurable fluid properties is given by:

$$(\rho\omega^2 - \gamma\bar{k}^3 - \rho g\bar{k})(\rho\omega^2 - m\bar{k}^2\bar{\varepsilon}) - \bar{\varepsilon}k^3(\gamma\bar{k}^3 + \rho g\bar{k}) + 4i\rho\mu\omega^3\bar{k}^2 + 4\mu^2\omega^2\bar{k}^3(m-\bar{k}) = 0 \tag{2.2}$$

[*Hansen and Ahmed*, 1971] where:

$$m^2 = k^2 - i\omega\rho/\mu \tag{2.3}$$

Using gravity, g, and measuring the density, ρ, and viscosity, μ, of the underlying fluid and surface tension, γ, and elasticity, ε, for the film covering the air-water interface one can determine the corresponding wavenumber for any desired frequency by finding the roots of Equation 2.2 which is sixth order in $\bar{k}$. A typical numerical method is to estimate the locations of valid roots then use Newton's Method, or the leading term in an expansion, to refine the root locations. Since the roots must satisfy the boundary conditions of zero displacement at infinite depth several roots can be discarded as improper solutions.

In the case where the elasticity, $\bar{\varepsilon}$, is equal to zero, equation 2.2 simplifies to:

$$(\rho\omega^2 - \gamma\bar{k}^3 - \rho g\bar{k})(\rho\omega^2) + 4i\rho\mu\omega^3\bar{k}^2 + 4\mu^2\omega^2\bar{k}^3(m-\bar{k}) = 0 \tag{2.4}$$

and the roots are located very close to the roots of first term which has the familiar form:

$$(\rho\omega^2 - \gamma\bar{k}^3 - \rho g\bar{k}) = 0 \tag{2.5}$$

When an elastic film is present the elasticity, $\bar{\varepsilon}$, will not be equal to zero. Furthermore the elasticity may have a real and imaginary part forming the complex term:

$$\bar{\varepsilon} = \varepsilon + i\varepsilon'\omega \tag{2.6}$$

where the real part of the elasticity, ε, represents pure elastic or quasi-static behavior, while the imaginary part, ε', is the film surface viscosity.

Hansen and Ahmed [*Waves at Interfaces,* 1971] show that the solution for transverse and longitudinal wavenumbers are approximated by:

$$\bar{k}_T^o = \left[\frac{\rho\omega^2}{\gamma}\right]^{1/3} \tag{2.7}$$

and

$$\bar{k}_L^0 = \rho^{1/4}\omega^{3/4}\mu^{1/4}\bar{\varepsilon}^{-1/2}e^{i\pi/8} \tag{2.8}$$

respectively. Then the roots are refined to:

$$\bar{k}_T = \bar{k}_T^o - \bar{k}_T^o\left[\frac{\bar{\varepsilon}k^2(\gamma k^3 + \rho gk) - 4i\rho\mu\omega^3 k - 4\mu^2\omega^2 k^2(m-k)}{(3\gamma k^2 + \rho g)(\rho\omega^2 - mk^2\bar{\varepsilon})}\right]_{k=\bar{k}_T^o} \tag{2.9}$$

$$\bar{k}_L = \bar{k}_L^o - \bar{k}_L^o\left[\frac{\bar{\varepsilon}k^2(\gamma k^3 + \rho gk) - 4i\rho\mu\omega^3 k - 4\mu^2\omega^2 k^2(m-k)}{2mk\bar{\varepsilon}(\rho\omega^2 - \gamma k^3 - \rho gk)}\right]_{k=\bar{k}_L^o} \tag{2.10}$$

In both cases the real portion of $\bar{k}$ gives information regarding the wavelength, $\lambda = 2\pi/k$, while the imaginary portion provides information about the decay rate, α. Figure 2.1 shows the dependence of longitudinal wavenumbers, k_L, on frequency and elasticity.

The first order correction to wavenumber in equation 2.10 is small and there is an inverse relationship between k and $\bar{\varepsilon}$; as the elasticity, ε, decreases the wavenumber, k, increases, resulting in shorter wavelengths. When the water is clean, $\varepsilon = 0$, the longitudinal wavelength is zero.

In the case of transverse waves, the estimated location of the roots in equation 2.7 has only a real component which is independent of elasticity. The corrected wavenumber, k_T, calculated in equation 2.9 has a relatively small dependence on $\bar{\varepsilon}$ such that the real portion of the root can be estimated by $k_T(\omega, g, \gamma, \rho, \bar{\varepsilon}) \approx k_T(\omega, g, \gamma, \rho)$. The change in elastic

properties will result in dramatic changes in longitudinal wavelength while leaving the transverse wavelength largely unaffected. The imaginary parts of the transverse and longitudinal wavenumbers provide information regarding the decay rates of the respective waves, both have a strong correlation with elasticity. The dependence of longitudinal waves on elasticity is discussed below and transverse waves in section 2.2.

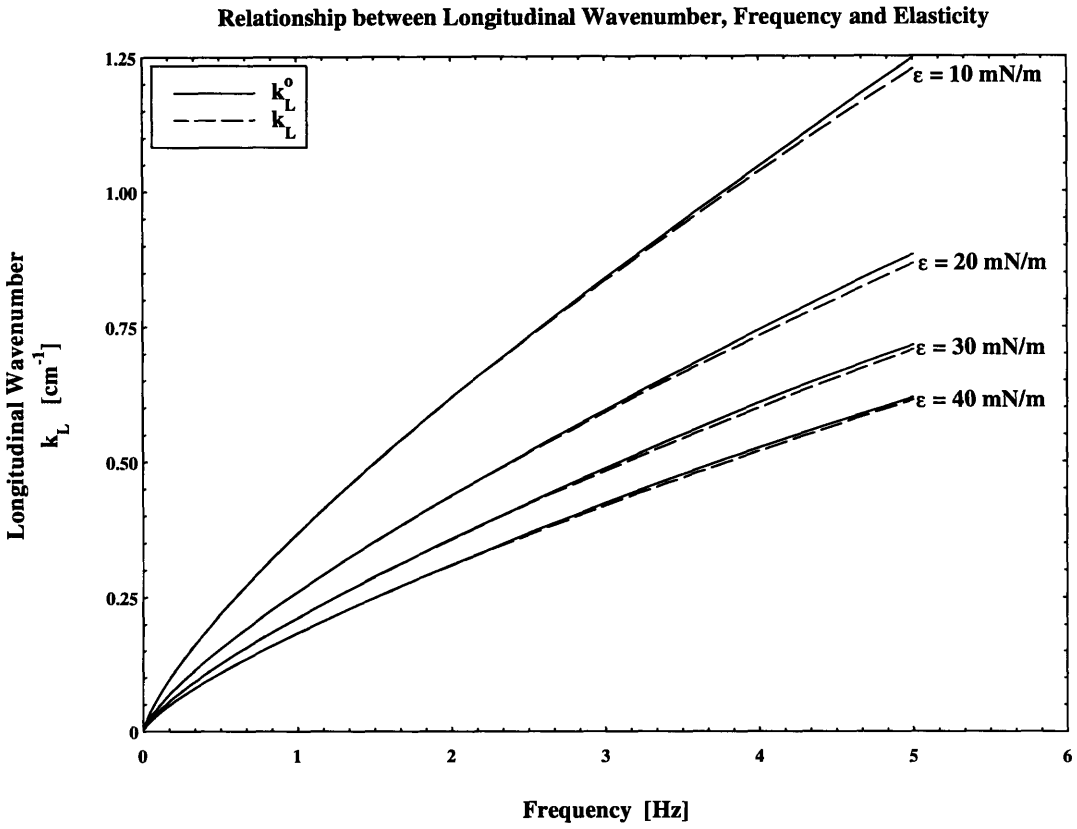

Figure 2.1 Relationship between Longitudinal Wave Number, Frequency and Elasticity for: $\gamma = 68.0\ mN/m, \varepsilon' = 0\ mN/m$/ sec.

2.1.1. Longitudinal Wave Decay and Variations in Surface Tension

In the open ocean a film covered surface with elastic properties will have longitudinal waves generated from transverse waves distorting the equilibrium surface film. One method of studying longitudinal waves is to de-couple them from transverse waves through the use of a longitudinal wavemaker and wave tank or trough. The following discussion is for a film covered surface in a wave tank equipped with a longitudinal wavemaker.

When a continuous monomolecular sheet or monolayer film exists, longitudinal waves can be generated without causing significant vertical particle motion by displacing surfactant molecules that form the monolayer film in the plane of the air-water interface. The waves are generated by horizontal displacement of the surfactant molecules with a film barrier. The barrier is placed on top the longitudinal wave tank piercing the monolayer with minimum penetration of the underlying fluid. Oscillating the film barrier horizontally

displaces the surface molecules. Motion of the bar causes displacement of particles on the air-water interface making up the surface film. A longitudinal wave is generated.

From classical wave theory, the displacement of a surface particle must satisfy equation 2.1. using the longitudinal wavenumber, $\bar{k}_L$, derived in equation 2.10. Furthermore, the particles on the surface near the wavemaker must have a displacement nearly equal to the wavemakers. If the displacement of the film barrier (wavemaker) is of the form:

$$\xi = Ae^{i(\pi/2-\omega t)} \tag{2.11}$$

The displacement of the film particles near the wavemaker will have to satisfy the same expression. Due to the finite length of the trough, reflection can occur off the wall opposite the oscillating film barrier. Particles near the wall will have the same displacement as the wall, zero. If the solution is to account for one reflection off the wall it will be of the form:

$$\xi = Be^{i(\bar{k}_L x-\omega t)} + Ce^{i(-\bar{k}_L x-\omega t)} \tag{2.12}$$

The first term on the right represents a wave traveling in the $+x$ direction (right) and the second term represents a wave traveling in the $-x$ direction (left). From the first boundary condition, equation 2.11, film displacement must equal film barrier displacement near the film barrier, one gets the equality:

$$\xi_{x=0} = Ae^{i(-\pi/2-\omega t)} = Be^{i(-\omega t)} + Ce^{i(-\omega t)} \tag{2.13}$$

or

$$B + C = Ae^{i(-\pi/2)} \tag{2.14}$$

The second boundary condition dictates that the fluid displacement at the wall must zero. If d is the distance between the wavemaker and far wall and the distance is much larger than the wavemaker amplitude, A, the boundary condition at d is:

$$\xi_{x=d} = Be^{i(\bar{k}_L d-\omega t)} + Ce^{i(-\bar{k}_L d-\omega t)} = 0 \tag{2.15}$$

or

$$Be^{i(\bar{k}_L d)} + Ce^{i(-\bar{k}_L d)} = 0 \tag{2.16}$$

which gives two equations with two unknowns. Rearranging equation 2.14:

$$C = Ae^{i(-\pi/2)} - B \tag{2.17}$$

Substituting into equation 2.16 and simplifying yields:

$$B = Ae^{i\pi/2}\frac{e^{-i\bar{k}_L d}}{e^{i\bar{k}_L d} - e^{-i\bar{k}_L d}} \tag{2.18}$$

Substituting the coefficient B back into equation 2.17 and simplifying yields:

$$C = Ae^{i\pi/2}\frac{e^{i\bar{k}_L d}}{e^{i\bar{k}_L d} - e^{-i\bar{k}_L d}} \tag{2.19}$$

With the coefficients calculated one can state the specific solution for surface particle displacement at any point on the air-water interface.

$$\xi = Ae^{i\pi/2}\frac{e^{-i\bar{k}_L d}}{e^{i\bar{k}_L d} - e^{-i\bar{k}_L d}}e^{i(\bar{k}_L x - \omega t)} + Ae^{i\pi/2}\frac{e^{i\bar{k}_L d}}{e^{i\bar{k}_L d} - e^{-i\bar{k}_L d}}e^{i(-\bar{k}_L x - \omega t)} \tag{2.20}$$

or simplified;

$$\xi = Ae^{i(\pi/2-\omega t)}\left[\frac{e^{-i\bar{k}_L d}}{e^{i\bar{k}_L d} - e^{-i\bar{k}_L d}}e^{i\bar{k}_L x} + \frac{e^{i\bar{k}_L d}}{e^{i\bar{k}_L d} - e^{-i\bar{k}_L d}}e^{-i\bar{k}_L x}\right] \tag{2.21}$$

As the longitudinal wave travels in x, the particle motion causes the interface film to distort (stretch and compress). The elastic properties of the film dictate the local changes in surface film pressure and surface tension from the static equilibrium as the film is stretched and compressed to a larger and smaller area. The variation in surface tension, γ', is the elasticity multiplied by the horizontal strain for simple elastic behavior:

$$\gamma' = \bar{\varepsilon}\frac{d\xi}{dx} = i\bar{\varepsilon}A\bar{k}_L e^{i(\pi/2-\omega t)}\left[\frac{e^{-i\bar{k}_L d}}{e^{i\bar{k}_L d} - e^{-i\bar{k}_L d}}e^{i\bar{k}_L x} - \frac{e^{i\bar{k}_L d}}{e^{i\bar{k}_L d} - e^{-i\bar{k}_L d}}e^{-i\bar{k}_L x}\right] \tag{2.22}$$

The fact that elasticity, $\bar{\varepsilon}$, and wavenumber, $\bar{k}$ can be complex, dictates γ' can have real and imaginary parts or a magnitude and phase. The magnitude of γ' is the amplitude of variations in surface tension and the phase represents the phase shift of variations in surface tension at a distance x from the film barrier with respect to strain. Equation 2.22 shows sinusoidal oscillation of the longitudinal wavemaker generates sinusoidal variations in dilation and surface tension. The variation in surface tension is affected by the longitudinal wave and elastic properties of the film. The varying surface tension corresponds to:

$$\gamma = \gamma_0 + |\gamma'|\cos[phase(\gamma') - \omega t] \tag{2.23}$$

Several methods exist to measure variations in surface tension. One method measures the changes in surface tension with minimum interference of the film present at the air-water

interface [*Sohl, Miyano and Ketterson*, 1978]. Details of the device we developed are given in section 3 and appendix A.

The relationship between the magnitude of surface tension variation, elasticity and frequency at one position in the trough is shown in figure 2.2. The change in surface tension is normalized with respect to the amplitude of the oscillating film barrier (longitudinal wavemaker). This allows one to discern small changes in surface tension at the higher frequencies.

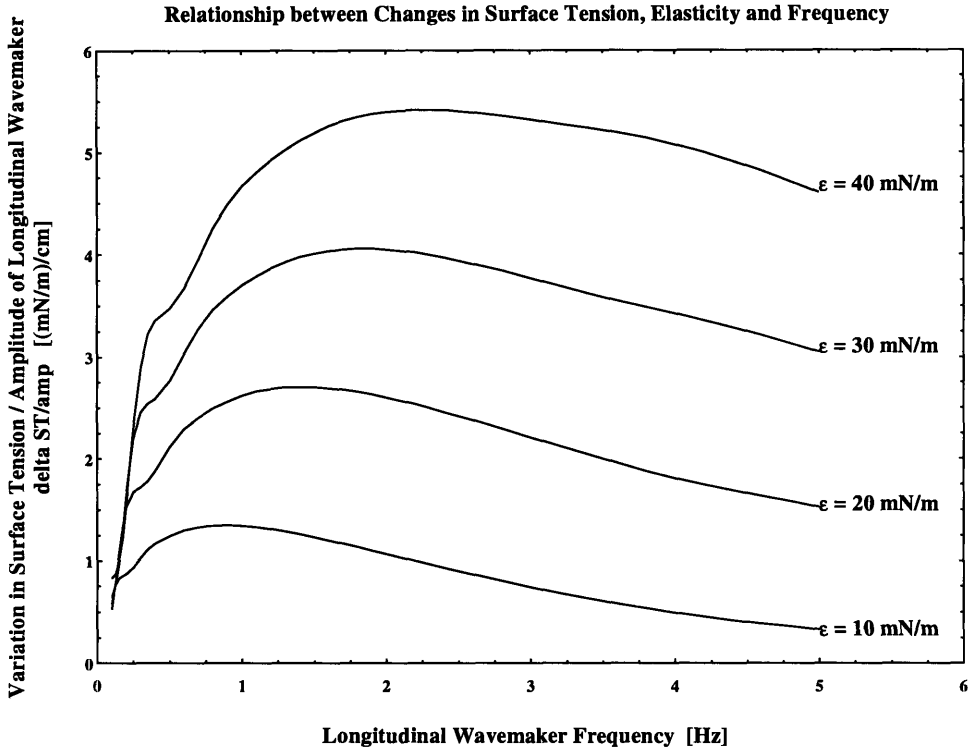

Figure 2.2 Relationship between Changes in Surface Tension, Elasticity and Frequency for $d = 40\ cm$, $x = 7\ cm$, $\gamma = 68.0\ mN/m$, $\varepsilon' = 0\ mN/m$ / sec.

Figure 2.3 shows the variations in phase dependence on elasticity and frequency at the same position as figure 2.2. The phase difference of the change in surface tension with respect to the oscillating film barrier is also sensitive to changes in elasticity.

After measuring the parameters which describe the fluid and surfactant, one can calculate theoretical values for the longitudinal wavelength, the displacement of particles on the film between the air-water interface and local variations in surface tension. The combination of the three allows one to compare theoretical dynamic behavior of a film with measured behavior.

Unfortunately, generating longitudinal waves at frequencies above 4 Hz without generating transverse waves is difficult. Transverse waves form from meniscus forming on the film

barrier and the bar's penetration into the underlying fluid. Analyzing dynamic behavior for higher frequencies requires another approach.

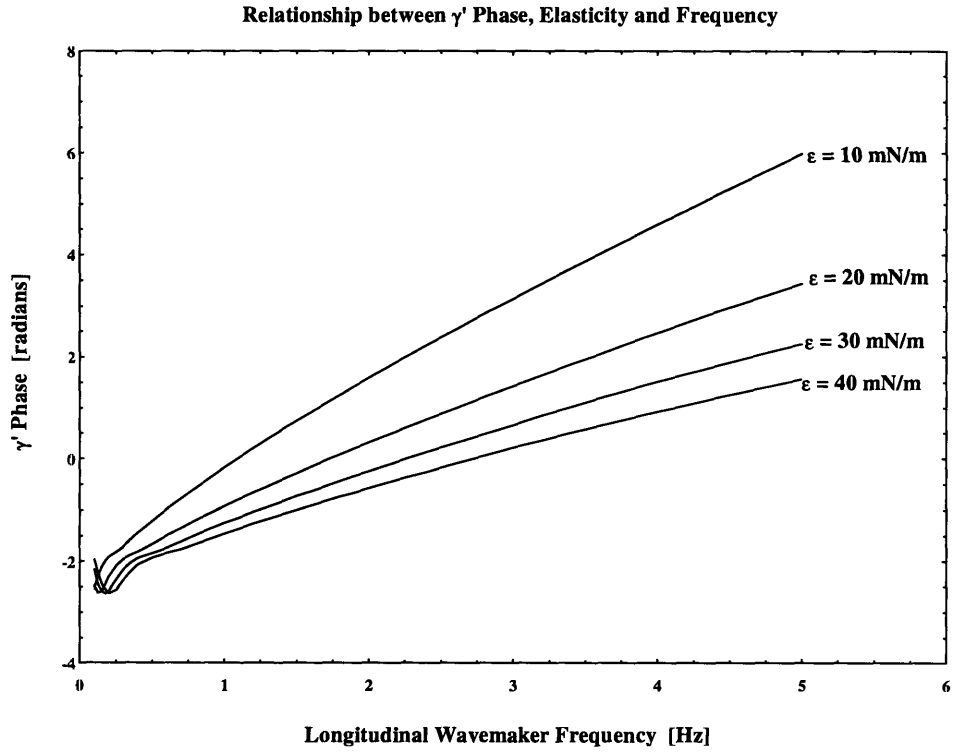

Figure 2.3 Relationship between Phase, Elasticity and Frequency for $d = 40\ cm$, $x = 7\ cm$, $\gamma = 68.0\ mN/m$, $\varepsilon' = 0 mN/m$ / sec.

2.1.2. Transverse Wave Decay

In the laboratory, transverse waves can be generated with frequencies ranging from ~4 Hz up to several hundred Hz with relative ease. Throughout this range the wave characteristics depend on surface tension and elasticity making transverse waves an ideal means to study surface film properties. As stated earlier, the real portion of the roots in the transverse dispersion relation (equation 2.9) are relatively insensitive to changes in elasticity. However, recalling equation 2.1 and 2.2

$$\zeta = \zeta_o e^{i(\bar{k}x - \omega t)} \tag{2.1}$$

$$\xi = \xi_0 e^{i(\bar{k}x - \omega t)} \tag{2.2}$$

the imaginary portion of the wavenumber, $\bar{k}$, is the real spatial decay rate. Equation 2.7 gives us an approximation or starting value of k that can be corrected using equation 2.9.

However, in the case of waves with frequencies in the range 4 ~ 15 Hz the gravitational effects must be included when determining the approximate location of the roots.

$$(\rho\omega^2 - \gamma\bar{k}^3 - \rho g\bar{k}) = 0 \tag{2.5}$$

Rather than finding the roots of equation 2.5, given a specific wavelength, λ, one can solve for the corresponding value of frequency, ω, and use the combination in equation 2.9 to resolve the first order estimate of the complex wavenumber, $\bar{k}$. The real portion of the complex wavenumber provides information about the wavelength and imaginary portion is the real decay rate, α. Figure 2.4 shows the dependence of decay rate on frequency and elasticity.

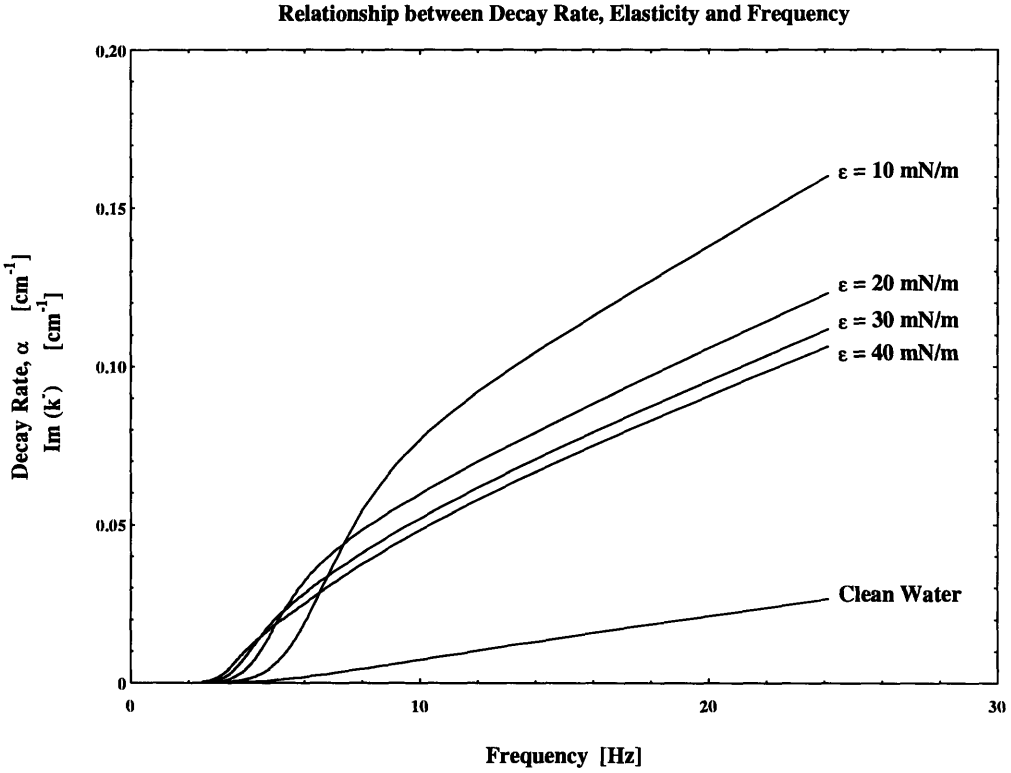

Figure 2.4 Relationship between Decay rate, Elasticity and Frequency for $\gamma = 68.0\ mN/m$, $\varepsilon' = 0 mN/m$ / sec.

Of immediate interest are the crossovers that take place between 4 - 8 Hz. Below the crossover point; low elasticities have lower decay rates but above the crossover point; low elasticities have higher decay rates. At first glance the high decay rates for films with low elasticities seem counter intuitive, but the decay is related to the phase between the film motion and the underlying fluid motion. The actual dissipation occurs in the upper water boundary layer. The relative phases are frequency dependent resulting in the crossovers.

A great deal of literature regarding wave decay is presented in non-dimensional form; where the decay rate, α, is normalized by the clean water decay rate, α_o. Hansen and Ahmed [1971] give clean water spatial decay for transverse waves as:

$$\alpha_0 = \frac{2k\upsilon\omega}{\rho g + 3\gamma k^2} \tag{2.24}$$

The benefits of normalizing the decay rates become apparent when reviewing data in the crossover region, 4 - 8 Hz. Here the clean water decay is very small while the film covered surface continues to have a significant damping effect. Figure 2.5 illustrates the relationship between normalized decay rates, elasticity and frequency.

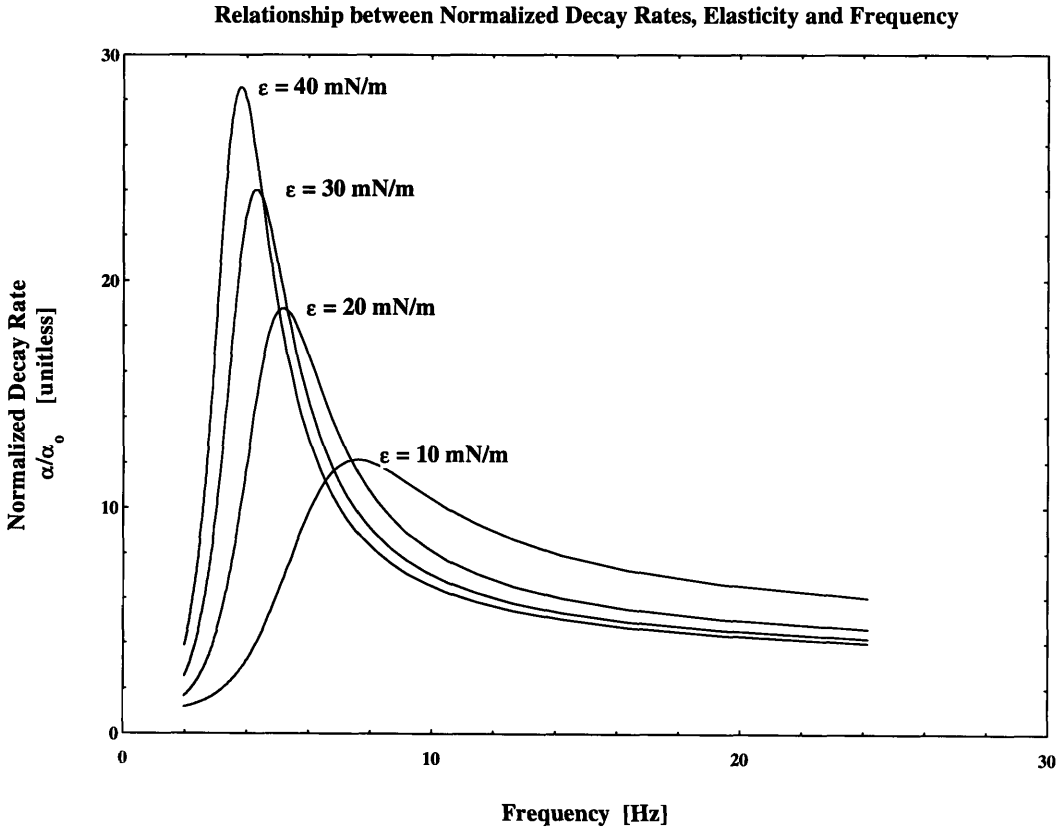

Figure 2.5 Relationship between Normalized Decay Rate, Elasticity and Frequency for: $\gamma = 68.0\ mN/m, \varepsilon' = 0 mN/m$ / sec.

Regardless of the method of viewing; gravity-capillary wave decay rates have a strong dependence upon elasticity and frequency making them suitable for evaluating film properties.

2.2. Quasi-Static Elastic Properties

Quasi-static elastic properties of surface films are determined experimentally through measurement of the pressure-area isotherms. The film pressure is the variation in surface

tension the film evokes when it forms into a continuos sheet or monolayer. In the case of elastic films, the films are usually made up of molecules with hydrophilic heads and hydrophobic tails forming into sheets one molecule thick. Present in such low concentrations the molecules are spaced widely apart and have no interaction. The surface tension is the same as the air-water interface. Sliding a film barrier compresses the molecules into a smaller surface area increases their concentration and interaction. Eventually the concentration increases to a critical level, the formation of a continuos monomolecular sheet. Any addition compression results in a drop in surface tension due to film pressure. The surface tension drops as film pressure increases. If compression continues, the resistance of the molecules to being packed closer together increases in a nonlinear relationship with increasing film pressure.

Macroscopically one can conceptualize the monolayer as a rubber sheet. Compressing it requires a sustained force, and its elastic properties result in local disturbances in pressure being transmitted trough the sheet.

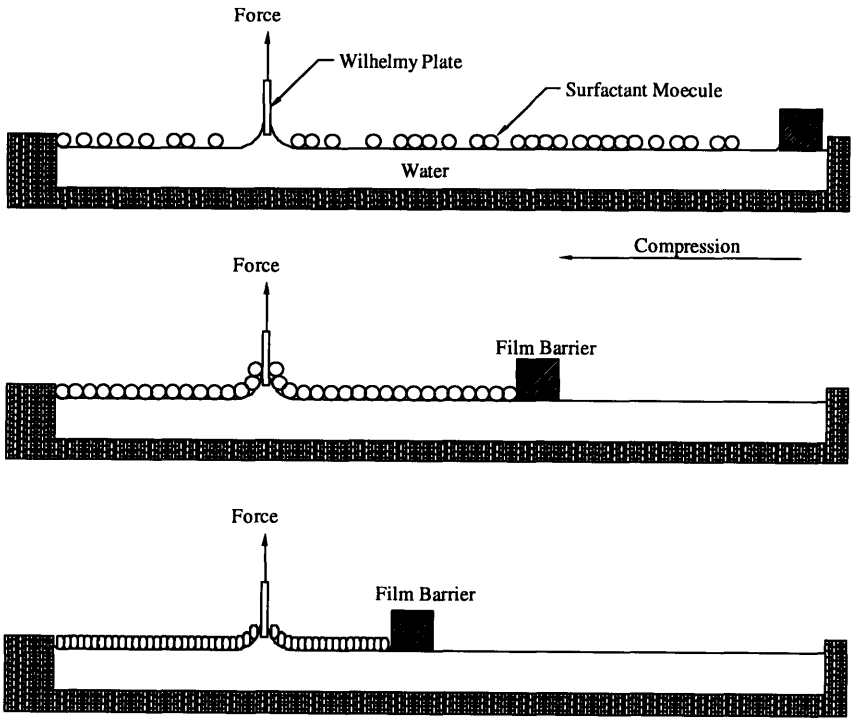

Figure 2.6 Compression Model of Surface Film

2.2.1. Experimental Determination of Surface Film Elastic Properties

Determining the elastic properties of a film requires accurate measurement of the film pressure. Surface film pressure, Π, is related to surface tension, γ, by:

$$\Pi = \gamma_o - \gamma \tag{2.25}$$

where, γ_o is the clean water surface tension measured before the film forms into a continuous monomolecular sheet or monolayer film and γ represents the surface tension after compression begins.

Several methods have been developed to measure surface tension. One method uses a platinum coated slide known as a Wilhelmy Plate. The plate is lowered into contact with the air-liquid boundary and the force exerted by the fluid meniscus on the plate is measured. The surface tension, γ, is related to the downward force, F, exerted by the fluid on the plate by equation 3.2; where L_p is the length of the plate.

$$F = 2\gamma L_p \tag{2.26}$$

Data points are collected by adjusting the film area, lowering the plate into the water and pulling it out till the meniscus is at a near breaking point, then measuring the force with a force balance. The force and film area are converted and recorded as film pressure and surface area for each data point. Data points are collected over a range of areas where the film pressures vary from 0 mN/m, surfactant molecules sparsely located, to a point where the monolayer film is near buckling. The film area is controlled by slowly moving a barrier and waiting for the film to stabilize. A conceptual visualization is offered in Figure 2.6 and a typical pressure-area isotherm for oleyl alcohol is shown in Figure 2.7.

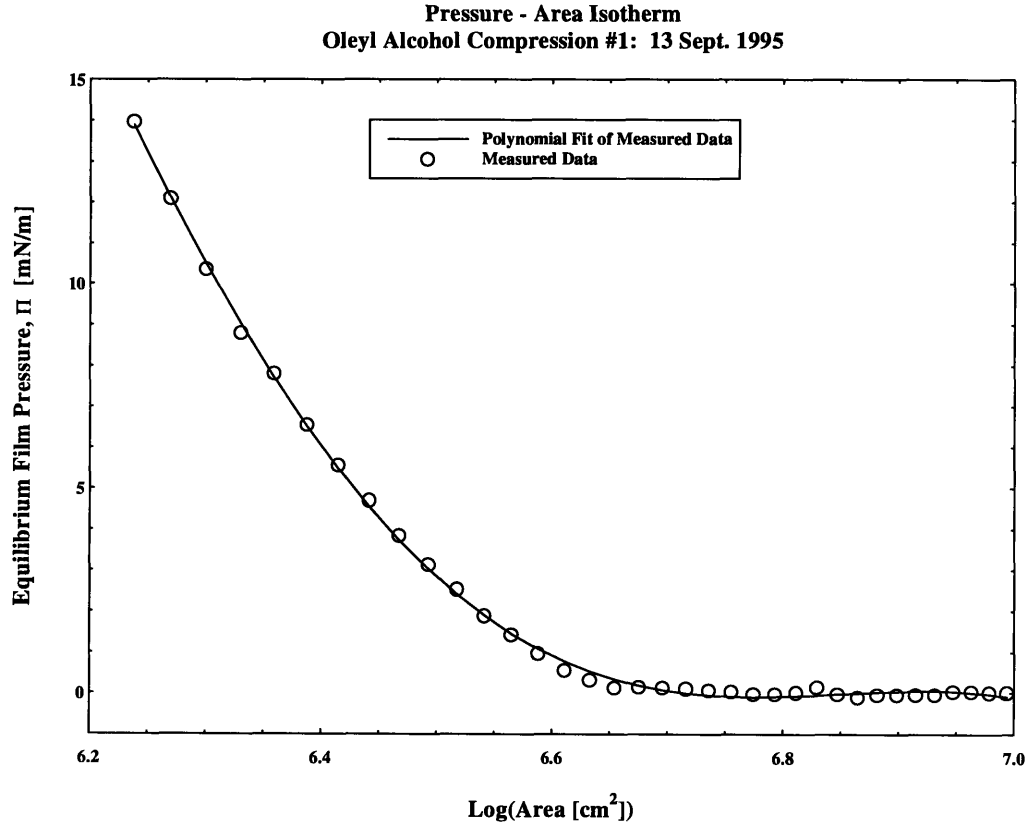

Figure 2.7 Quasi-Static Pressure-Area Isotherm

Once the pressure-area isotherm is collected the Gibbs' elasticity, ε, of a film is determined from the definition:

$$\varepsilon = \frac{d\Pi}{d[\ln(area)]} \tag{2.27}$$

A typical approach used to calculate quasi-static elasticity is to fit the pressure-area isotherm with a mathematical function then differentiate the function. Figure 2.7 shows a 5th order polynomial fit for the measurement of an oleyl alcohol film. Figure 2.8 shows the elasticity found by differentiating the polynomial fit.

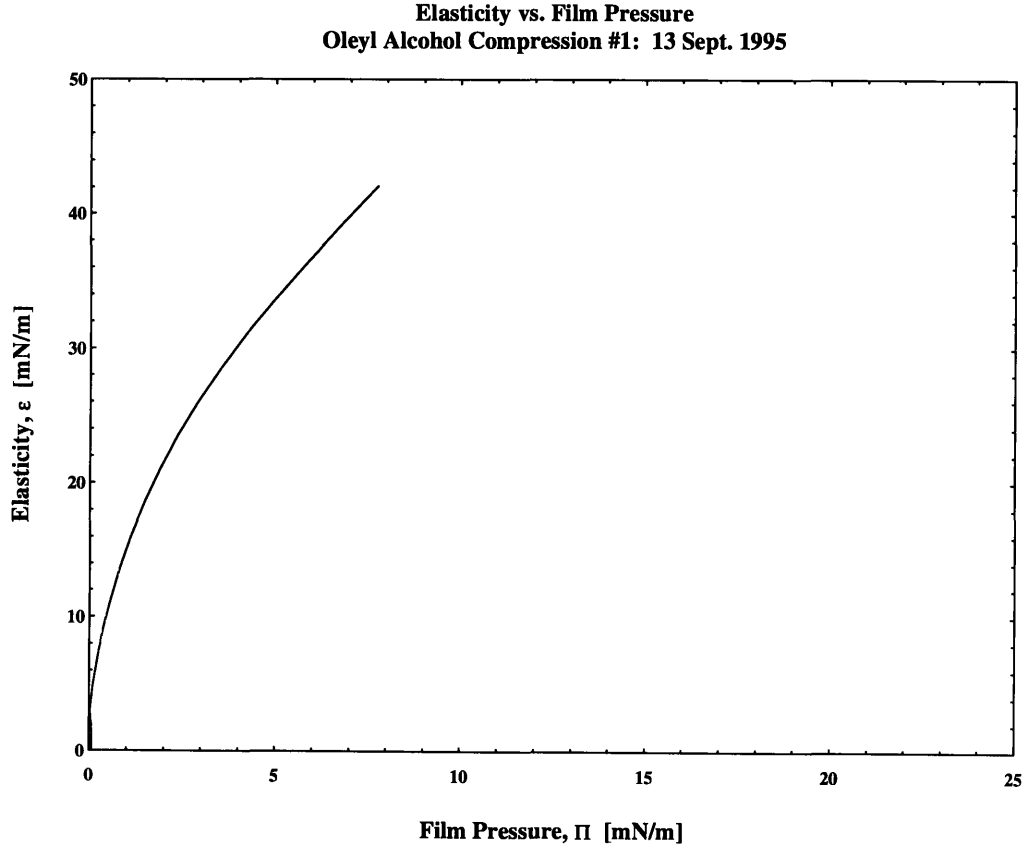

Figure 2.8 Elastic Properties from Quasi-Static Pressure-Area Isotherm

3. Apparatus

Two devices were built to measure the dynamic properties of elastic films. The Longitudinal Wave Trough, figure 3.1, was built to analyze dynamic properties from longitudinal waves with frequencies up to 4.5 Hz. An 80 cm long aluminum trough held water samples. When an elastic film is present as a monomolecular sheet, oscillating the film barrier horizontally generates longitudinal waves at the surface-air interface that propagate along the trough. The longitudinal waves create local variations in surface tension. The variations in surface tension are measured by monitoring changes in wavelength of high frequency capillary waves. A transverse wavemaker generates capillary waves at 200 Hz propagating across the tank and normal to the longitudinal waves. A laser slope gauge is used to determine the time varying wavelengths of the 200 Hz transverse waves. The dispersion relationship for capillary waves, equation 2.7, is used to relate changes in wavelength to changes in surface tension.

A full explanation of the design, construction and operation of the device is given in Appendix A.

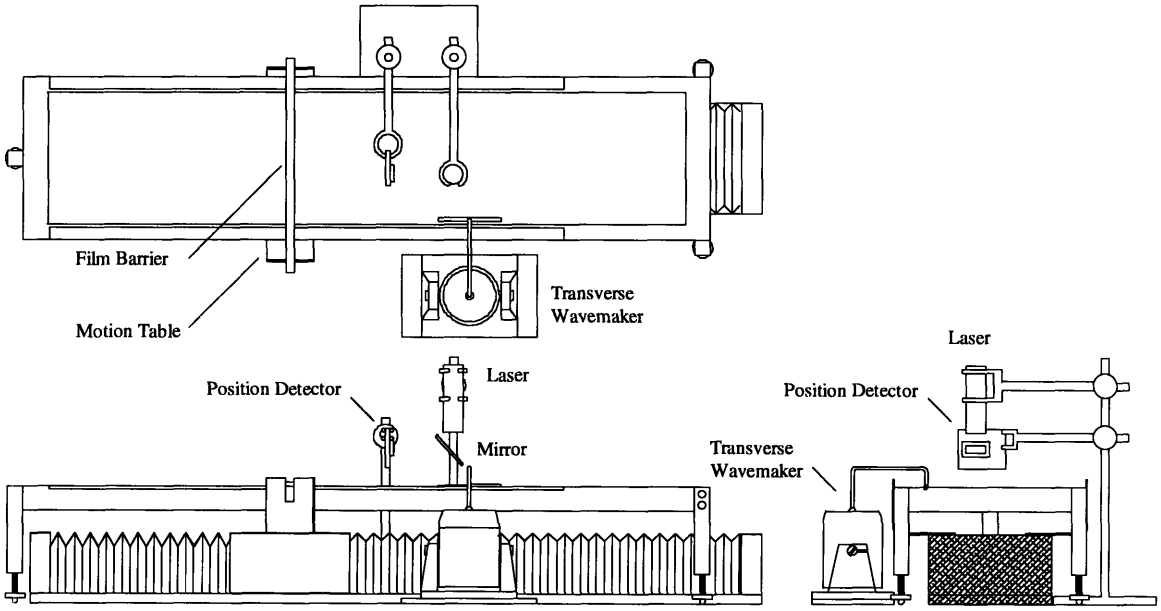

Figure 3.1 Longitudinal Wave Trough

The Wave Decay Tank, figure 3.2, was built to measure the dynamic properties of elastic films at frequencies between 4 and 25 Hz. A paddle type wavemaker generated 2D transverse waves. Four laser slope gauges mounted on a sliding carriage measured the amplitude decay of the transverse waves. Software calculated and averaged the four decay rates which were compared to theoretical decay rates; the imaginary portion of the transverse wavenumber, equation 2.10.

The tank was 2.4 m in length, 0.42 m in width and filled to a depth of 0.1 m. An acoustic speaker driving a wavemaker generated transverse waves. A beach minimized reflection of the transverse waves once they had passed through the data window. The electronic balance and Wilhelmy Plate were used to measure pressure-area isotherms in the calculation of the film quasi-static elasticity, and monitor the film pressure during wave decay experiments.

A full explanation of the design, construction and operation of the device is given in Appendix B.

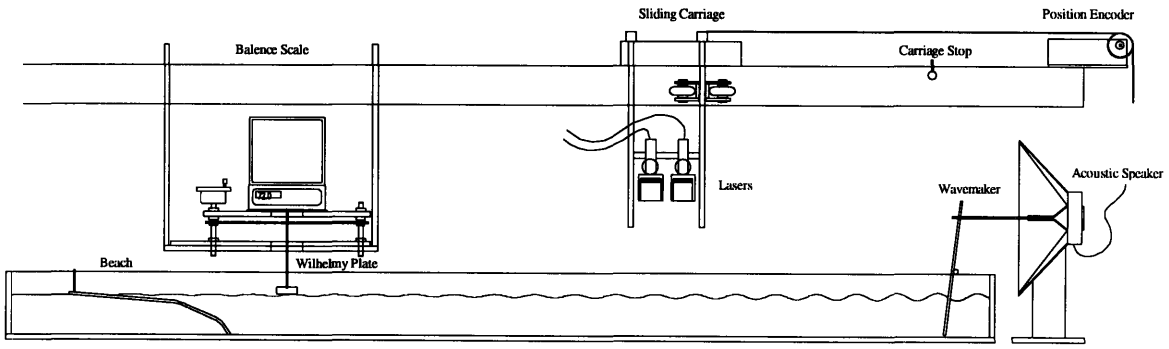

Figure 3.2 Wave Decay Tank

Both devices were equipped with components enabling the measurement of pressure-area isotherms and calculation of quasi-static elasticity.

4. Experiments and Results

Prior to testing natural films several "confidence" tests were performed on films with known characteristics. The dynamic properties of oleyl alcohol were measured in both devices and the dynamic properties of clean water, transverse wave decay rates, were measured in the Wave Decay Tank. The tests provided a baseline to ensure the devices were working properly.

4.1. Sample Collection

Seawater samples were collected from two shore based locations with free flowing connection to the ocean. Little Harbor near Cohasset, Ma. is a 100 acre pond with an inlet cross section area of approximately 150 square meters. The inlet faces the Atlantic Ocean on the north side of Cape Cod. Seawater was collected from the coastal road bridge on the incoming tide when water was near the high tide mark. The bridge forms the narrowest constriction of the inlet creating a large eddy during flood tide. The eddy naturally concentrates surface films. The samples gathered during flood tide were representative of coastal ocean surfactant. The second location was a 5 acre salt pond located near Falmouth Ma. The pond is free flooding through a narrow viaduct connecting it to Vineyard Sound. The inlet has a cross section area of approximately 3 square meters. Collection of water at the inlet during ebb tide provided surfactant of different origin than the Cohasset samples.

The seawater samples were collected by immersing containers into film covered seawater. The containers were positioned with their openings piercing the surface creating a waterfall into the container. This process captured surface material. Water samples were transported to the laboratory and tested within 24 hours.

4.2. Testing Sequence

Once seawater samples were collected and transported to the laboratory experiments were conducted in the following manner

1. Fill Wave Decay Tank and Adjust Film Concentration by letting a film adsorb to the surface and compressing it with a film barrier.
    a. Measure Quasi-Static Elasticity (minimum of 3 times)
    b. Measure Dynamic behavior for frequencies of 4.0 - 25 Hz
    c. Measure Quasi-Static Elasticity (minimum of 2 times)

2. Wave Decay Tank and Adjust Film Concentration by compression with a barrier.
    a. Measure Quasi-Static Elasticity (minimum of 3 times)
    b. Measure Dynamic behavior for variations up to 4.0 Hz
    c. Measure Quasi-Static Elasticity (minimum of 2 times)

The characteristics of the quasi-static elasticity varied with repeated compression creating a work hardening of the elastic properties (See Chapter 7).

5. Dynamic Properties of Surface Films: 0.5 to 4.0 Hz

The propagation of longitudinal waves and the variations in surface tension they invoke were discussed in section 2.1. Using the Longitudinal Wave Trough, described in Appendix A, we were able to measure variations in surface tension generated from longitudinal waves and compare them to predictions based on the film's quasi-static elastic properties.

5.1. Experimental Procedure

Experimental Procedure can be broken down into three areas; cleaning, setup and data collection. A brief description of each area follows.

5.1.1. Cleaning

Prior to testing great care must be taken to remove contaminants. Everything encountering the fluid and film must be cleansed of oils and solvents. Hands, beakers, thermometers, pipettes and stirrers are washed in hot tap water and dried using surfactant free paper wipes. The trough was hot waxed with paraffin and washed in tap water. The wavemakers, longitudinal and transverse, and film barriers were washed in hot tap water and stored submerged in tap water until use. The Wilhelmy Plate was washed in tap water and flame cleaned with a butane torch.

In two cases, oleyl alcohol and Woods Hole concentrate, films were spread on water. The tank was filled either tap or distilled water and the air-water interface was "wiped" clean. Wiping ensures the removal of contaminants from the water surface and is accomplished by sliding a film barrier the length of the trough. Contaminants are trapped behind the barrier and pushed away from the area of interest. Once the surface was clean, concentrate was spread on the surface by floating a drop on the air-water interface.

5.1.2. Setup

The trough was positioned over the motion control table with the laser beam positioned 33 cm from the right end wall, figure 3.1, and 6 cm from the side wall. The fluid of interest was placed in the trough until the fluid level was even with the side walls, depth ~ 2.5 cm. The trough was leveled using the three leveling screws. In the case of spread films, a barrier was used to wipe the air-liquid interface trapping unwanted surfactant behind a temporary film barrier. Spread films were applied to the clean interface and adsorbed films were given time to concentrate at the interface. The Wilhelmy Plate was attached to the electronic balance and wetted by submerging it in the fluid. Upon extraction the electronic balance was zeroed and the plate was lowered into contact with the surface to the point where the meniscus was at a near breaking point.

Once surfactant molecules were present on the surface the film barrier, attached to the motion control table, was used to generate longitudinal waves. The transverse wavemaker was attached to the shaker and positioned near the side wall. The laser beam reflection point on the interface was double checked and beam location on the position sensing device (PSD) was adjusted until output voltage was zero.

5.1.3. Data Collection

Data collection is composed of three phases. The first and third phases determine the film's quasi-static elastic properties. Movement of the film barrier in 1 cm increments compresses sparsely located surfactant molecules. The motion table records barrier position and force exerted on the Wilhelmy Plate by the fluid. Equations in Section 2.2. were used to calculate the quasi-static elastic properties from the pressure-area isotherm. Isotherms were measured until repeatable elastic properties were shown. Repeated compression of natural films caused hardening; in which case repeated compression was done until repeatable stiffness was achieved. When hardening was present the elastic properties measured on the first isotherm following dynamic measurements were used in the theoretical comparisons.

The second phase of data collection measured the dynamic properties of the film. After the quasi-static properties were determined the longitudinal wavemaker was moved to a position 40 cm from the right wall, $d = 40\,cm$. The transverse wavemaker and laser and laser slope gauge were set up 7 cm from the film barrier, $x = 7\,cm$. The film pressure was adjusted to ~ 2.5 mN/m by releasing excess film around the longitudinal wavemaker. The motion table drives the longitudinal wavemaker (film barrier) at a prescribed frequency while the second computer records bar position and laser/transverse wavemaker phase. Software converts the data to time dependent variations in surface tension. For more details regarding data collection and reduction see Appendix A. Several frequencies were run over a range from 0.5 Hz to 4.0 Hz. The high frequency limit of 4 Hz represents the point where the oscillating film barrier begins generating transverse waves along the length of the trough.

5.2. Analysis of a Known Film: Oleyl Alcohol

Oleyl alcohol was tested on several occasions to serve as a baseline for data comparison. After cleaning, the trough was filled with distilled water and one drop of oleyl alcohol, $\sim 15\,\mu l$, was applied to the surface. Due to the disparity in surface tension and density between water and oleyl alcohol the later is a self spreading compound. Excess droplets, when present, were wiped to the left end of the trough and contained behind a film barrier. In all cases the elastic properties measured before and after data collection adequately explained the dynamic behavior for frequencies up to 3 Hz. Data collected above 3 Hz showed considerable scatter. The scatter was due to the longitudinal wavemaker generating transverse waves in the direction of the longitudinal waves.

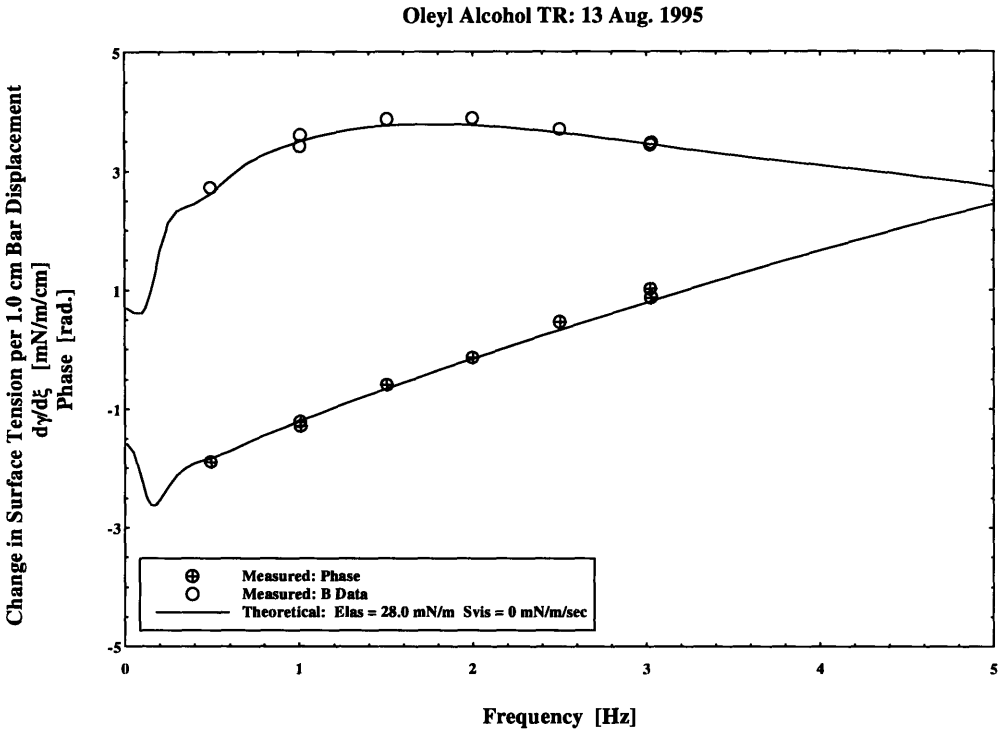

Figure 5.1 Variation in Surface Tension: Oleyl Alcohol $\gamma = 68.0\ mN\ /\ m$

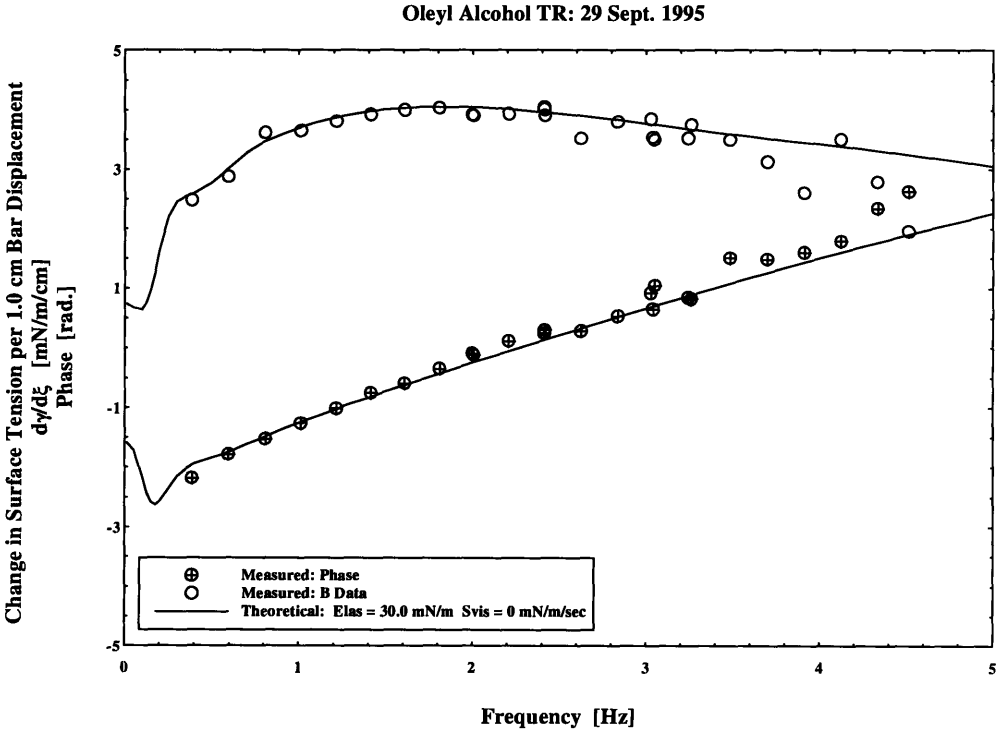

Figure 5.2 Variation in Surface Tension: Oleyl Alcohol $\gamma = 67.0\ mN\ /\ m$

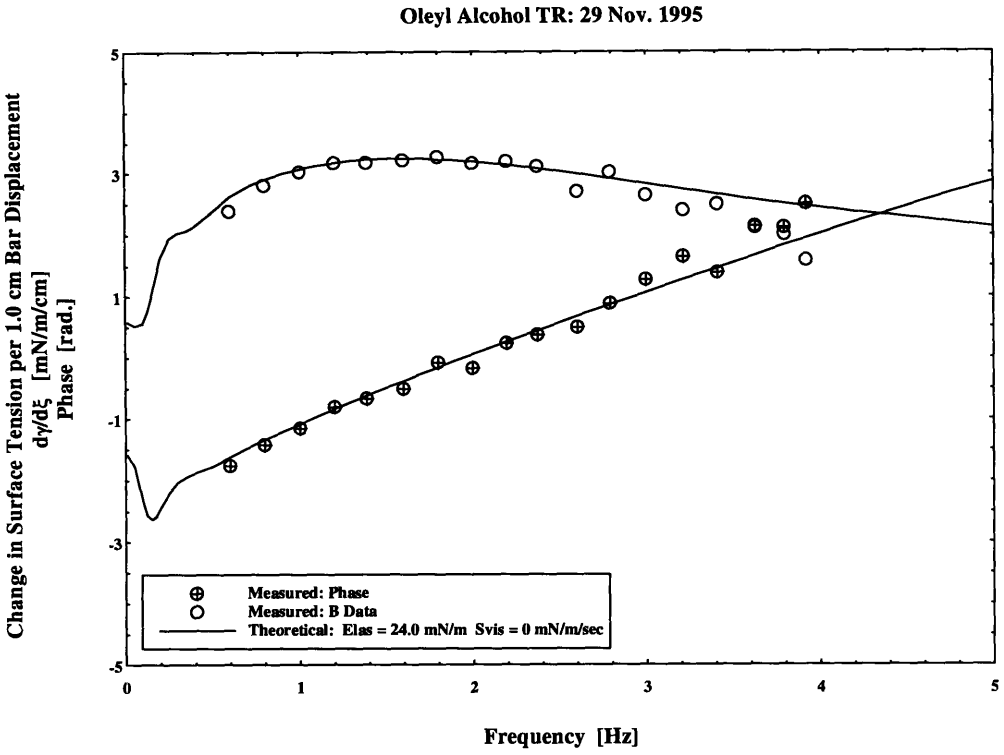

Figure 5.3 Variation in Surface Tension: Oleyl Alcohol $\gamma = 70.0\ mN\ /\ m$

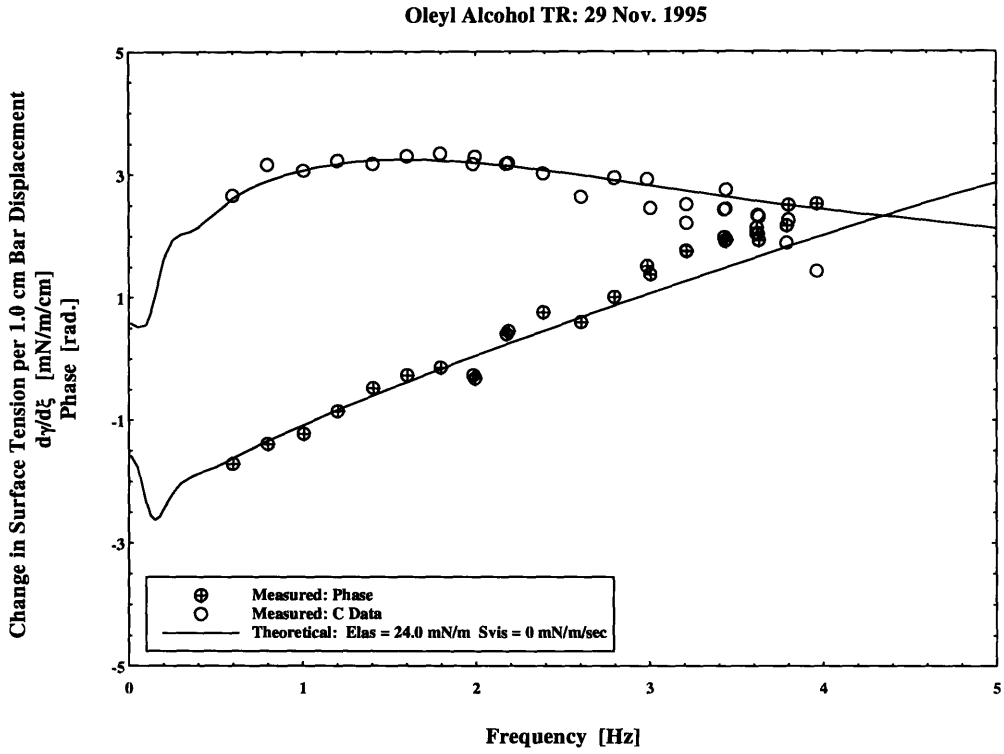

Figure 5.4 Variation in Surface Tension: Oleyl Alcohol $\gamma = 70.0\ mN\ /\ m$

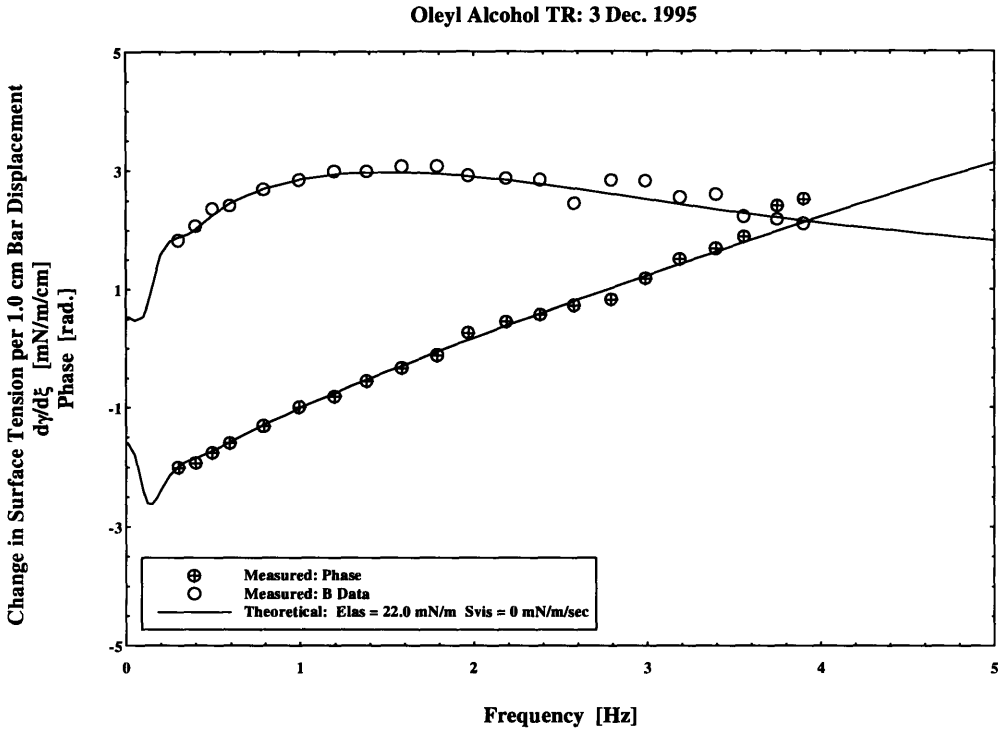

Figure 5.5 Variation in Surface Tension: Oleyl Alcohol $\gamma = 69.0\ mN\ /\ m$

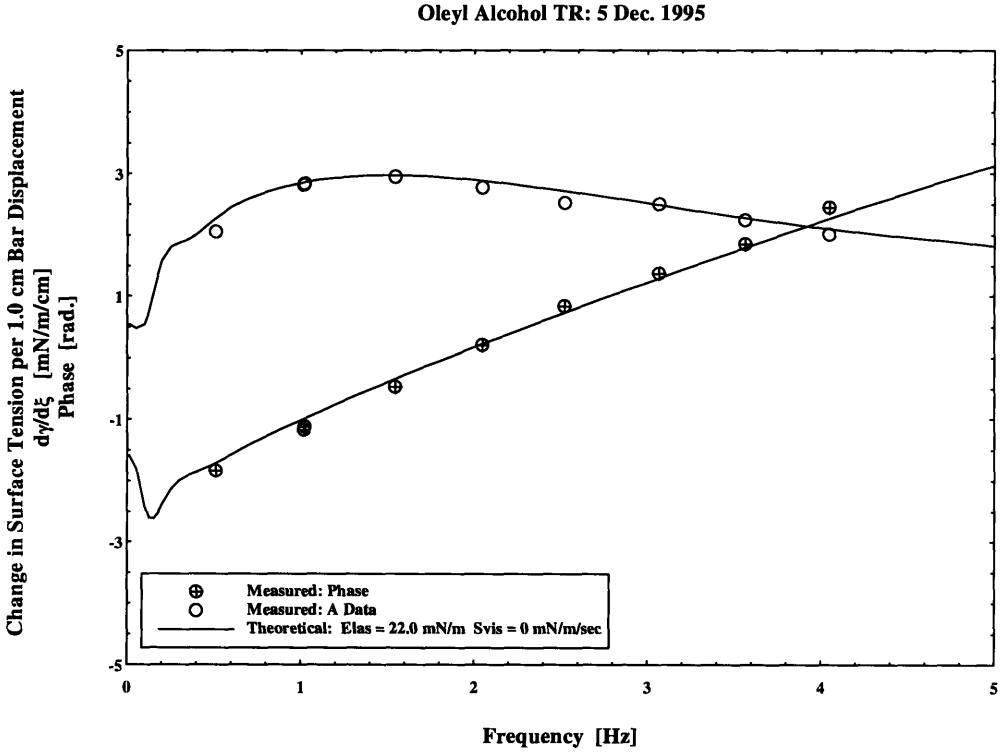

Figure 5.6 Variation in Surface Tension: Oleyl Alcohol $\gamma = 70.0\ mN\ /\ m$

5.3. Analysis of Seawater Surfactants

5.3.1. Analysis of Cohasset Seawater

On several occasions, water was collected and analyzed from the inlet to Little Harbor near Cohasset Ma. Little Harbor is located on the northern shore of Cape Cod taking in water from the Bay of Massachusetts. Water was collected during daylight hours near the end of the flood tide. The shape of the inlet allows a large eddy to form during flood tide, concentrating surface surfactant when present.

After collection and transportation to the laboratory, seawater samples were placed in the Wave Decay Tank or, in the case of a smaller sample, a 50 liter holding tank equipped with surface skimming apparatus. The Longitudinal Wave Trough was filled with water skimmed off the larger tank. This process ensured an adequate supply of surfactant. In those cases where samples were tested for both wave decay properties and variations in surface tension, wave decay experiments were performed and surfactant was skimmed off the Wave Decay Tank. Prior to dynamic testing several pressure-area isotherms were measured to determine the quasi-static elasticity. Dynamic data is compared to theoretical predictions based on quasi-static elasticity measured following the dynamic tests

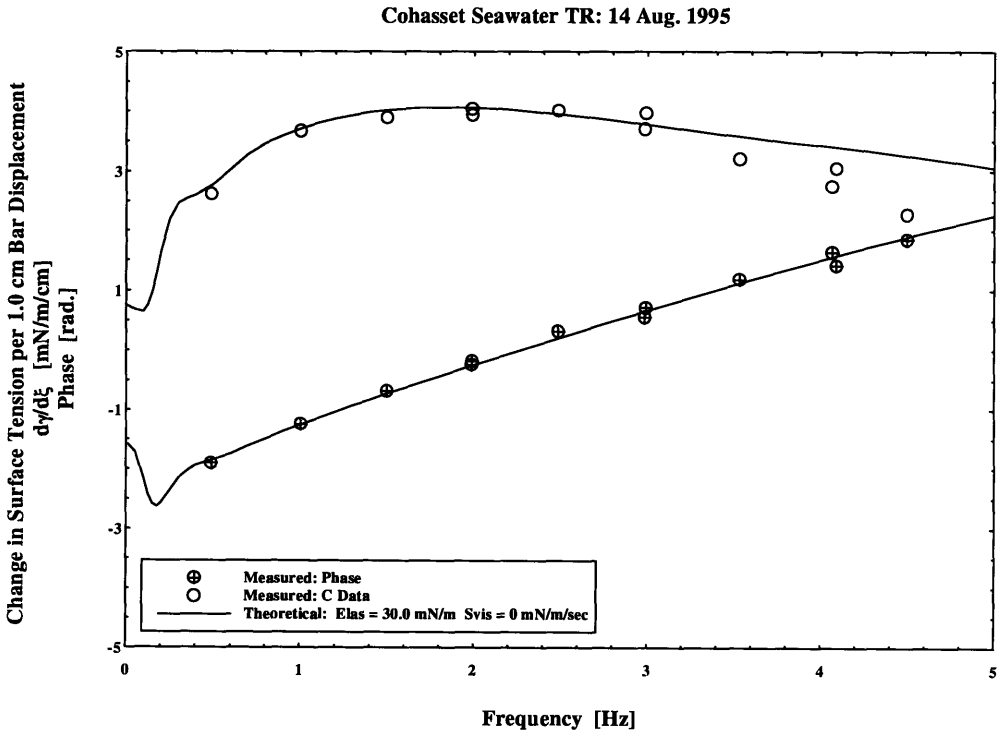

Figure 5.7 Variation in Surface Tension: Cohasset Seawater $\gamma = 69.0\ mN / m$

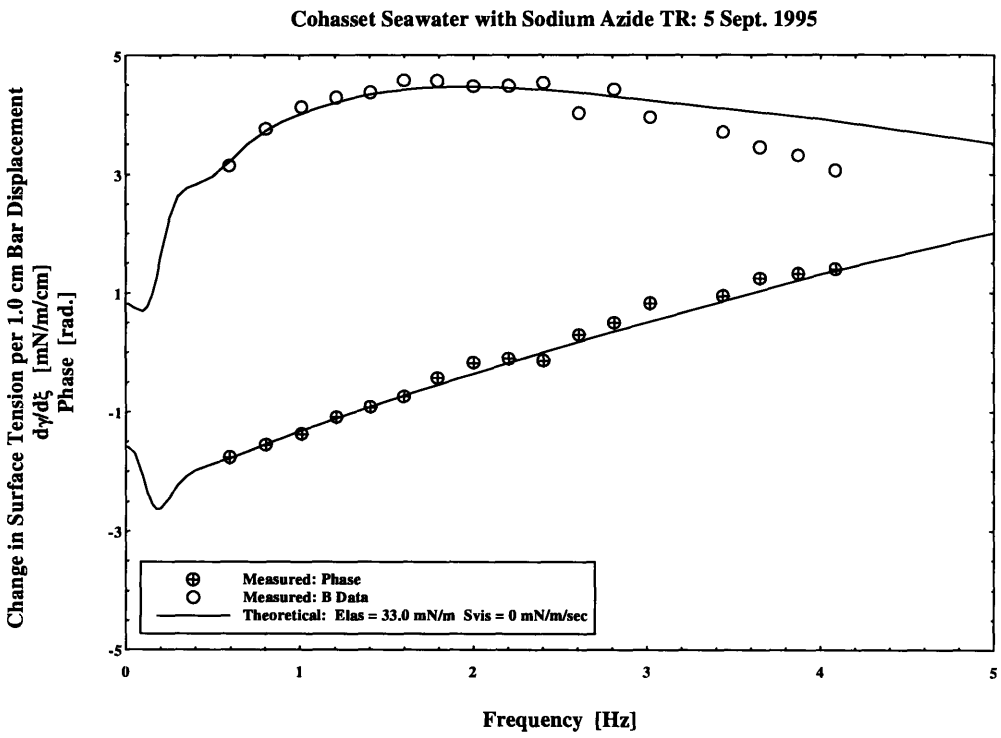

Figure 5.8 Variation in Surface Tension: Cohasset Seawater $\gamma = 68.0\ mN\ /\ m$

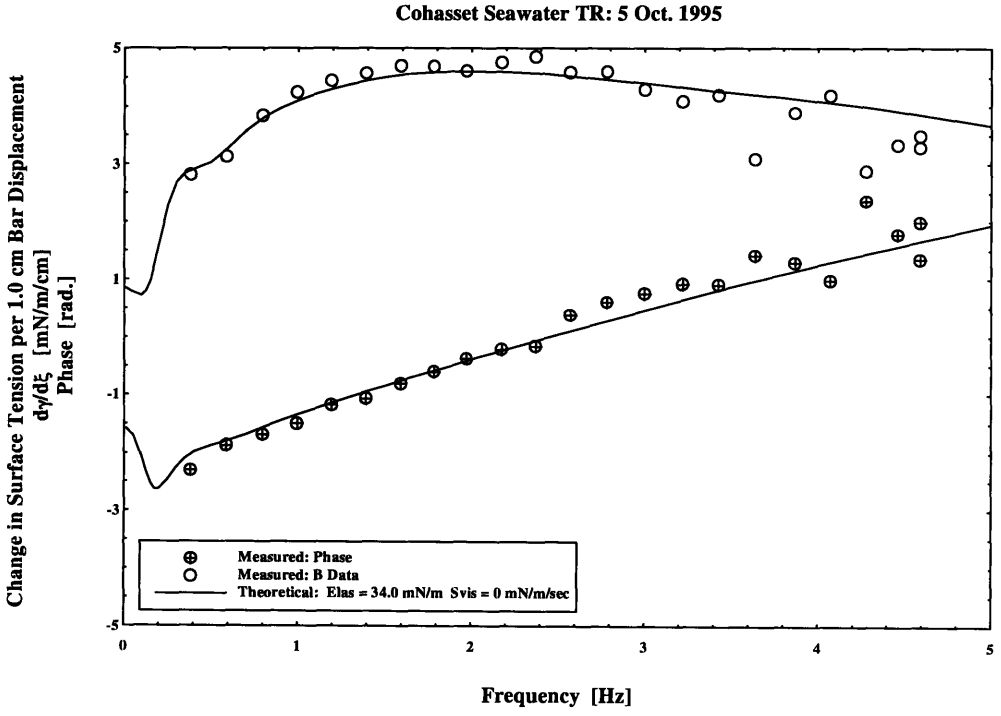

Figure 5.9 Variation in Surface Tension: Cohasset Seawater $\gamma = 69.0\ mN\ /\ m$

5.3.2. Analysis of Woods Hole Seawater

Two water samples were collected from a salt pond on the south shore of Cape Cod fed by an inlet to Vineyard Sound. The first sample was collected from the inlet during ebb tide on the morning of November 18. Containers were lowered into the flow out of the inlet taking care not to disturb the material on the bottom or banks. Water was transferred from collection containers to 50 liter containers allowing 400 liters to be transferred to the Marine Instrumentation Laboratory MIT. Samples were stored overnight in the 50 liter transport containers and dynamic properties were measured on November 19. Upon completion of wave decay experiments seawater and surface films were transferred to the Longitudinal Wave Trough by skimming film off the surface of the Wave Decay Tank.

Variations in surface tension were measured in the longitudinal wave trough at frequencies between 0.6 to 3.2 Hz. Variations in surface tension magnitude corresponded to predictions made from the quasi-static elastic properties. However, the measured phase relationship between the longitudinal wavemaker and variations in surface tension for low frequency deviated slightly from predicted values. The error in phase for 0.6 Hz represents variations in surface tension occurring 0.1 sec before predicted variations. The error may be due to a change in film properties due to its age but remains unexplainable without future experiments.

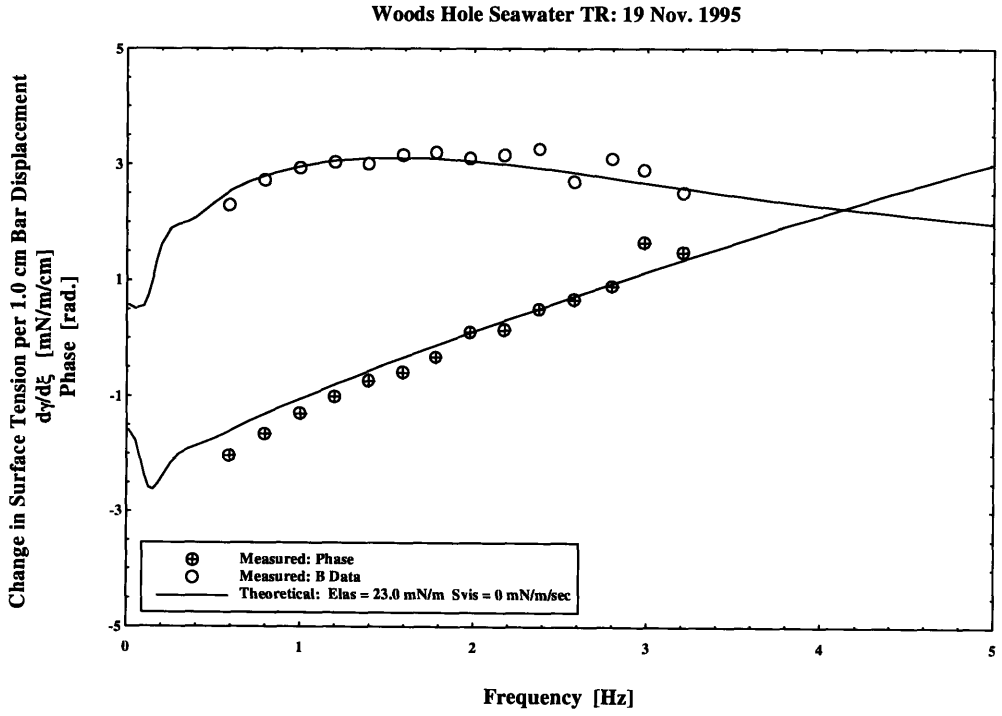

Figure 5.10 Variation in Surface Tension: Woods Hole Seawater $\gamma = 70.0\ mN\ /\ m$

The second sample was collected from the salt pond, concentrated using a centrifuge and eluted with methanol into a concentrate. Collection and concentration were carried out by

Robert Nelson of the Woods Hole Oceanographic Institute. The concentrate was spread onto tap water that had been wiped clean. A micro pipette was used to spread ~ 200 μl of the concentrate on the water surface.

During concentrate spreading for the December 5 experiment several droplets of concentrate sank to the bottom of the trough. The droplets could not be moved from below the laser apparatus resulting in difficulties maintaining a constant surface film pressure during the experiment. The variation in film pressure resulted in variations in elasticity and increased scatter during the experiment.

During concentrate spreading for the December 6 experiment care was taken to spread concentrate behind the longitudinal wavemaker in smaller quantities. Several small droplets sank but leakage was confined outside the test area. Data scatter was reduced and the dynamic behavior corresponds to predictions made from the quasi-static elasticity.

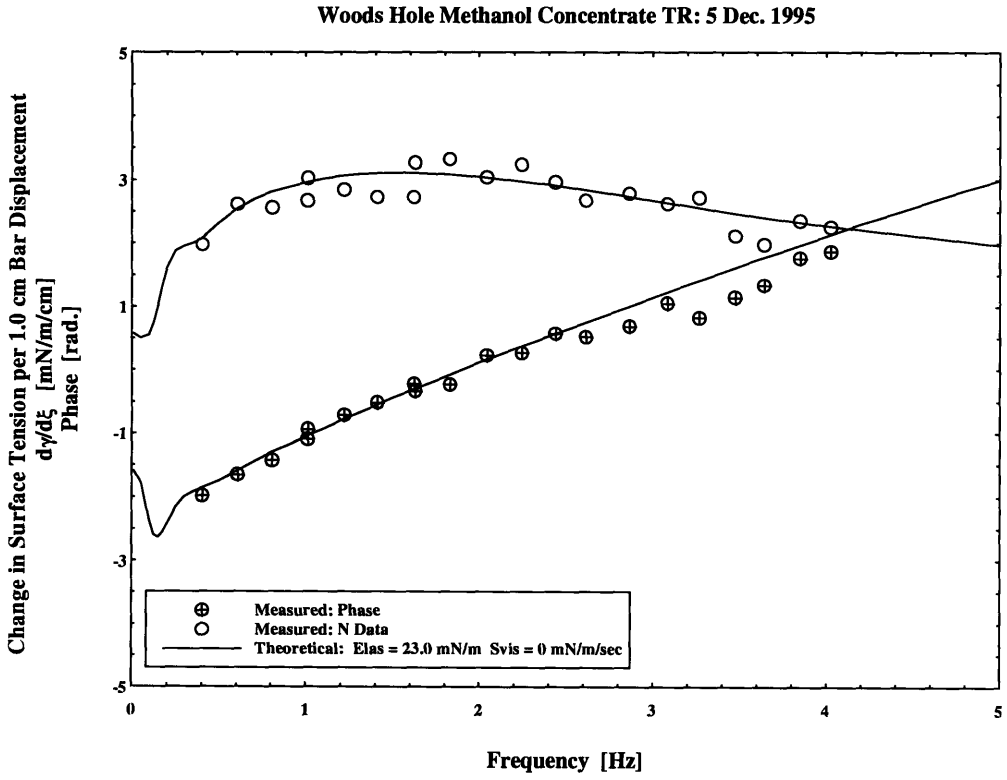

Figure 5.11 Variation in Surface Tension: Woods Hole Concentrate $\gamma = 70.0\ mN / m$

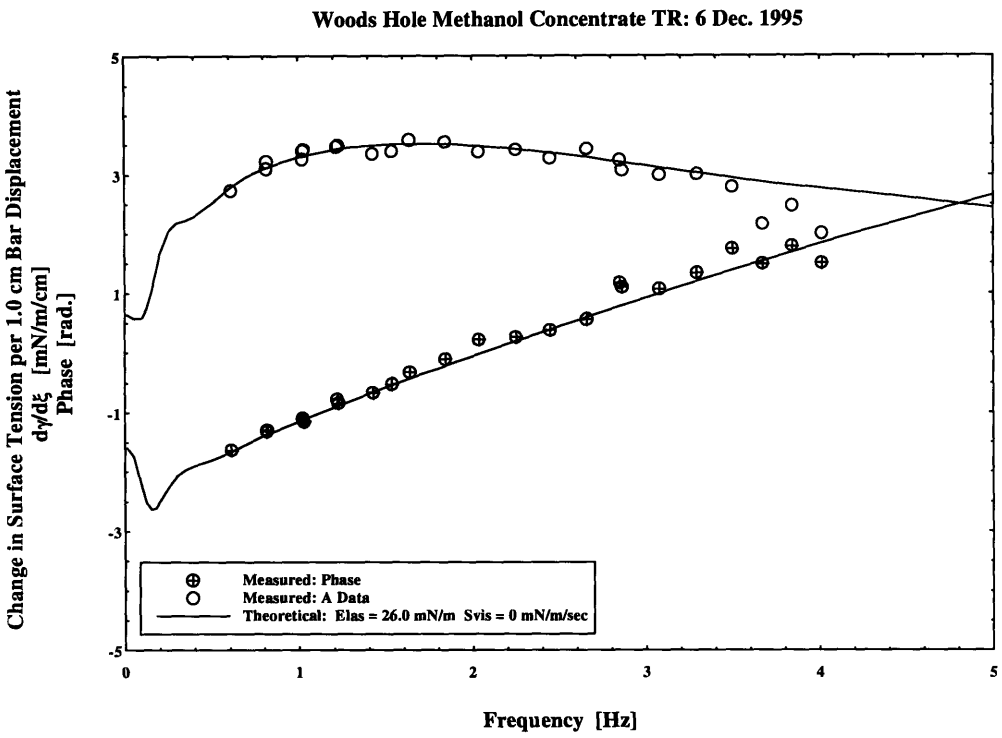

Figure 5.12 Variation in Surface Tension: Woods Hole Concentrate $\gamma = 70.0\ mN\ /\ m$

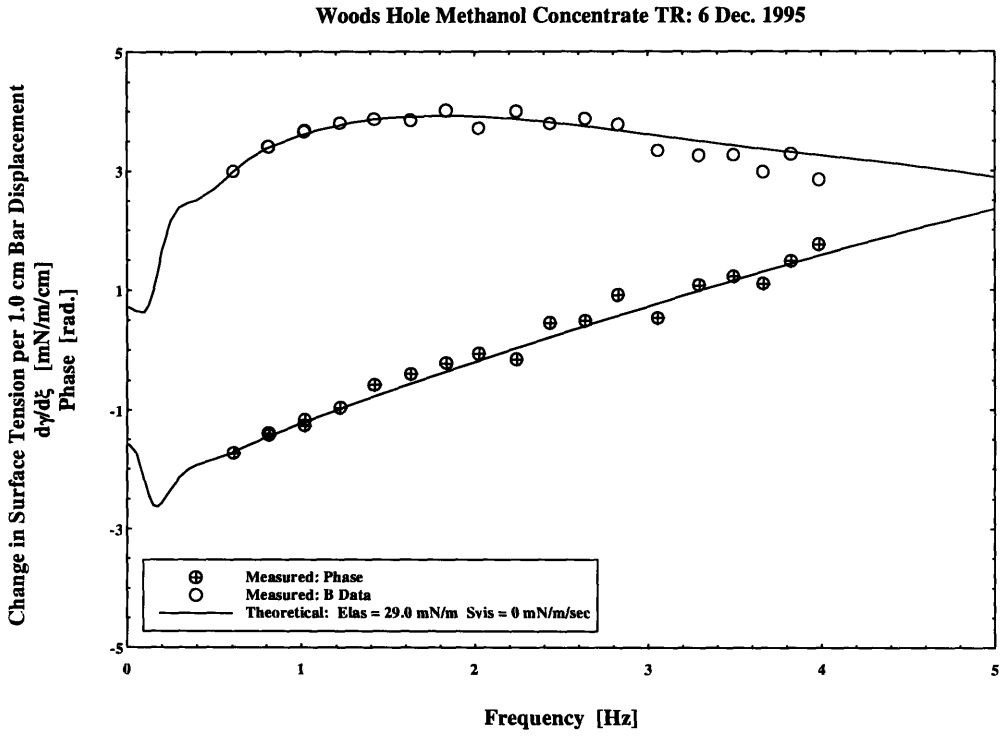

Figure 5.13 Variation in Surface Tension: Woods Hole Concentrate $\gamma = 69.0\ mN\ /\ m$

5.4. Surface Viscosity Sensitivity Analysis

In an effort to quantify whether surface films possess significant surface viscosity, several test cases were run through the surface tension modeling program for a constant elasticity. Surface viscosity values ranging from 0.0 mN/m/sec to 1.0 mN/m/sec were used. The model predicts a significant reduction in the magnitude of surface tension variation with surface viscosity values greater than 0.1 mN/m/sec.

The phase relationship between the longitudinal wavemaker and variations in surface tension at the point where surface tension measurements are made is also affected by changes in surface viscosity. Varying surface viscosity shows changes in the phase relationship between wavemaker and measurement points for frequencies above 2 Hz and for surface viscosity values greater than 0.5 mN/m/sec.

Examination of the experiential data with respect to surface viscosity reveals that surface viscosity must be negligible in the films tested.

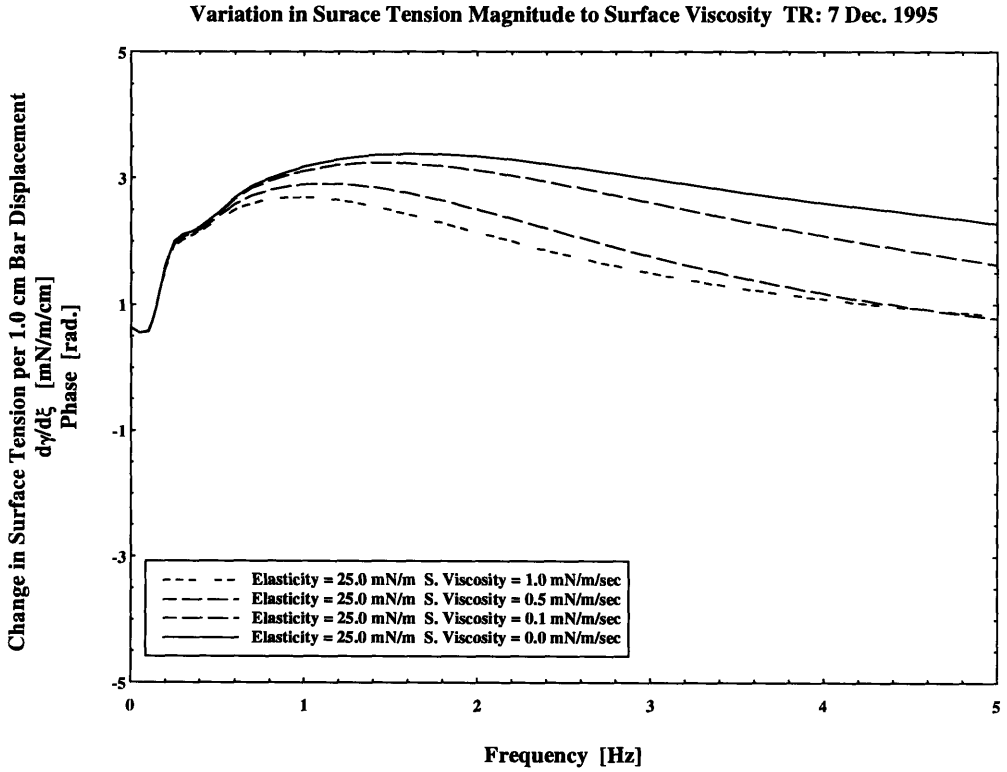

Figure 5.14 Variation in Surface Tension Magnitude due to Surface Viscosity

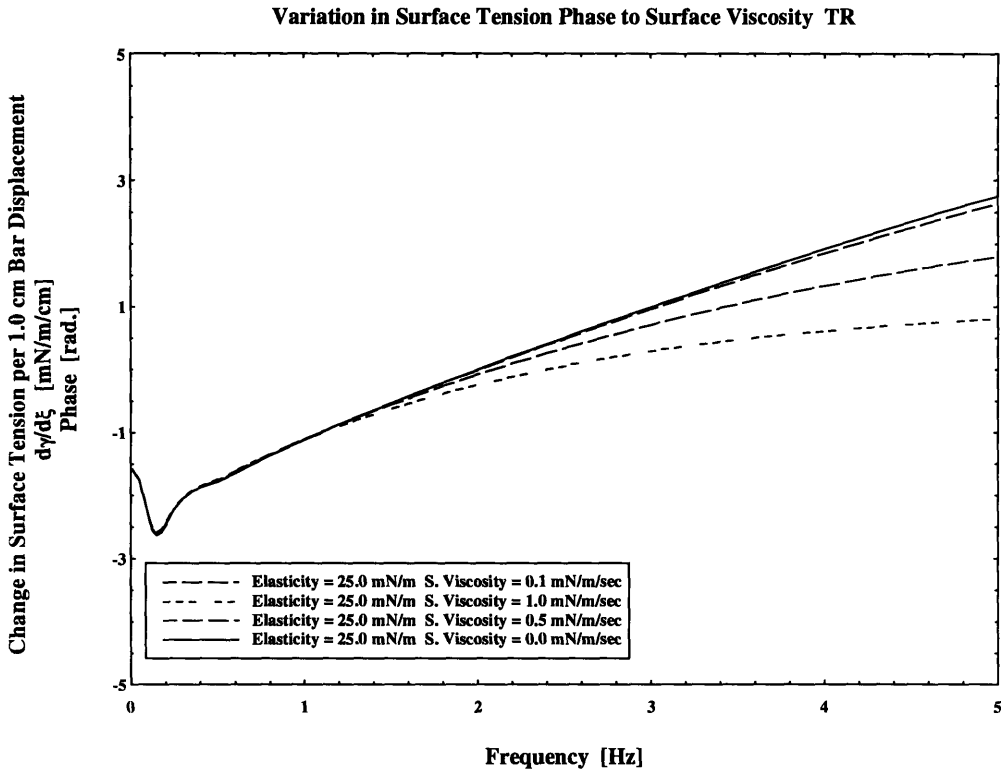

Figure 5.15 Variation in Surface Tension Phase due to Surface Viscosity

6. Dynamic Properties of Surface Films: 4.0 to 24.0 Hz

The decay rate of transverse water waves propagating on a film covered surfaces were discussed in section 2.1. Using the Wave Decay Tank, described in Appendix B, we were able measure decay rates over a range of frequencies from 4.0 to 24.0 Hz.

6.1. Experimental Procedure

Procedure can be broken down into three areas; cleaning, setup and data collection.

6.1.1. Cleaning

Prior to testing great care must be taken to remove contaminants. The Wave Decay Tank was rinsed with tap water and dried using a vacuum squeegee. The wavemaker, beach and skimmers were washed with tap water and dried using solvent free paper wipes.

Prior to testing decay rates of clean water and spread films on tap water the surface was "wiped" clean or skimmed to remove any contaminants. Two film barriers were constructed to slide on the tank walls. The barriers pierced the air-water interface with seals along the tank walls. Sliding the barriers along the tank trapped and compressed contaminants to the point where they could be vacuumed off.

6.1.2. Setup

Two types of underlying fluid were tested in the wave decay tank. The first, tap water, was used during the measurement of clean water decay and as a base for spread films. After cleaning, the tank was filled with tap water through a garden hose to a depth of 10 cm. The water was left to stand for 20 minutes and the surface was skimmed. After skimming, cleanliness was ensured by measuring the surface tension of and comparing it to typical values for clean water.

Two types of tests were conducted using tap water as a base. Decay tests were performed checking clean water decay rates. The clean water decay rates served as a baseline check testing the apparatus for repeatability. Upon completion of successful clean water decay tests, surfactant was spread on the tap water surface. Two spread films were tested, oleyl alcohol and Woods Hole seawater concentrate.

Seawater was the second base fluid. The tank was cleaned with tap water and filled with seawater that had been transported to the laboratory from site collection. Once filled to a depth of 10 cm the water was left to stabilize for ½ hour. In the event more surfactant was needed a smaller tank equipped with a skimming apparatus was filled with seawater and surface surfactant was skimmed into a 200 ml beaker and transferred to the Wave Decay Tank.

Several pieces of equipment were shared between the wave decay experiments and the variation in surface tension experiments. Moving from one experiment to the other required

relocating the electronic balance and reconfiguring the data processing and collection equipment.

6.1.3. Data Collection

Data collection was done in three steps. 1) Pressure-Area Isotherm. 2) Decay Data and 3) Pressure-Area Isotherm. The isotherm data was collected by submerging the beach, placing a film barrier at the "0" location and using a second film barrier to compress the surface film. After the pressure-area isotherm was completed the film pressure was adjusted to ~2mN/m by moving the film barrier, the beach was raised into position, and the transverse wavemaker was installed. Decay data collection started with a frequency of 4 Hz and then was done at progressively higher frequencies. The electronic balance and Wilhelmy Plate were located forward of the beach and kept in contact with the water during decay data collection ensuring continuous monitoring of film pressure.

6.2. Measured Decay Rates of Clean Water

Clean water was used as a baseline checking the test apparatus and data reduction software. The tank was filled with MIT tap water to a depth of 10 cm. The surface was wiped clean by removing any surfactants from the surface area of interest.

Transverse wave decay was measured over frequencies ranging from 4 to 30 Hz. In all cases the decay rates matched those predicted by equation 2.24.

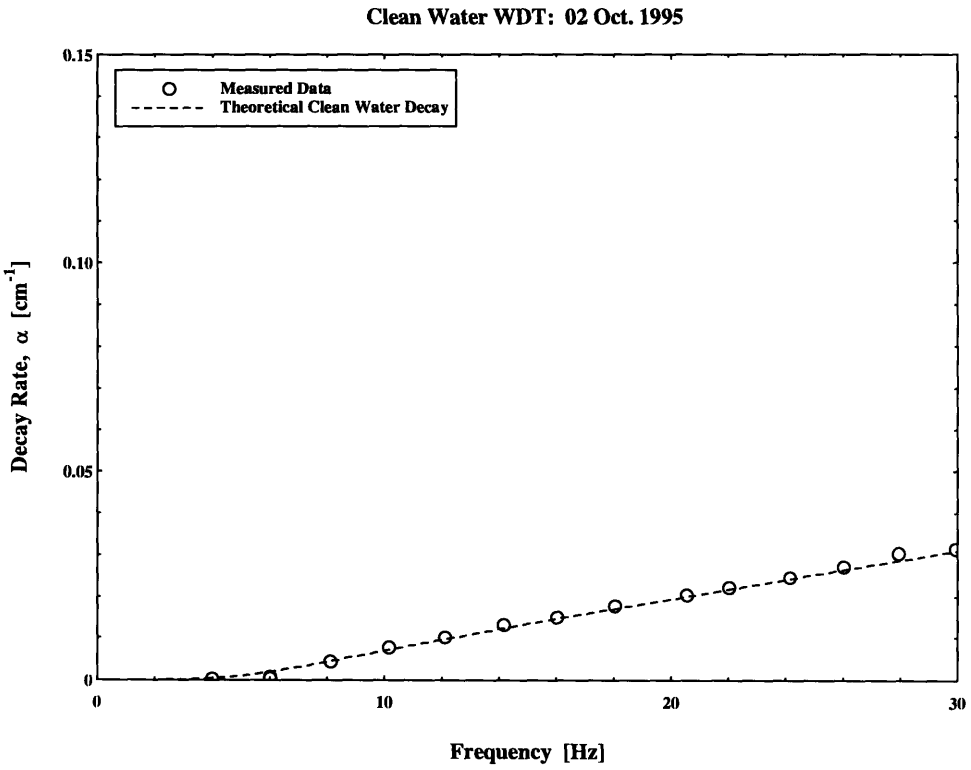

Figure 6.1 Transverse Wave Decay Rates: Clean Water $\gamma = 72.0\ mN / m$

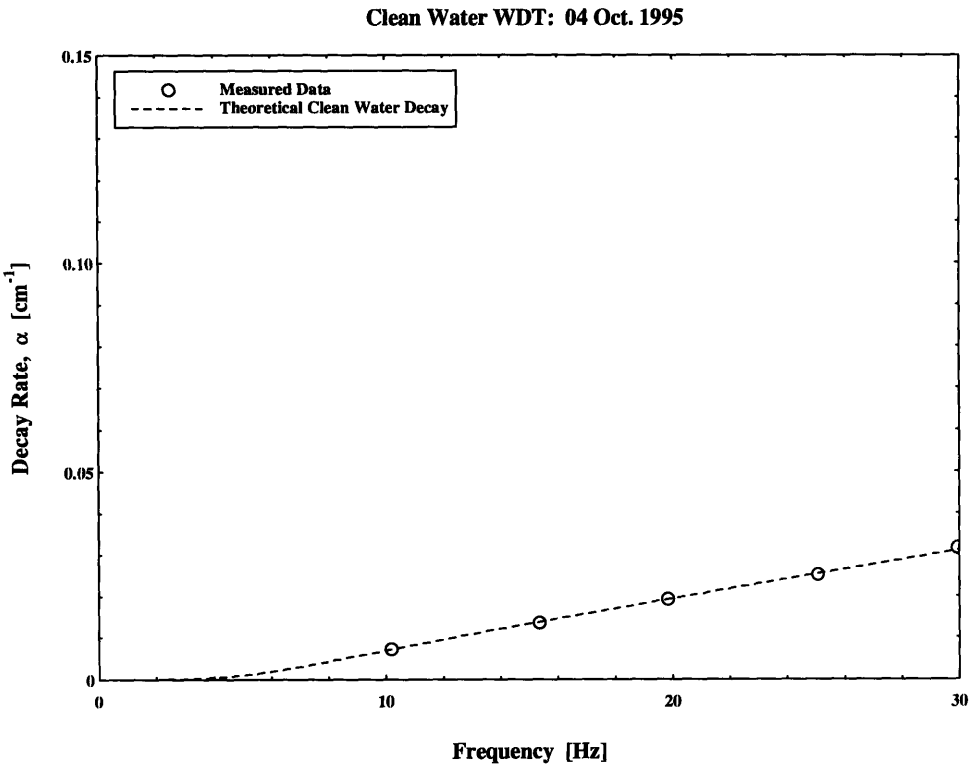

Figure 6.2 Transverse Wave Decay Rates: Clean Water $\gamma = 72.0\ mN / m$

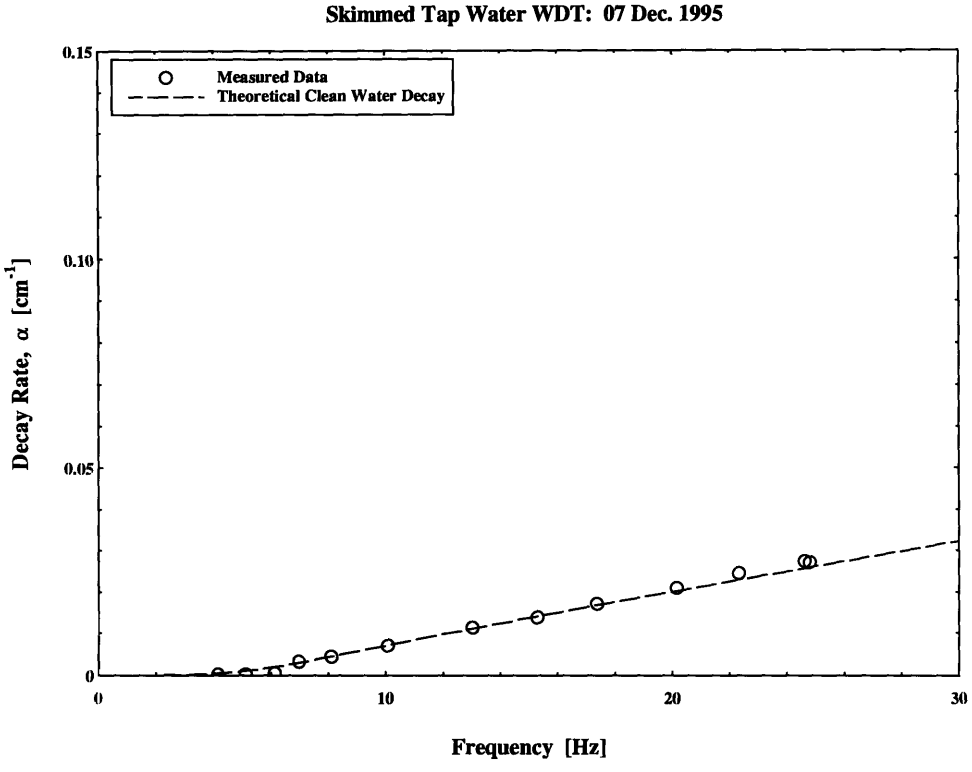

Figure 6.3 Transverse Wave Decay Rates: Clean Water $\gamma = 72.0\ mN / m$

6.3. Transverse Wave Decay Rates for Oleyl Alcohol

A second baseline was established by testing the dynamic properties of oleyl alcohol spread on tap water. A film was spread on the surface, repeated pressure-area isotherms were measured to determine the quasi-static isotherm and transverse wave decay data was collected. Transverse waves were generated in 1 Hz increments from 4 to 10 Hz and in 2 Hz increments from 12 to 24 Hz. The data is shown compared to theoretical predictions based on quasi-static elasticity measured before and after transverse wave data collection. The decay data is shown in the figure below.

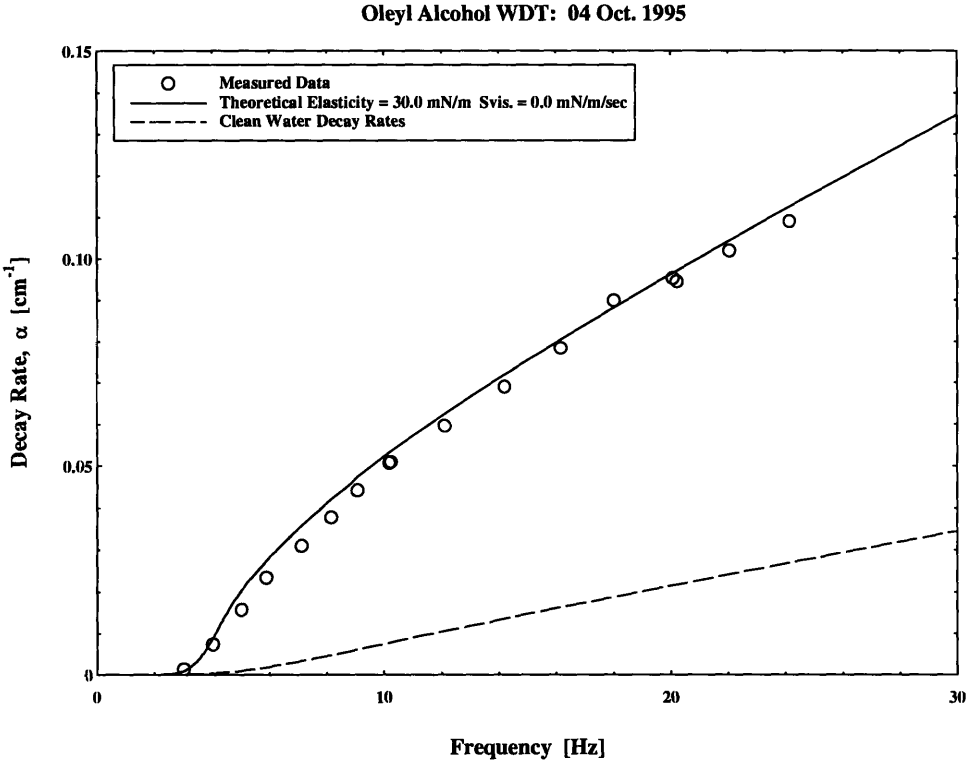

Figure 6.4 Transverse Wave Decay Rates: Oleyl Alcohol $\gamma = 67.0\ mN / m$

6.4. Transverse Wave Decay Rates for Seawater

In an effort to characterize natural films seawater samples were collected at two locations along the Massachusetts coastline. Water was collected by piercing the free surface with a container creating a waterfall effect. The waterfall allowed surface surfactant to be skimmed off the surface and transferred to larger containers.

6.4.1. Analysis of Cohasset Seawater

On several occasions, water was collected and analyzed from the inlet to Little Harbor near Cohasset Ma. Little Harbor is located on the northern shore of Cape Cod taking in water from the Bay of Maine. Water was collected during daylight hours at the end of the flood tide.

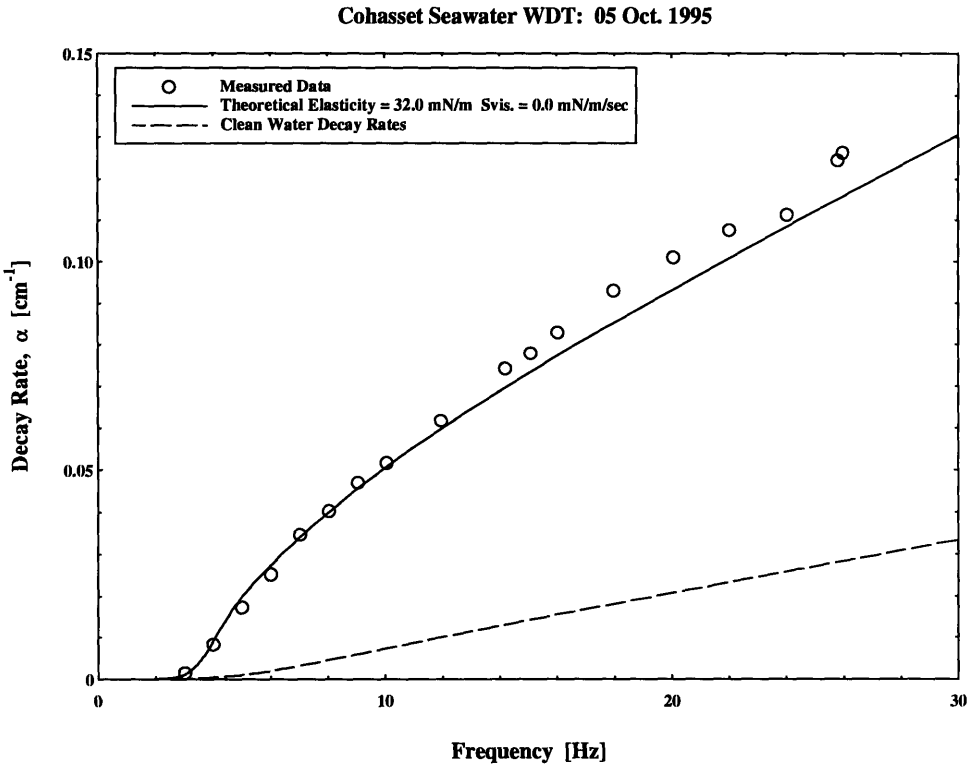

Figure 6.5 Transverse Wave Decay Rates: Cohasset Seawater $\gamma = 69.0\ mN / m$

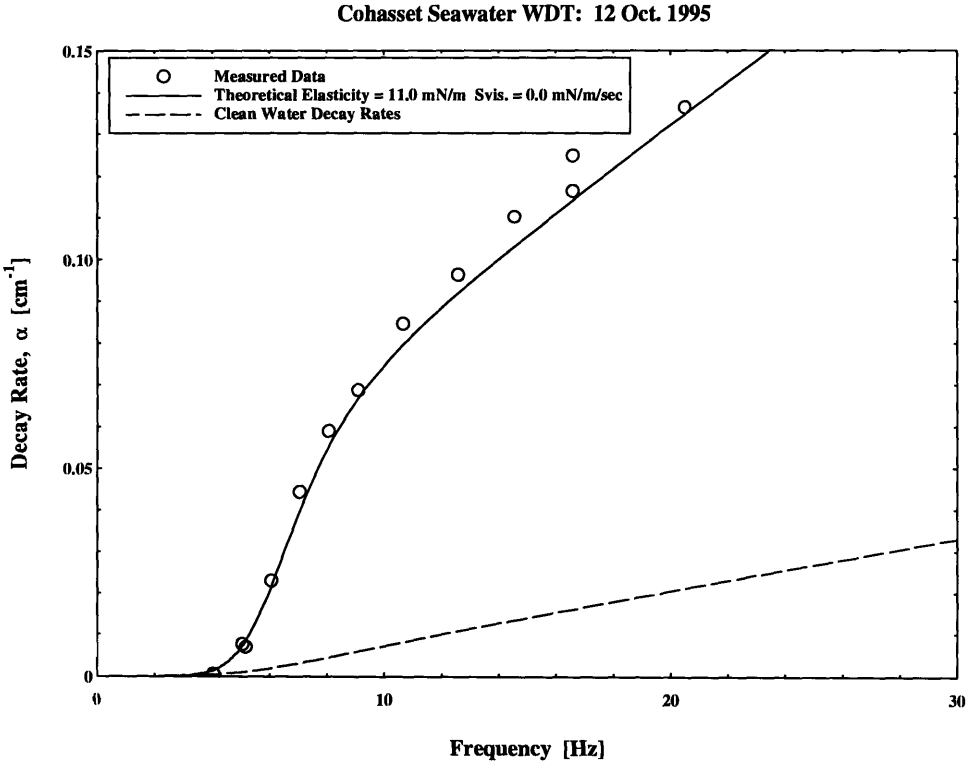

Figure 6.6 Transverse Wave Decay Rates: Cohasset Seawater $\gamma = 72.0\ mN / m$

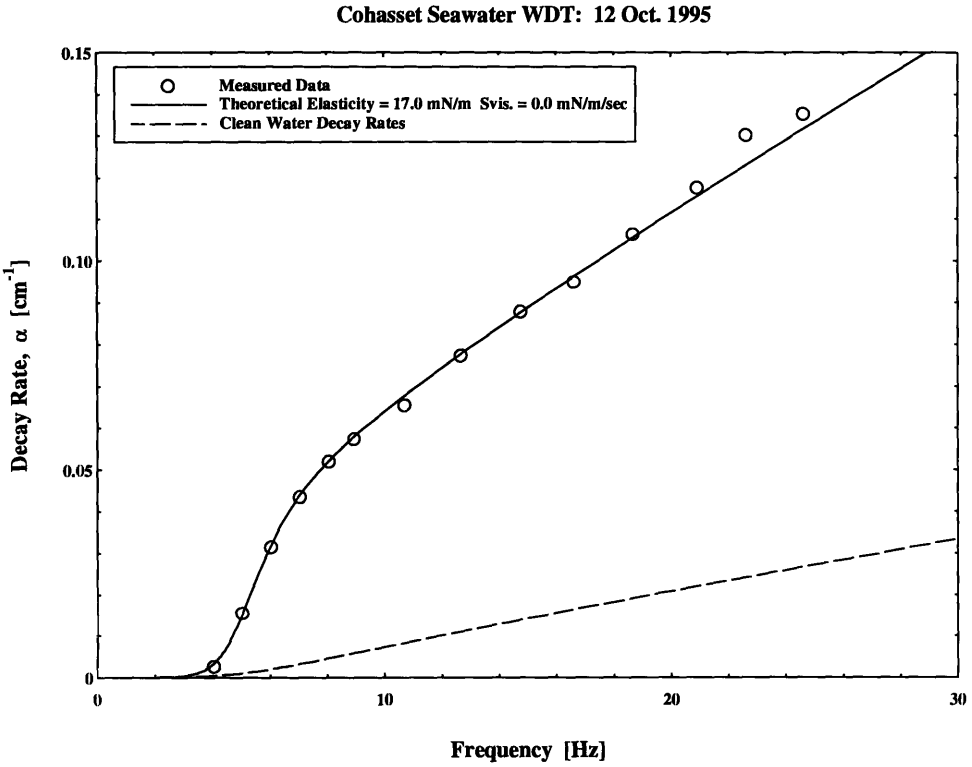

Figure 6.7 Transverse Wave Decay Rates: Cohasset Seawater $\gamma = 71.0\ mN / m$

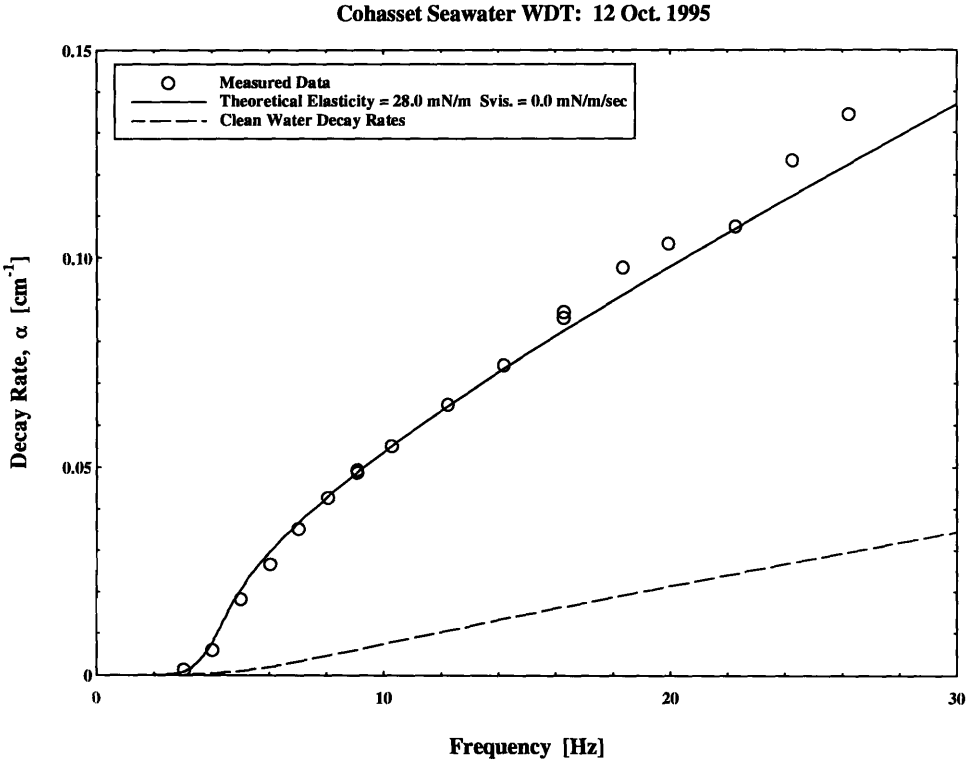

Figure 6.8 Transverse Wave Decay Rates: Cohasset Seawater $\gamma = 69.0\ mN / m$

6.4.2. Analysis of Woods Hole Seawater

Two water samples were collected from a salt pond on the south shore of Cape Cod fed by an inlet to Vineyard Sound. The first sample was collected from the inlet during ebb tide on the morning of November 18. Containers were lowered into the flow of the inlet taking care not to disturb the material on the bottom or banks. Water was transferred from collection containers to 50 liter containers allowing 400 liters to be transferred to the Marine Instrumentation Laboratory. Wave decay and variation in surface tension experiments were conducted on the evening of November 19.

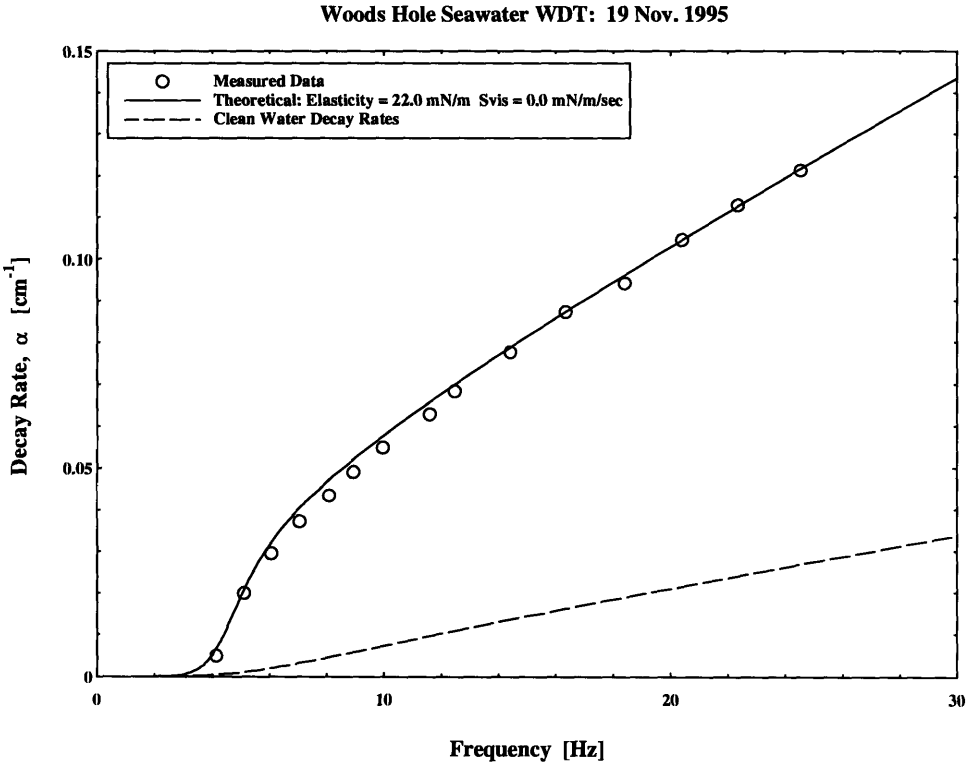

Figure 6.9 Transverse Wave Decay Rates: Woods Hole Seawater $\gamma = 70.0\ mN\ /\ m$

The second sample was collected from the salt pond, centrifuged and eluted into a methanol concentrate by Robert Nelson of the Woods Hole Oceanographic Institute. The concentrate was spread onto tap water that had been wiped clean. A micro pipette was used to spread ~ 2.0 *ml* of the concentrate on the Wave Decay Tank surface.

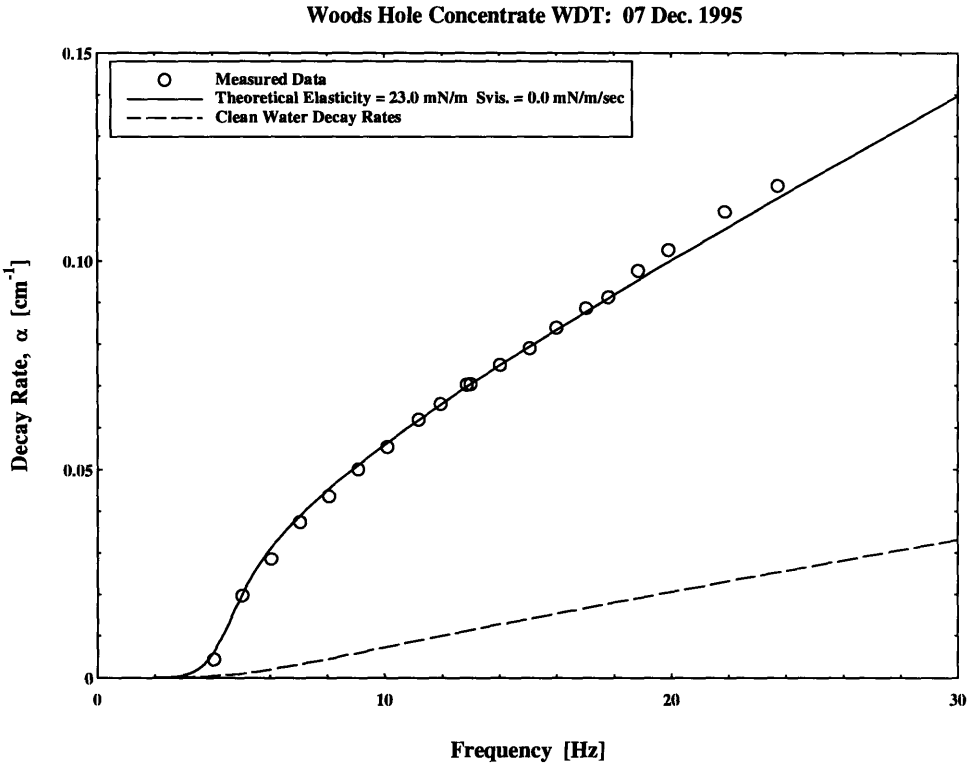

Figure 6.10 Transverse Wave Decay Rates: Woods Hole Concentrate $\gamma = 70.0\ mN / m$

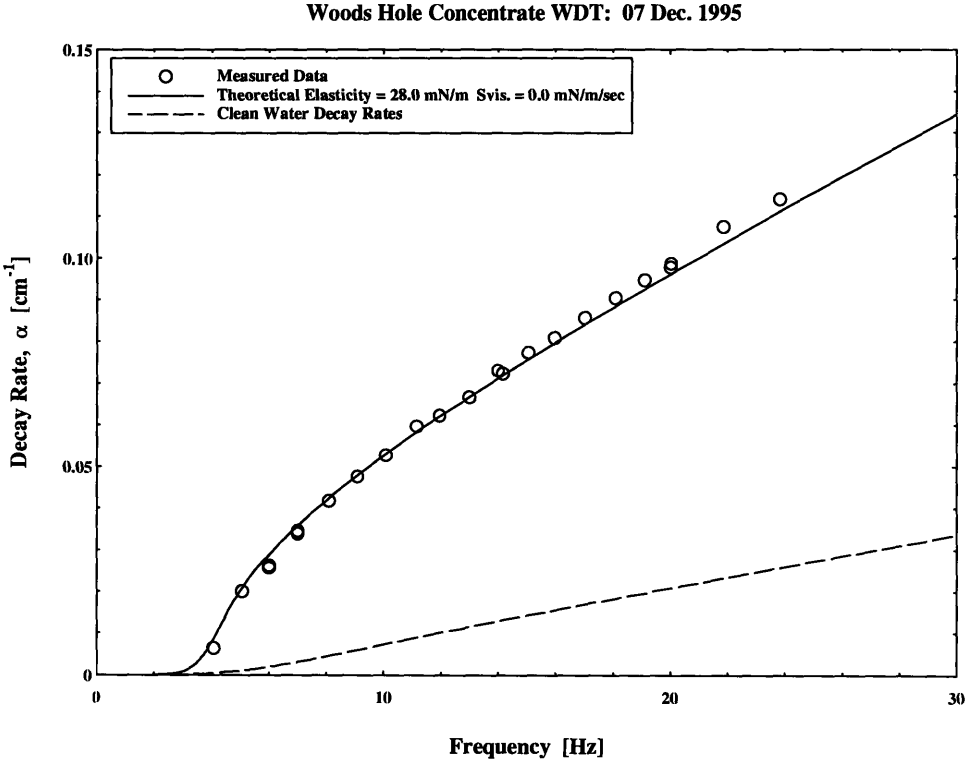

Figure 6.11 Transverse Wave Decay Rates: Woods Hole Concentrate $\gamma = 69.0\ mN / m$

6.5. Surface Viscosity Sensitivity Analysis

In an effort to quantify whether surface films posse surface viscosity several test cases were run through the wave decay modeling program for a constant elasticity. Surface viscosity values ranging from 0.0 mN/m/sec to 1.0 mN/m/sec were used. The model predicts a significant reduction in the magnitude of wave decay rates with surface viscosity values greater than 0.1 mN/m/sec.

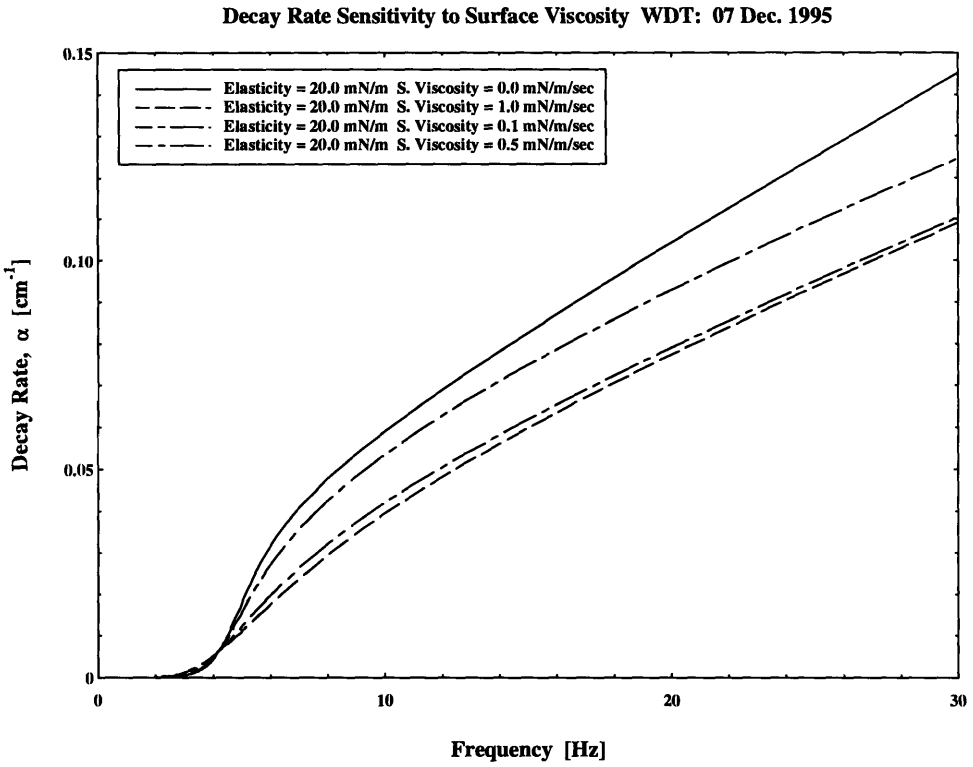

Figure 6.12 Variation in Decay rate due to Surface Viscosity

Examination of the experiential data with respect to surface viscosity reveals that surface viscosity is insignificant in the films we studied.

7. Variations in Quasi-Static Elasticity

Several experiments were performed to quantify the variations in elasticity associated with repeated compression. The first experiment tested a film known to be free of work hardening characteristics. The second experiment tested seawater from Little Harbor (Cohasset, Ma.) containing a natural film. The third experiment compared repeated compression of salt pond film (Woods Hole) and salt pond film concentrate spread on tap water (Woods Hole Concentrate). Films were compressed over a period of 15 minutes after which the film barrier was returned to it starting position. The film was allowed to expand for 5 to 10 minutes and the compressed again. Care was taken not to agitate or disturb the film during expansion. The sequence was repeated several times until the film ceased to harden.

7.1. Elastic Properties of Oleyl Alcohol

Oleyl alcohol, a film with known elastic properties that do not harden, was spread on distilled water and compressed repeatedly while measuring the pressure-area isotherm. Because oleyl alcohol is free of hardening characteristics, variations in elasticity illustrate the repeatability of the device. The compound was spread on distilled water in the Longitudinal Wave Trough (TR) forming a continuous monolayer sheet. Excess compound was trapped behind a movable film barrier and wiped to one end of the trough, See Figure 2.6. Molecules, now sparsely located on the area of interest, were compressed by slowly moving the film barrier in 1 cm increments compressing the film area from ~ 1000 cm^2 to 640 cm^2. The bar was stopped after each step giving the film time to stabilize before a data point was acquired. Repeatability was found to be on the order of ±2 mN/m. Quasi-static elasticity from repeated compression of oleyl alcohol is shown in figures 7.1 and 7.2.

7.2. Elastic Properties of Cohasset Seawater

During the evaluation of dynamic properties for films collected near Cohasset Ma. repeated pressure-area isotherms were measured. Samples were placed in the Wave Decay Tank (WDT) and left to stand ½ hour. Isotherms were calculated by compressing the film area from ~9000 cm^2 to 4000 cm^2 . The film barrier was moved in 5 cm increments allowing 15 seconds for the film to stabilize before a data point was collected. Repeated compression revealed the films harden, figures 7.3 and 7.4.

7.3. Elastic Properties of Woods Hole Seawater

To correlate our findings with other's work in the field [Bock & Frew,1993] we tested two samples of collected water from a salt pond near Woods Hole. The first sample was collected in 50 liter Nygalene jugs and tested in the Wave Decay Tank within 24 hours of collection. The second sample consisted of condensed surfactant extracted from seawater using a centrifuge and methanol process [Frew & Nelson, 1992]. The condensed surfactant was spread on tap water that had been wiped clean. The elastic property of the spread film was similar to those with a film adsorbed on the surface from natural surfactants in it.

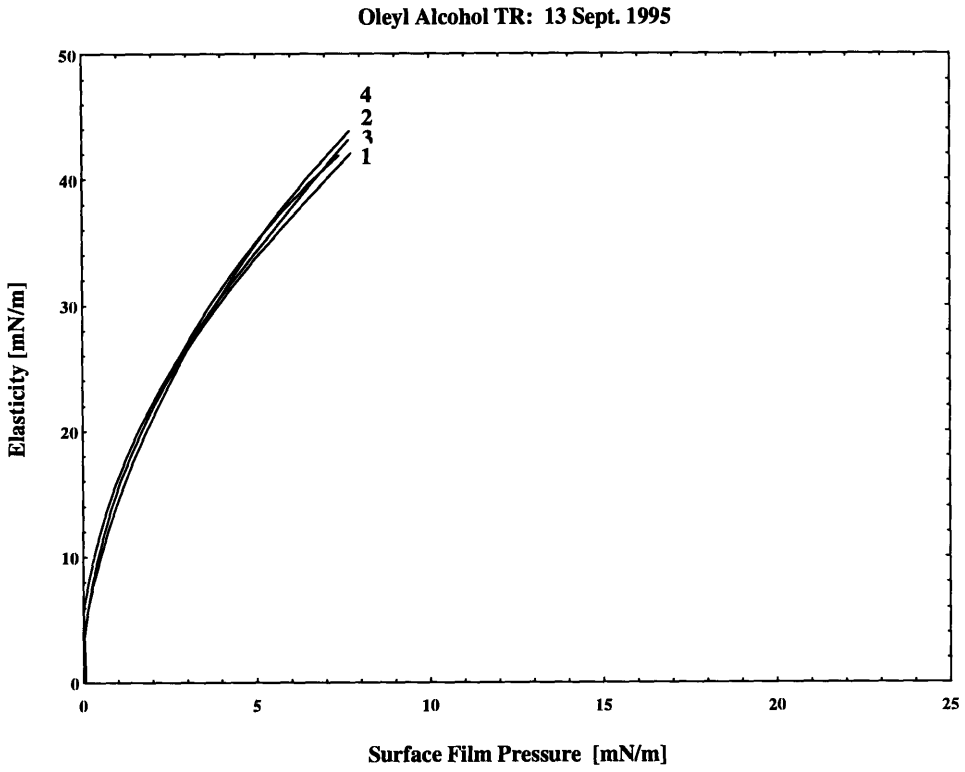

Figure 7.1 Elastic Properties of Oleyl Alcohol: I

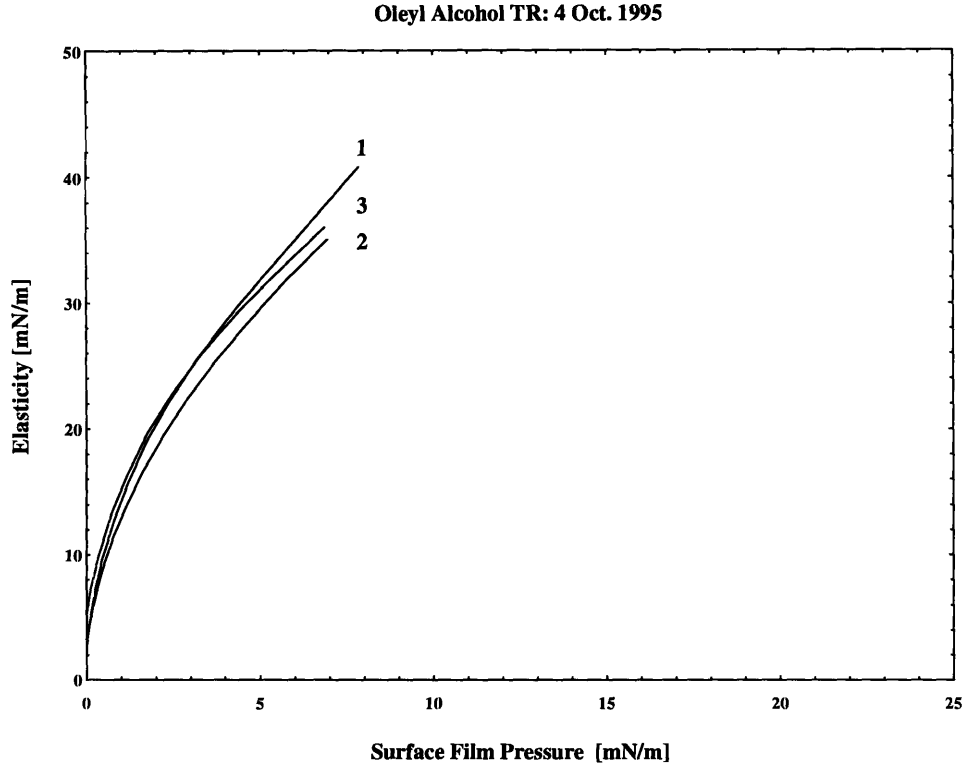

Figure 7.2 Elastic Properties of Oleyl Alcohol: II

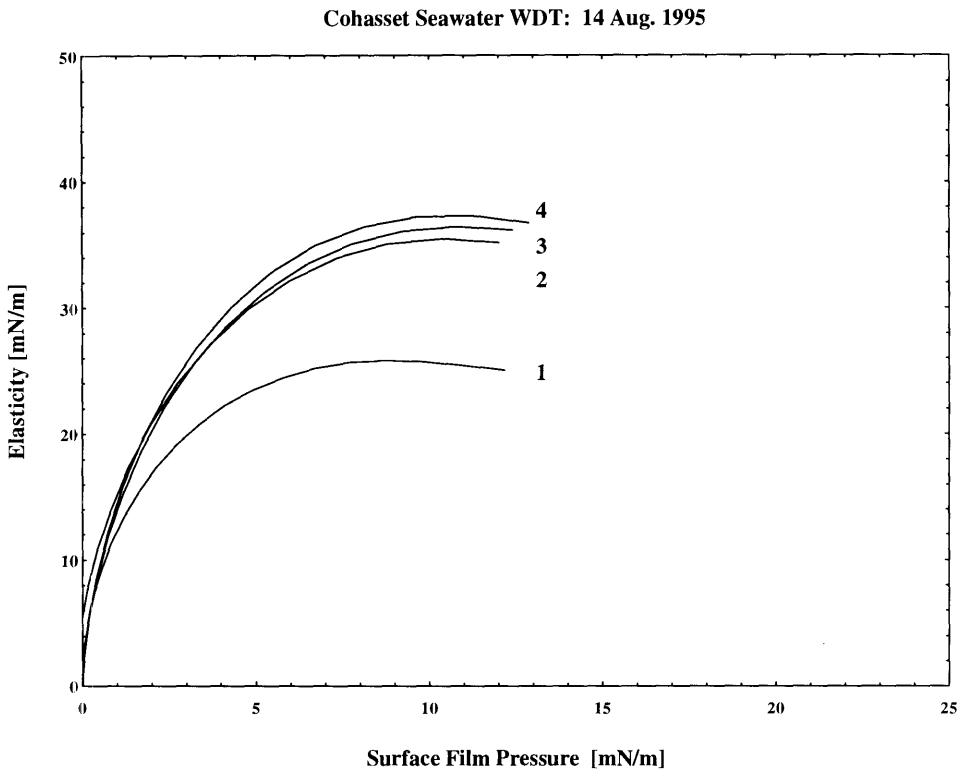

Figure 7.3 Elastic Properties of Cohasset Seawater: I

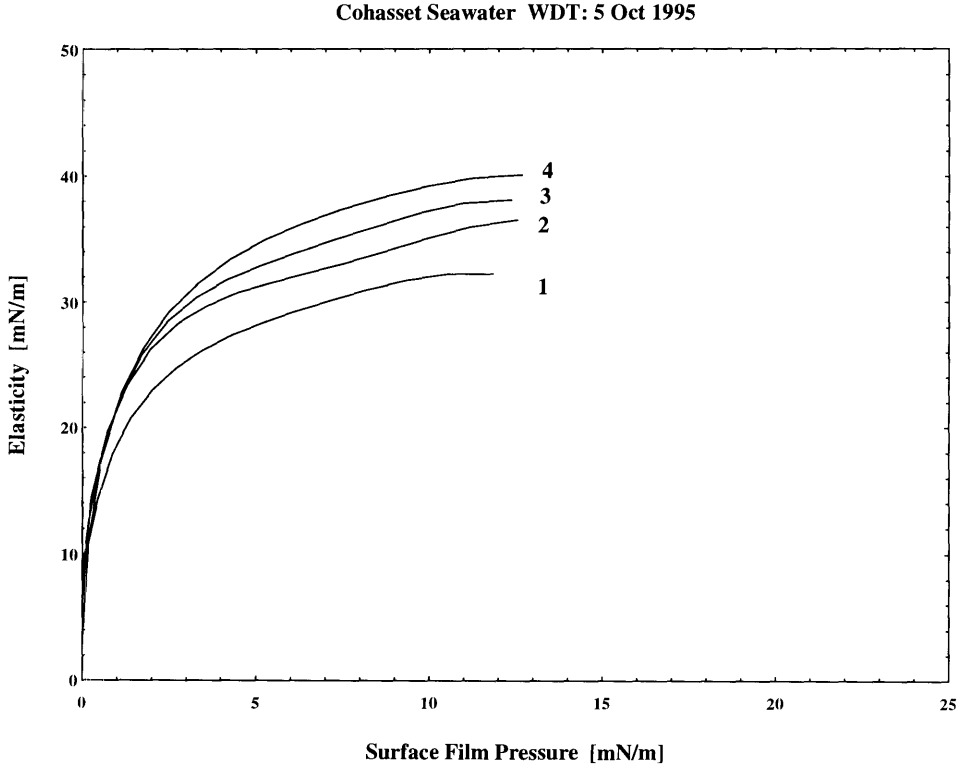

Figure 7.4 Elastic Properties of Cohasset Seawater: II

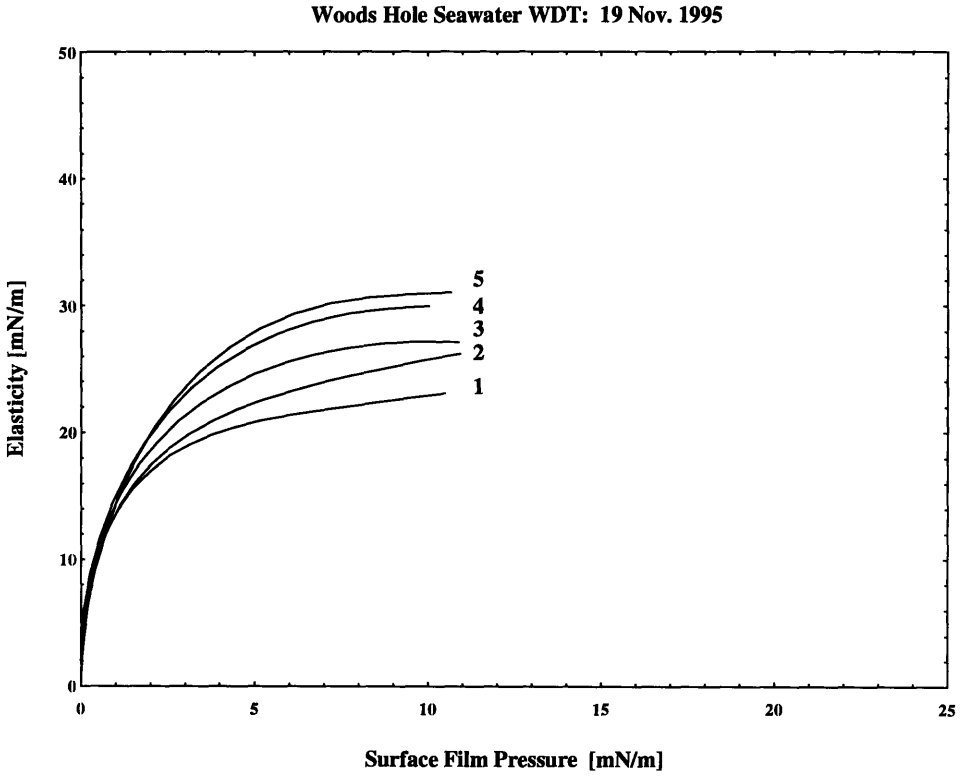

Figure 7.5 Elastic Properties of Woods Hole Seawater

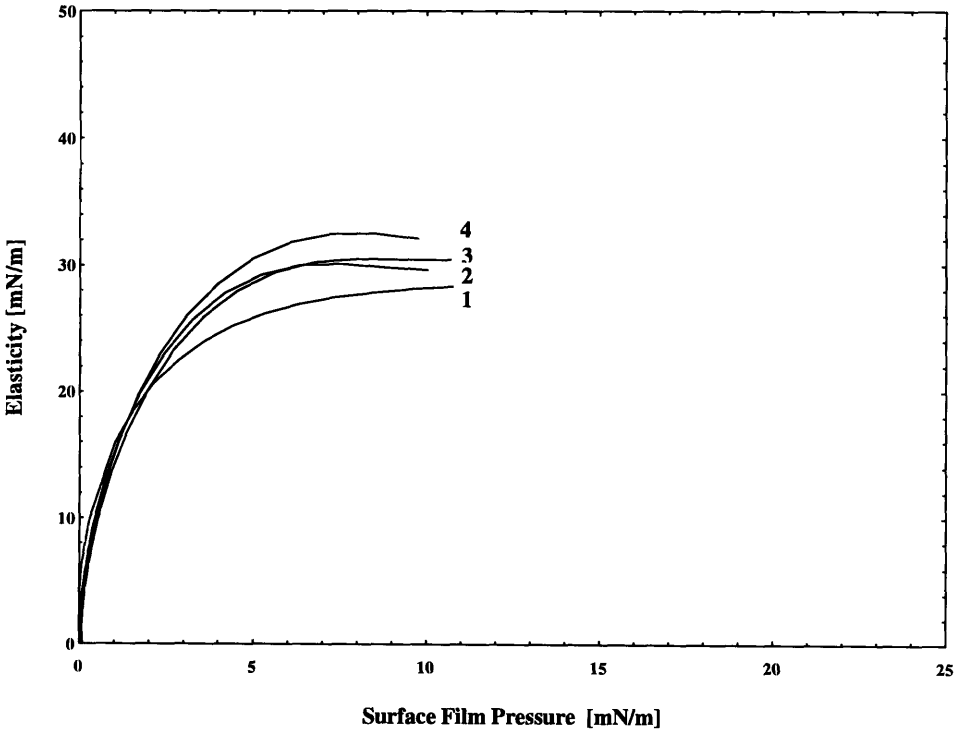

Figure 7.6 Elastic Properties of Woods Hole Concentrate

Sources of error in the determination of the quasi-static elasticity include; contamination, leakage, function fit error and measurement error. Due to the difficulty in quantifying contamination and leakage errors, isotherms were measured in two different tanks with different barrier types. Furthermore, isotherm measurements were repeated several times to provide a statistical basis to the elasticity curves. Given a stable surfactant, the repeated isotherms provided elasticity values with a variance of $\pm 2\ mN/m$. Prior to all measurements the Wilhelmy Plate was washed in tap water and flame cleaned with a butane torch.

8. Conclusions and Recommendations

8.1. Quasi-Static Elastic Properties of Natural Films

Large scale dilations were found to alter the quasi-static elastic properties of naturally occurring films. The altered characteristics, referred to as "work hardening", result in an increased elasticity (~40%) per unit change in film pressure after repeated large scale compression of the film area. Applied to the open ocean, films forming with nearly uniform film pressures can contain large differences in elastic properties. The difference in elasticity will create variation in capillary wave decay. Ships passing through such a film could conceivably leave a work hardened film bands on the edges of their wakes.

8.2. Dynamic Behavior

In the naturally occurring films studied the elastic properties were found to predict dynamic behavior for distortion frequencies ranging up to 25 Hz. The elastic properties used in the predictions were free from frequency dependence and surface viscosity. The dynamic properties were predictable from the quasi-static elasticity.

Correct measurement of the elastic properties is crucial. The fact that natural films tend to harden with repeated compression makes choosing the correct quasi-static elasticity difficult. Measuring pressure-area isotherms before and after dynamic testing and closely monitoring film pressure during dynamic testing is important if accurate elastic properties are to be used.

In the future new methods of measuring film pressure should be explored. One method, monitoring film pressure with a surface potential probe, could improve the measurement of film pressure. The process measures the voltage potential of the surface film which can be related to surface pressure. Measuring film pressure via surface potential is less intrusive than the Wilhelmy Plate method because it does not pierce the surface. Furthermore, due to the fact the probe can be smaller, potential probes do not average measurements over as large an area producing faster response times. The reduced reaction time may provide insight into whether films can harden from repeated small scale dilations and compressions.

8.3. Future Experiments

Future experiments can be broken down into two categories. The first involves improved understanding of the mechanisms at work in hardening the elasticity of natural films. Experiments should concentrate on determining the relaxation time of hardened films and to what extent mixing and turbulence returns the film to an non-hardened state. From a chemical point of view is the chemical composition of the monolayer changing during hardening.

The second category involves dynamic understanding of hardened films. It would be beneficial to determine if areas of differing elasticity can coexist in natural films and if so what is the dissipation time of the hardened portion. The static dissipation should be compared to dissipation times for a composite film in the presence of transverse waves. A composite film could be constructed consisting of patches of film at various elasticities in the Wave Decay Tank. Monitoring transverse wave decay through the various patches over a period of time would provide a means to determine dissipation time.

Appendix A. Longitudinal Wave Trough Apparatus[1]

The apparatus built to measure variations in surface tension due to dilation of the surface film by longitudinal waves, consists of several components. A computer controlled motion table moves the film barrier; compressing the film during quasi-static elasticity measurements and oscillated the barrier making longitudinal waves during dynamic surface tension tests. An electromechanical shaker drives a plunger type wavemaker generating transverse waves. A laser and laser beam position sensing detector measure transverse wave slopes. An electronic balance and Wilhelmy Plate serve two purposes. First, the balance and plate measure pressure-area isotherms to determine quasi-static elasticity properties. Second, they monitor film pressure during dynamic tests. Finally, great care is taken to mount components in a manner that allows the different aspects of the experiment to take place without disruption, minimize vibrations and maximize accessibility for cleaning. The design and construction of the apparatus is broken down into six groups based on functionality.

1. Wave Trough
2. Longitudinal Wavemaker and Film Barrier Motion
3. Transverse Wavemaker
4. Laser Slope Gauge
5. Measurement of Elastic Properties
6. Data Acquisition & Analysis for Variations in Surface tension

Figure A.1 shows a sketch of the apparatus components used to perform the variation in surface tension experiments.

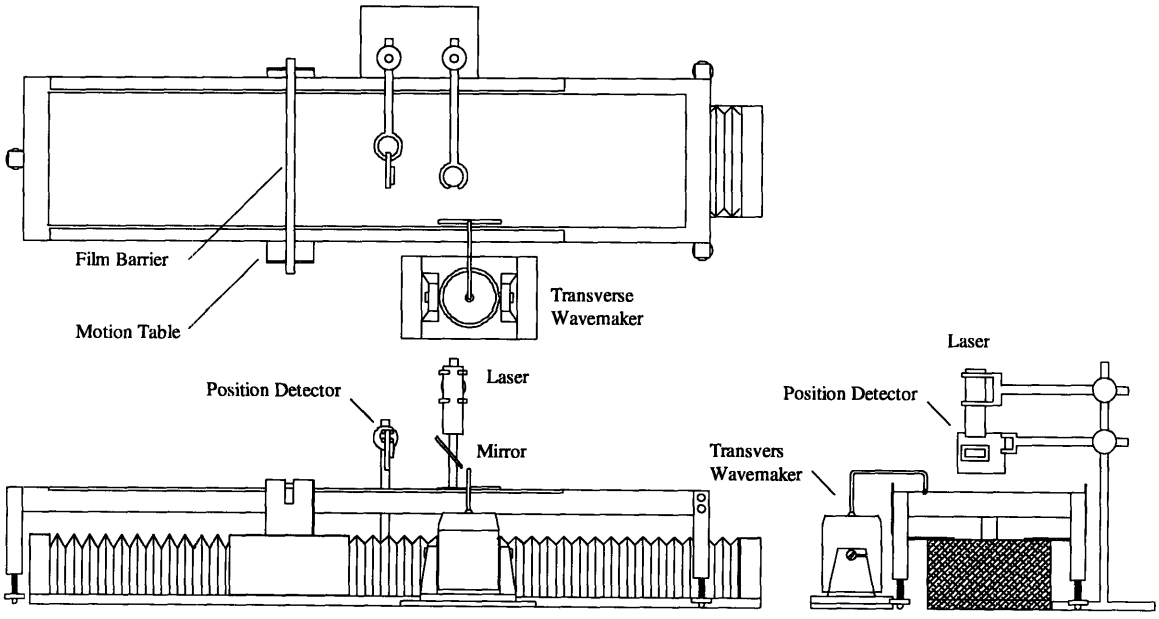

Figure A.1 Sketch of Longitudinal Wave Trough

[1] Portions of Appendix A.1, A.7 and A.9 first appeared in an independent studies report on Development of a Computer Phase Angle Meter to Track Variations in Surface Tension. The report is unpublished.

Missing from figure A.1 is the electronic balance that measures the force on the Wilhelmy Plate during the measurement of pressure-area isotherms. The force is used to determine quasi-static elasticity. Following is a brief discussion of the design and construction of each component.

Appendix A.1. Dynamic Measurement of Variations in Surface Tension

Equations 2.22 and 2.23 give the theoretical variation in surface tension, due to dilation of the surface film area, for a film covered surface. The electronic balance that measures surface tension quasi-statically with a Wilhelmy Plate does not have a high enough frequency response for dynamic measurements. Furthermore, due to the fact that the Wilhelmy Plate penetrates the film, the plate is film intrusive making it unsuitable for dynamic measurements. Sohl, Miyano and Ketterson [1978] propose a technique using high frequency transverse waves and laser reflections to measure variations in surface tension. We developed an apparatus using a similar approach coupled with a longitudinal wavemaker and computer interfaced phase measurement to determine time-varying variations in surface tension over a range of longitudinal wave frequencies, 0.5 - 4.0 Hz.

Frequency is conserved in the dispersion relationship. In the case of capillary waves, changes in surface tension are offset inversely by changes in the wavenumber until the same frequency is reached. The dispersion relationship for gravity-capillary waves is given in the simplified form by equation 2.5.

$$\omega^2 = g\bar{k} + \frac{\gamma \bar{k}^3}{\rho} \tag{2.5}$$

If the wavenumber, k, is large enough the gravitational influenced in the dispersion relationship is much less than the surface tension influence and can be neglected. Conservation of frequency dictates that any changes surface tension will be offset by changes in wavenumber. Surface tension measurements are reduced to measuring changes in wavenumber.

One method of measuring changes in wavenumber is to track the number of waves separating two wave gauges. When two wave gauges are held in a fixed position any change in the number of the waves separating the gauges will produce a change in the phase angle between the two gauges.

Reviewing wave theory, a two dimensional transverse wave field with waves progressing in the x direction will have vertical displacements given by equation 2.1.

$$\zeta = \zeta_0 e^{i(\bar{k}x - \omega t)} \tag{2.1}$$

Comparing the elevations of two probes placed in the fluid; one near the transverse (capillary) wavemaker, $x \approx 0$, and another at a fixed distance, $x = l$, the difference in elevation will be given by:

$$\partial\zeta = \frac{\zeta_2}{\zeta_1} = \frac{\zeta_0 e^{i(\bar{k}l-\omega t)}}{\zeta_0 e^{-i\omega t}} \tag{A.1}$$

Which simplifies to:

$$\partial\zeta = e^{i\bar{k}l} \tag{A.2}$$

The percentage decrease in elevation is then:

$$\partial\zeta = e^{-\alpha l}\cos(kl) \tag{A.3}$$

The imaginary portion of the wave number becomes the decay rate, α, while the wavenumber-separation distance combination, kl, represents an angular phase shift. The fixed separation distance, l, and the dispersion relationship dictates that changes in the phase between the two signals represents a change in wavenumber.

When the separation distance, l, is fixed the number of capillary waves, N, separating the gauges is given by:

$$N = \frac{l}{\lambda_o} = \frac{k_o l}{2\pi} = \frac{l\omega^{2/3}\rho^{1/3}}{2\pi\gamma_o^{1/3}} \tag{A.4}$$

Any change in wavenumber represents a change in the number of waves separating the gauges changing. The new number of waves separating the gauges is given by:

$$N_{new} = N_{old} + \frac{\partial\theta}{2\pi} \tag{A.5}$$

Combining the two equations and simplifying, one gets an equation for the new surface tension based on the old surface tension, wavenumber, separation distance and change in phase.

$$\gamma_{new} = \gamma_o\left[\frac{kl}{kl+\partial\theta}\right]^3 \tag{A.6}$$

The situation can be further simplified by removing the wave gauge near the transverse wavemaker and monitoring the phase relationship between the wavemaker and wave gauge. The method can only measure changes in surface tension and requires the measurement of a starting surface tension by another device such as a Wilhelmy Plate.

The variations in surface tension are generated by longitudinal waves propagating on a film covered surface and measured by capillary waves. The approach results in two wave fields

being present. The longitudinal waves propagating in the x direction are two dimensional and variations in surface tension are independent of location across the tank, y. The transverse wave field propagates in the y direction, orthogonal to the longitudinal waves. Due to the orthogonal orientation the surface tension between the wave gauge and transverse wavemaker varies with time as the longitudinal waves pass but is constant at any instant in time. In other words, the variations in surface tension in the trough are dependent on time and location in x; the transverse wave propagates waves in the y direction.

Note, the transverse waves mentioned above are transverse in two senses of the word. The waves have vertical particle displacements of the same magnitude as their horizontal particle displacements in which case they are transverse waves as mentioned in chapter 2, and, they are propagating across the longitudinal waves and trough.

Appendix A.2. Design and Construction of the Longitudinal Wave Tank

A 'Langamuir' trough was milled out of aluminum and hard coated using the anodization process. Three legs with leveling screws provide trough support, height adjustment, and leveling. The fluid cavity measures 80 cm long, 16.7 cm wide and 2.5 cm deep. The trough fluid volume is 3340 cm^3 with an air-water interfacial area of 1336 cm^2. During use, the trough is coated with a thin layer of paraffin. The coating facilitates cleaning and prevents film leakage in the region where the longitudinal wavemaker seals with the trough. Several experiments were carried out to ensure the coating did not alter film characteristics. Experiments showed no difference in results with and without the paraffin coating.

Appendix A.3. Longitudinal Wavemaker and Film Barrier Motion.

The longitudinal waves are generated by oscillating a film barrier at a desired frequency and amplitude. The barrier consists of a 6 mm square acrylic bar that spans across the trough. The bar rests on the trough walls and is attached to the linear motion table with two sets of elastic straps. The first set of straps exerts a downward force, ensuring the bar does not ride off the trough. The second set of straps exerts a force transversely keeping the bar in contact with the motion table supports.

The point of contact between the barrier and trough is very susceptible to leakage. The straps ensure the barrier is held firmly against the motion table supports with a constant downward pressure on the table. The latter is necessary to prevent film leakage around the barrier. If the barrier does not seal with the trough walls, the film pressure gradient that exists from one side of the barrier to the other causes the surface film to flow under the barrier. The escaping surface film reduces the film concentration resulting in a drop in film pressure. The seal must remain intact as the barrier slides on the trough during pressure-area isotherms and dynamic measurements, however, to much downward pressure causes the barrier to vibrate creating waves. To reduce friction, the edges of the trough were coated with paraffin and the acrylic bar was milled flat. The elastic straps, paraffin and milled bar resulted in a barrier that did not leak and moved without vibration.

The motion table moves the barrier during pressure-area isotherms and dynamic testing where longitudinal waves are needed. The motion table, purchased from DCI Inc., contains

a set of precision ground rails, linear bearings, and lead screw to control position. Table position and velocity are controlled by a pulse width modulated DC servo motor, model TO3L-QU11 manufactured by YASKAWA, and motion controller, model 5A5 manufactured by ADVANCED MOTION CONTROLS. Motor and controller are interfaced with a personal computer using hardware manufactured by OMNITECH ROBOTICS, model MC-1000S. A computer program, written by the author, controls table position and velocities while collecting data.

It can be difficult getting a linear motion table to oscillate in a sinusoid. The author achieved this by using velocity control with position feedback. Sinusoidal velocity and position profiles are calculated and stored in an array. The motor is velocity controlled with position feedback. The motor position is compared to theoretical position and velocity was adjusted accordingly. The result is a velocity profile dependent on location instead of time. Period (frequency) is adjusted by varying the magnitude of the distance the bar travels. Through the use of clockwise and counterclockwise velocity calibration the table motions compare favorably with sinusoidal input data.

The longitudinal wavemaker is able to generate longitudinal waves with frequencies up to 4 Hz. When attempts were made to generate longitudinal waves with frequencies above 4 Hz the barrier began generating both longitudinal and transverse waves propagating along the tank. The latter produced an unacceptable vertical displacement that interfered with the capillary waves propagating across the trough and pushed the reflected light beam off the position sensing device.

Appendix A.4. Transverse Wavemaker.

Transverse waves, used in the dynamic measurement of surface tension, are generated using a function generator, audio amplifier, shaker and Teflon wedge. The function generator produces a 200 Hz square wave. The audio amplifier increases the power of the signal. The shaker, model number V203 manufactured by LDI Ltd., transform the electrical signal into linear motions oscillating the Teflon wedge. The wedge, in contact with the air-water interface, produces a two dimensional wave field propagating across the trough.

Several wavemakers were tried and discarded before choosing the Teflon wedge. Metal wavemaker disturb the electrical potential of the surface film [*Adamson 1976* and *Barger, 1985*] and acrylic proved too fragile when trying to machine the small wedge. Teflon samples were tested to ensure they did not alter properties of the films. The tests showed that Teflon did not affect the film properties.

Appendix A.5. Laser Slope Gauge.

Once longitudinal and transverse wave fields are established, transverse waves induce variations in surface slope that are measured using a laser slope gauge. Traditional wave gauges use wires that pierce the surface to measure variations in amplitude; but, they lack resolution and frequency response when measuring high frequency surface waves. Furthermore, by piercing the surface the wires run the risk of disturbing both wave fields and the integrity of the surface film. An alternative to wire wave gauges, a laser slope

gauge provides a non-intrusive means to collect transverse wave slopes. The variation in slope is proportional to variations in amplitude with a 90° phase shift.

The laser slope gauge measures variations in location of a light beam reflecting off the air-water interface. The laser is positioned with the light beam shining directly down on the surface of the water. When the light beam passes through the free surface a portion of the beam reflects back into the incident beam. A mirror directs the reflected portion of the laser beam onto a laser beam position detector. Vertical surface displacements, generated from the transverse wavemaker, create variations in the surface slope. The variations in slope alter the angle of incidence and reflectance of the light beam (*The Law of Reflection).* The altering angle of reflection results in an oscillation of the reflected beam location. The displacement of the reflected beam location is measured by a position detector; see figure A.1.

The laser slope gauge consists of a laser beam generator, mirror and beam position detection device. The incident beam has a wavelength of 670 nm; produced by a 19 mw diode laser. The laser is manufactured by LASERMAX Inc. The laser is equipped with a cylindrical lens producing a beam with a diameter of 1mm. (In one experiment the laser was fitted with a 5 degree line generator. The laser line was oriented orthogonal to the propagation direction of the transverse waves. The reflected beam produced an oscillating laser line on the position detector.) The beam passes through the back side of a first face mirror onto the air-water interface. The mirror allows the downward light to pass through and redirects the reflected beam onto the laser beam position detector.

The position sensing detector, model IL-10SP manufactured by SiTek, is a p-n semiconductor with one anode and two cathodes. The anode is connected to ground. The cathodes are located on opposite ends of the p-n material and biased with constant voltage. When the p-n material is excited by incoming light, resistance changes across the p-n junction altered the current flow through each cathode. Comparing the current flow through each cathode one can locate the point of excitation on the p-n material, i.e. equal current flow the beam is centered on the p-n material.

Companion circuitry, model OT-300 manufactured by On-Trak Photonics, converts changes in current flow into voltage changes; then compares the relative values at each cathode and outputs a signal, -10 *v* to 10 *v* ,that is a function of beam position.

Building vibrations create waves on the air-water interface that need to be filtered out of the slope measurements. Persons walking in the lab and vehicle traffic on the adjacent street produce vibrations in the building. The vibrations produce waves in the trough, which in turn, are measured by the laser slope gauge. The vibration frequencies were typically less than 5 Hz. The magnitudes of the slope variations are on the same order of magnitude as the transverse waves. From a signal processing point of view, the slope variations due to building vibration are "noise" in the laser slope signal. The large difference in frequencies allows the use of active signal processing to remove the "noise". The output signal from the OT-300 is bandpass filtered using a 4 channel high and low pass Butterworth filter with

adjustable gain. The filter, model 3384, is manufactured by Krohn-Hite. Values of 190 Hz and 210 Hz are chosen for high and low cutoff frequencies respectively. A typical amplitude gain value of 20 dB is used to increase signal strength.

In summary, the laser slope gauge converts variations in surface slope into an electrical signal. The phase angle of the slope signal is compared to the signal driving the transverse wavemaker. Variations in phase angle reflect changes in the number of waves between the wavemaker and the point where the laser beam reflects off the air-water interface; see equation A.5. Furthermore, the variations in phase angle are converted to variations in surface tension; see equation A.6.

The position of the laser slope gauge with respect to the transverse wavemaker and the frequency of the transverse wavemaker are dictated by fluid properties, resolution of the laser slope gauge and phase calculation software. A separation distance of 6 cm is used due to the high decay rates of capillary waves on surfactant covered surfaces. The frequency of the wavemaker is 200 Hz due to sampling limits of the analog to digital board.

Several confidence tests showed the transverse wave-laser slope gauge to be an excellent method of measuring variations in surface tension; see section A.9 *Confidence Testing Phase Measurement of Surface Tension* and figure A.4.

Appendix A.6. Measurement of Elastic Properties .

Section 2.2 covers the principles that govern the elastic properties of a surface film. The practical aspect of determining the elastic properties requires compression of the surface film, measurement of surface area and surface tension, curve fitting and differential analysis.

Several programs carry out the tasks. The main program *TABLE* has several operating modes. One of which, Quasi-Static data collection, moves the film barrier in step increments waits for the film to stabilize then collects a surface tension measurement via the electronic force balance and Wilhelmy Plate. The user is required to input start and stop locations, step size and transition speed. The program writes area and force to a file. The program *STCOMP* converts the force measurements into surface tension using equation 2.26. The program *QS_FIT* analyzes the pressure-area isotherm to determine the pressure-elasticity relationship. The program *QS_FIT* finds the coefficients of a 5^{th} order polynomial having a minimum mean squared error relative to the pressure-area data, and calculates the first derivative with respect to film pressure.

Appendix A.7. Phase Measurement between Laser Slope Gauge and Wavemaker.

The angular phase shift between two signals, excited at the same frequency, can be resolved in two ways, spectrally or directly. The spectral method translates the time domain data to the frequency domain through the use of Fourier transforms, yielding magnitude and phase for each signal. The direct method compares signal attributes in the time domain, namely time lag or lead between zero crossings. The direct method is used to determine the angular phase relationship between the laser slope gauge and transverse wavemaker signals.

Measuring variations in surface tension created by longitudinal waves requires discrete sampling of surface tension several times per longitudinal wave period *vis a vis* changes in the phase relationship between the transverse wavemaker signal and laser slope gauge signal. Two computers control the film barrier position and acquire data. The first computer uses a subroutine in the computer program *Table* to control the motion table generating longitudinal waves, export the film barrier location and gate data collection on the second computer. The computer uses an analog to digital converter, model DAS-16G, manufactured by Metrabyte to trigger data collection on the second computer and export the film barrier position. The trigger consists of a 40 Hz square wave. The square wave starts when the film barrier begins to oscillate.

On the leading edge of every square wave, the second computer collects film barrier position, transverse wave and laser slope gauge signals to determine the phase angle between the transverse wavemaker and laser slope gauge. A sample hold technique measures phase changes in the transverse wavemaker and laser slope gauge signals. The second computer is equipped with an analog to digital converter, model CIO-DAS1600 manufactured by Computer Boards. The program *SPR2* measures changes in phase angle between the signals. It uses a three step process consisting of wait for trigger, collect film barrier and signals, and calculate phase angle. After phase angle collection, the program returns to wait mode repeating the cycle at 40 Hz until the required number of data points have been collected. During the second step, the second computer collects one data point recording the film barrier position and 1300 samples of the wavemaker and laser slope signals. The latter samples are recorded at 125 K bytes/second resulting in 650 samples in 0.010 seconds. The transverse waves, generated at a frequency of 200 Hz, have a period of 0.005 seconds resulting two cycles of data sampled at 325 samples per cycle. After collecting 1300 samples, the program enters the third step and calculates the phase relationship between the wavemaker and laser slope gauge signals by finding the time difference in upward zero crossings of the signals. The film barrier position and phase angle are written to a file and the program enters wait mode until the next gate signal.

Time to calculate the phase relationship between the two signals and write it to a file becomes a limiting factor in the trigger speed and therefore the sampling rate of variations in surface tension. A 25 MHz 486 computer is used to sample and calculate phase angles. Using integer calculations to calculate phase the program was able to calculate the phase relationship and write it to a file in 0.017 seconds. The trigger time was set at 0.025 seconds resulting in 0.008 seconds of wait between phase angle calculations.

Appendix A.8. Data Acquisition and Analysis Programs.

Several programs acquire phase data, convert it to surface tension data and compare it to theoretical predictions. Following is a brief description of each program.

Appendix A.8.1. SPR2: Data acquisition.

The program *SPR2* acquires transverse wavemaker and laser data, calculates the phase relationship, acquires longitudinal wavemaker position, and writes longitudinal wavemaker position and phase data to a file. Upon execution the program reads an input file, *SPR2.IN*,

containing the distance separating the longitudinal wavemaker and the reflecting wall, distance separating the longitudinal wavemaker and the laser slope gauge, distance separating the transverse wavemaker and the laser slope gauge, frequency of the transverse wavemaker, static surface tension, and quasi-static elasticity and viscosity. The program then collects 16 seconds of phase data using the sample hold technique described in section A.7, estimates the frequency of the variation in phase angles using zero crossings and writes the data file *ST.DAT*. Finally, the program performs several system calls executing the data analysis programs.

Appendix A.8.2. MWAVE6: Theoretical Variations in Surface Tension

The first program executed from *SPR2* reads the header information in *ST.DAT* containing fluid and trough information and calculates the theoretical variation in surface tension and phase relationship between the longitudinal wavemaker and a point on the fluid where the laser slope gauge was located. The equations 2.10 and 2.22 are used to calculate the magnitude and phase of variations in surface tension. The program rewrites *ST.DAT* including the theoretical information in the in the header and returns computer control to *SPR2*.

Appendix A.8.3. ST2: Conversion of Phase Data to Surface Tension Data

ST2, the second program executed as a function call in *SPR2*, reads the header and phase information in *ST.DAT* and uses equation A.6 to convert the phase data into variations in surface tension. The program also calculates discrete values for the theoretical variations in surface tension using equation 2.23 and theoretical values calculated by *MWAVE6*. Finally, *ST2* writes; time, bar position, theoretical bar position, theoretical surface tension and measured surface tension into the output file *ST.OUT* for the 16 seconds of data.

Appendix A.8.4. STFIL: Low Pass Filtering Surface Tension Data

Comparison of measured variation in surface tension to theoretical calculation is done in both the frequency and time domains by *STFIL* and *STAMP2* respectively. *STFIL* uses a Fast Fourier Transform on 512 data points (12.8 seconds of data) converting the measured and theoretical surface tension data to the frequency domain. Magnitude and phase are then compared at the fundamental frequency. Magnitudes are normalized by dividing the magnitude by longitudinal wavemaker amplitude. Normalized theoretical and measured amplitude and phase were then written to the output file *ST.ERR*.

In an effort to "clean up" the data for time domain comparisons of measured time varying surface tension vs. theory, the measured data is low pass filtered by setting Fourier coefficients with frequencies greater than 2.5 times the fundamental equal to zero and inverse transforming the frequency domain data back to the time domain. The filtered data is written to the output file *STFIL.OUT*.

Appendix A.8.5. STAMP2: Surface Tension Magnitude and Phase Data

The program *STAMP2* computes the amplitude and phase of the filtered surface tension data in the time domain. Time domain comparison of measured verse theoretical magnitude of variations in surface tension is accomplished by calculating average maximum and

minimums of the filtered data and theoretical predictions. The amplitude of variations in surface tension are calculated by subtracting the average minimum from the average maximum and dividing by two. The amplitudes were normalized through division by longitudinal wavemaker amplitude.

The time domain phase relationship is calculated by subtracting the signal mean and determining the starting phase needed to satisfy each upward zero crossing. The starting phases were then averaged to determine a mean starting phase. Normalized amplitude and average starting phase for both theoretical and measured data are written to the output file *ST2.ERR*. Figure A.2 gives a summary of the data collection programs, analysis programs and data files. Typically the **.DAT* and **.ERR* files were saved for each experiment.

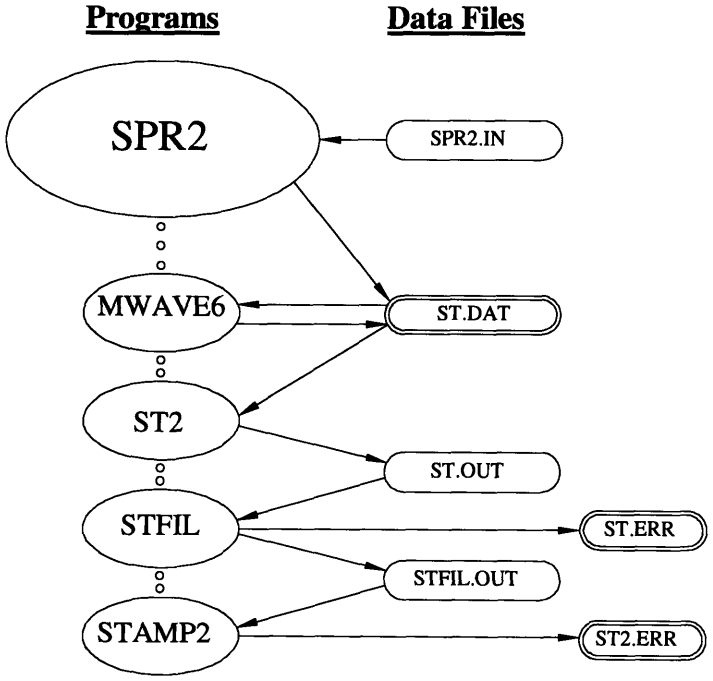

Figure A.2 Programs and Data Files

Appendix A.9. Confidence Testing for Phase Measurement of Surface Tension.

The Phase Measurement of Surface Tension method was tested by comparing variations in surface tension measured during a pressure-area isotherm. The variations were measured by monitoring changes phase angle and force exerted on a Wilhelmy Plate.

Appendix A.9.1. Apparatus

The longitudinal wave trough was used to test the transverse wave-laser slope gauge method of measuring surface tension. The program *PH_METER* was written to resolve phase data between the transverse wavemaker and the laser slope gauge signals during film compression in the pressure-area isotherm . The program uses the subroutine described in section A.7 to measure phase changes then outputs the phase data to the motion control PC

(first computer) through serial port communication. The quasi-static mode in the program *TABLE* was modified to record bar position, electronic balance force and phase in the output file.

During film compression the number of transverse waves separating the transverse wavemaker and the laser slope gauge changes by more than 1 resulting in jumps in the phase measurement ranging from $-\pi$ to $+\pi$. The program *PHCOR* corrects phase data stepping through $\pm\pi$ and the program *STCOMP* calculates the variation in surface tension using equation A.6.

Appendix A.9.2. Methods and Results

The experiment was done in the same manner as the usual pressure-area isotherm with the addition of the transverse wavemaker and laser reflecting off the surface. Prior to measurements the trough, film barrier and Teflon wedge were washed in hot water. The trough was coated with paraffin, positioned over the motion table and filled with distilled water. The transverse wavemaker was positioned near the trough wall and propagated 200 Hz transverse wave across the trough. The laser slope gauge was positioned with the laser beam reflecting off the surface at a point 6 cm from the transverse wavemaker.

Oleyl alcohol was spread on the surface and the film barrier was placed 68 cm from the right end of the tank. The Wilhelmy Plate was lowered into contact with the surface. The program *TABLE* moved the film barrier in 1 cm steps and recorded the bar position, force on the Wilhemy Plate and phase relationship calculated by the *PH_METER* program.

Figure A.3 shows the measured phase relationship between the transverse wavemaker and, laser slope gauge as the surface was decreased. The difference in phase angle jumps through 360 degrees as the number of capillary waves separating the wavemaker and laser slope gauge decreases. The phase relationship is given in degrees and area in cm^2.

Figure A.4 shows the surface tension measurements from the transverse wave-laser slope gauge and Wilhelmy Plate methods.

Appendix A.9.3.Conclusion

The method of measuring surface tension by monitoring changes in phase difference between transverse wavemaker and laser slope gauge signals proved adequate means of determining variations in surface tension, see figure A.4.

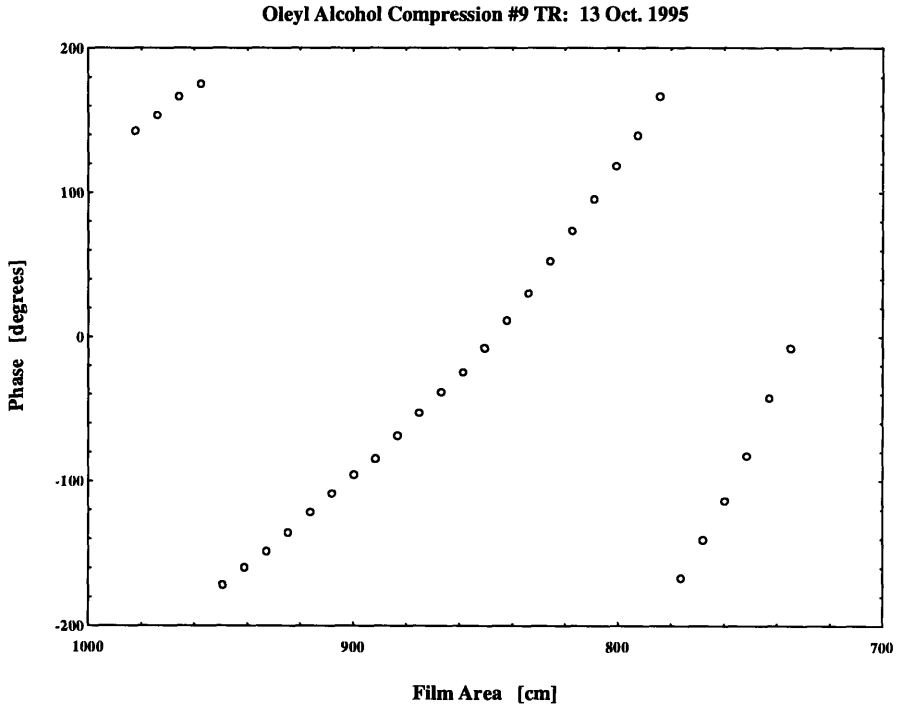

Figure A.3 Measured Phase Angle between Transverse Wavemaker and Laser Slope Gauge

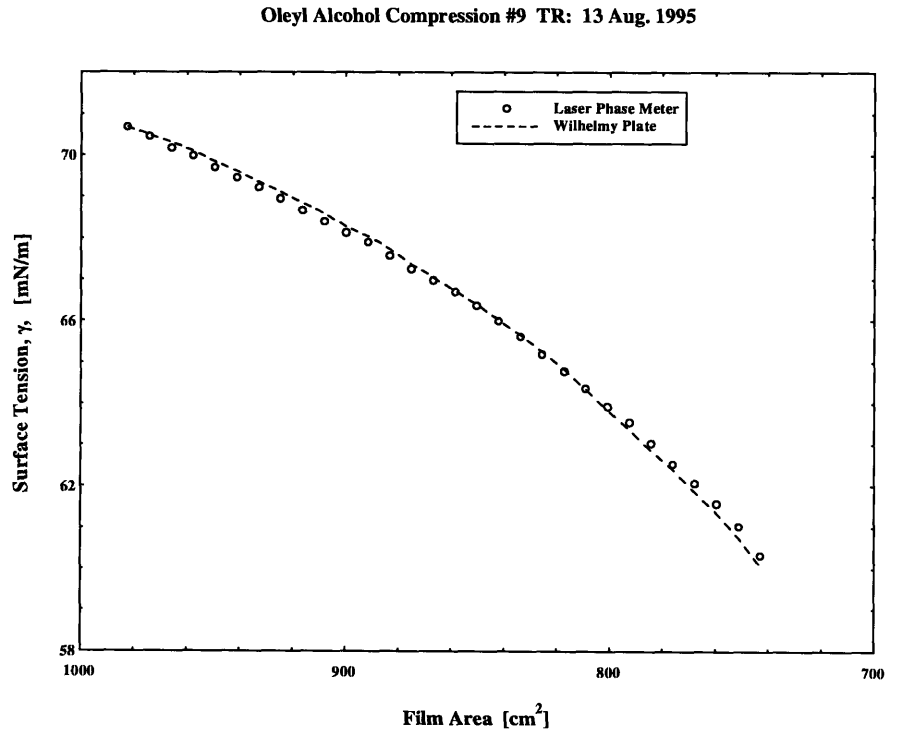

Figure A.4 Comparision of Surface Tension Measurements

Appendix A.10. Longitudinal Wave Phase Error Due to Signal Processing Delays in Components and Transverse Wave propagation

Measurements of longitudinal wave induced variations in surface tension revealed the presence of a phase shift in the phase relationship between the longitudinal wavemaker and variation in surface tension at the point where the laser reflects off the surface. Measurements showed magnitudes that corresponded with theory but a phase shift showed the measured variation in surface tension lagging that predicted in chapter 2. Two possible explanations include an error in the theoretical equations and a failure to account for delays in data acquisition. Due to the fact that the measured magnitudes were close to theoretically predicted values, the latter error was investigated. Figure A.5 shows the extent of the phase shift for data collected with oleyl alcohol spread on water.

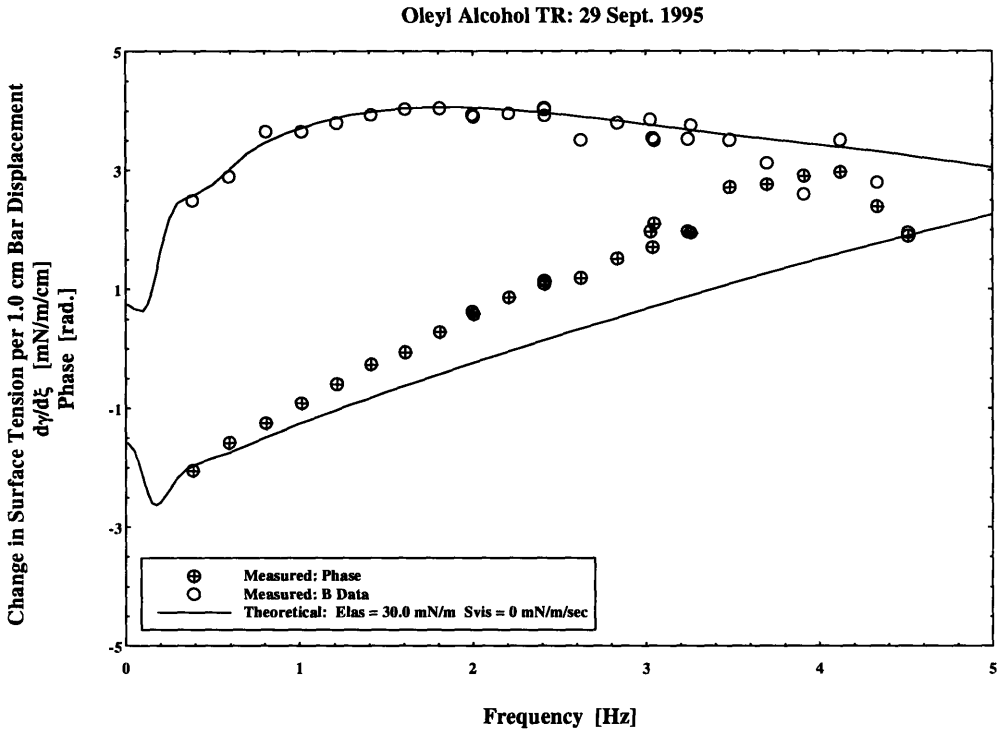

Figure A.5 Change in Surface Tension Phase Error

The phase error is small at low frequencies and increases with frequency. The error is frequency dependent. A constant time delay in the signal produces this type of phase error. The constant time delay, in seconds, shows up as an increasing phase delay because its ratio with wave period grows as the wave period decreases (frequency increases).

Appendix A.10.1. Time Delay Caused Signal Processing

Categorizing the delay requires evaluating time delays in all the components that process the wave signal between the fluid through the data acquisition system. Those components include the laser, laser position sensing device, current to voltage amplifier, bandpass filter and data acquisition system. The laser signal, traveling at the speed of light, has essentially

zero delay. The remaining component's delays were measured using a step response. The laser signal was phase shifted at the laser position sensing device. The time delay of the components was determined by comparing the time of the phase shift with the time the phase shift was measured through the components. The time delay measured was approximately 0.025 seconds.

The component processing error accounted for approximately 1/2 the observed error. With the signal processing components accounted for, interest turned to fluid effects and the possibility of a time delay associated with the method of measuring variations in surface tension.

Appendix A.10.2. Time Delay Caused by Fluid Propagation

The method used to measure changes in surface tension relies on the fact that surface tension and wavelength are related in the dispersion relationship. Resolving changes in wavelength facilitates calculation of changes in surface tension. Changes in wavelength are measured by determining the number of waves separating the transverse wavemaker and the point where the laser wave gauge reflects off the surface. Surface tension measurements were made with the wavemaker oscillating at 200 Hz. The distance separating the transverse wavemaker and laser slope gauge was 7 cm.

A time delay between when the surface tension changes and when the number of waves separating the wavemaker and wave gauge changes would produce a phase shift similar to the one observed in figure A.5. Calculating a theoretical value for the delay is difficult and beyond the scope of this project. An alternative to calculating a theoretical value for the time delay is to quantify the time delay through measurements and determine its dependence on fluid and wave properties.

Appendix A.10.2.1. Dimensional Analysis

In an effort to quantify the time delay due to transverse wave propagation, we used dimensional analysis to create a dimensional parameter that would relate fluid properties in units of time. The relevant parameters were:

d	Distance separating wavemaker and wave gauge	m
ω	Frequency of transverse waves	rad./sec
γ	Surface Tension	N/m
ρ	Density	kg/m^3
t	Time delay	sec
A	Constant	---

Combining the terms into a dimensionally correct expression yields

$$t = A\frac{d}{[\omega\frac{\gamma}{\rho}]^{1/3}} \tag{A.6}$$

Substituting

$$X = \frac{d}{[\omega \frac{\gamma}{\rho}]^{1/3}} \tag{A.7}$$

results in a linear relationship between time delay and the parameter X. The two are related by the coefficient A. The value of the coefficient can be determined experimentally by measuring time delays for several frequencies.

Appendix A.10.2.2. Apparatus

The Longitudinal Wave Tank was used to carry out experiments in determining the time delay of the transverse waves to respond to changes in surface tension. Longitudinal waves and an oleyl alcohol film were used to generate the variations in surface tension. The transverse wavemaker, laser, laser position sensing device, current to voltage amplifier, bandpass filter and data acquisition system were used to measure longitudinal wavemaker position and variation in surface tension. The delay time was calculated by comparing the measured phase to theoretical predictions. The error, in radians, was converted to a time delay, in seconds.

Appendix A.10.2.3. Methods and Results

The method used to determine the time delay consisted of varying the transverse wave frequency while the distance, mean surface tension, and density were held constant. The approach was used for three different longitudinal wave frequencies creating 3x3 data matrix of time delays. Transverse waves were generated at 100 Hz, 200 Hz and 300 Hz and for each longitudinal frequency of 2.0 Hz, 2.5 Hz, and 3.0 Hz. A linear least squares fit was used was to compare the time delay and X for each longitudinal frequency, resulting in the calculation of three values of the coefficient A.

Table 1.1 gives the values for the time delays and coefficient A using the values: $d = 7.1\ cm$, $\gamma = 65\ mN/m$, $\rho = 1000\ kg/m^3$

	Time Delay [ms]			
Long. Freq.	Transverse Wavemaker Frequency			
[Hz]	100 Hz	200 Hz	300 Hz	A
2.0	39	24	19	32.2
2.5	39	27	19	31.1
3.0	39	28	21	28.1

Table A.1 Time delay for Transverse wave propagation

The data in table A.1 shows a strong correlation between time delay and the frequency of transverse waves used to measure variations in surface tension. Given the parameters above and using 200 Hz transverse waves, the phase shift at the position of the laser beam requires approximately 26 ms to respond to changes in surface tension.

Appendix A.10.2.4. Conclusion

Time delays in signal processing and transverse wave propagation induce errors in the measured phase relationship. The measured phase relationship between the longitudinal wavemaker and surface tension variations on the fluid needs to be corrected for signal processing delay, 25 ms, and transverse wave propagation delay, 26 ms. The figure below shows the data in figure A.5 with the phase delays removed.

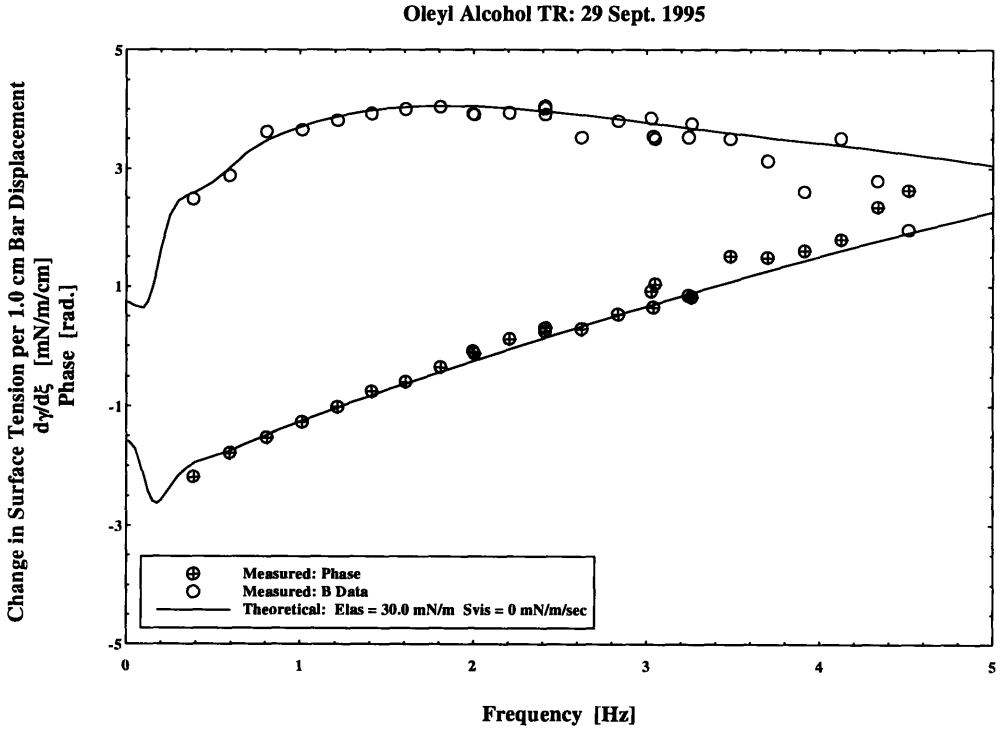

Figure A.6 Time Delay Subtracted from Measured Phase

The measured data, with the phase error due to time delays removed, agrees with the theoretical predictions; see figure A.6.

Appendix B. Development of the Transverse Wave Decay Tank

In the spring of 1994 it became clear another wave decay tank would be needed to analyze dynamic surfactant properties for frequencies greater than 4 Hz. Prior to this time, amplitude decay experiments were carried out in the Marine Instrumentation Laboratories Turbulence tank. The tank, built to conduct amplitude decay tests in the presence of turbulence, measures 3.66 meters square by 1.5 meters deep and requires approximately 3,000 gallons to fill. In the past seawater samples were collected by pumping seawater into a 5,000 gallon tank truck then pumping the water into the laboratory tank with 3hp gasoline driven centrifugal pump. Though assured by the trucking company that the tank truck, pump, and hoses were clean, the chance of introducing contamination was high.

The primary design objective of the new tank was for one person to be able to go to a site where surface films were present, collect a seawater and surface film sample and transport it back to the laboratory for static and dynamic analysis. The following design objectives were placed on the new apparatus:

1. Analysis using deep water theory.
2. Sensitivity high enough to measure clean water amplitude decay
3. Minimize amplitude decay due to viscous effects of edge walls
4. Minimize wave reflection from far wall
5. Wave Generation from 3 Hz to 15 Hz
6. Ability to compress surface film area
7. Ability to measure changes in surface tension

Figure B.1 shows a profile sketch of the apparatus built. The apparatus is able to measure pressure-area isotherms and amplitude decay of a film covered fluid. The following sections contain a brief description of each component.

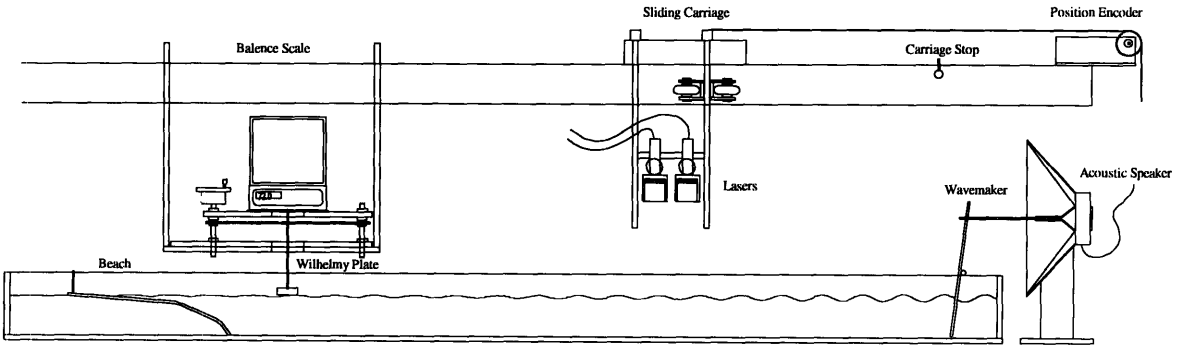

Figure B.1 Sketch of Wave Decay Measurement Apparatus

Appendix B.1. Development of the Wave Decay Tank.

The orbital particle velocities that characterize transverse waves decay rapidly as one moves from the surface further into the fluid. The decay rate given by Newman (p. 243), $e^{(-kz)}$, shows the orbital radius reduces to 4 % when $kz = \pi$, water depth equal to ½ the wavelength. In the case of 3 Hz waves the wavelength is approximately 17 cm. A water depth of 10 cm was chosen for the new tank .

The length of the tank is based on clean water transverse wave decay rates. Transverse waves in clean water decay at a rate of:

$$\alpha_0 = \frac{2k\upsilon\omega}{\rho g + 3\gamma k^2} \tag{2.24}$$

In the case of a 5 Hz clean water wave the decay rate is approximately 0.1/m. With a measurement window length of 1 meter, the amplitude is reduced by 10%. In order to provide length for the measurement window, wavemaker, beach and skimming apparatus, the length is 2.4 meter. The width of the tank is 40 cm giving a volume of ~ 25 gallons. The tank construction material is clear acrylic sheet with a thickness of 12.7 mm. Acrylic was chosen for its ease of construction and cleaning. Prior to choosing acrylic, it was tested for surfactant leeching by submerging a sample into distilled water and monitoring the surface tension. The acrylic did not affect the surface tension. The material was purchased pre-cut and joined with Weld-On 4 acrylic cement.

Appendix B.2. Wavemaker design.

The Wavemaker proved to be the most troublesome component of the Wave Decay Tank apparatus to design. The design requirements required generation of a two dimensional wave field with a device that is easy to remove and clean. After reviewing literature on wavemaker construction [*Wang 1974*], several plunger type wavemakers were milled out of acrylic. In every case, the wavemaker generated a wave field with null points in it. Investigation found the null points are due to the combination of the desired 2D waves and radial waves coming from each of the intersections of the wavemaker and tank wall. The incentive to build the laser carriage was provided by the need to locate the null points in the 2D wave field. The laser carriage measures wave slopes along the length of the data window. The carriage allows quantitative evaluation of the wavemaker designs by determining which wavemaker produces the smallest null points. For more details regarding the laser carriage see section B.6 and B.7.

After several trial and error attempts a "paddle" type wavemaker was adopted. The paddle wavemaker is built out of a sheet of 6.4 mm thick acrylic that spans across the tank. A 6.4 mm rod is attached across the sheet to support it. When the wavemaker is placed in the tank, the rod rests on the tank walls making a pivot point. The paddle is connected to an audio speaker with an adjustable drive-rod. The speaker is driven with a single-ended input differential amplifier. A sine wave of desired amplitude and frequency is input into the amplifier by a function generator.

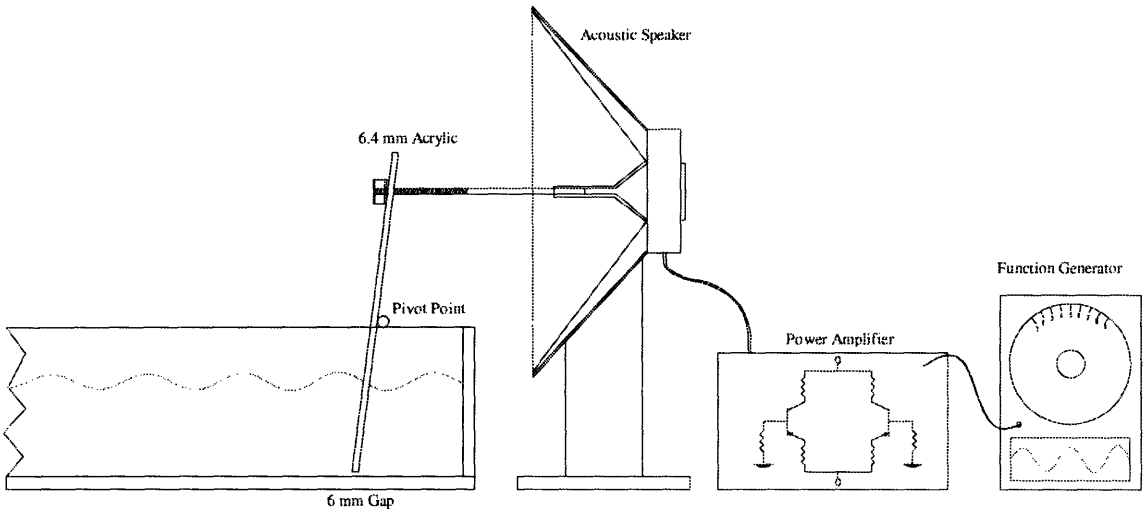

Figure B.2 Sketch of Transverse Wavemaker

Figure B.2 shows a profile sketch of the "paddle" type wavemaker, and electronic components used to produce transverse waves.

Typical audio amplifiers have a low frequency cutoff value of approximately 20 Hz making them unsuitable as power amplifiers for the apparatus. An amplifier was built in the laboratory to drive the speaker was. Figure B.3 shows a schematic drawing of the single-ended input differential amplifier that built to drive the audio speaker. V_{in} represents the input signal from the function generator and V_{out} represents the signal sent to the speaker.

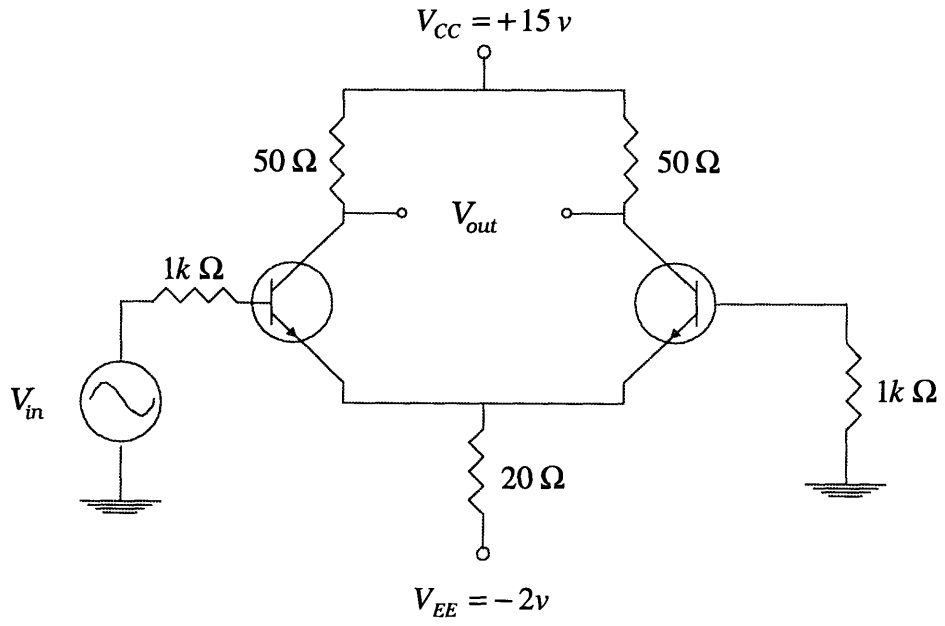

Figure B.3 Schematic of the Single-Ended Input Differential Amplifier

The amplifier allowed waves with frequencies as low as 3 Hz to be generated in the Wave Decay Tank. The paddle wavemaker produced an excellent 2D wave field.

Appendix B.3. Beach Design.

The beach serves as a wave damping device to accelerate decay once the waves have passed the data collection window. When waves enter shallow water they experience a change in group velocity. The crest, upper portion of the wave, outdistances the trough, lower portion of the wave, resulting in a "breaking" wave. The design criteria for the beach requires it to be removable during film pressure-area isotherms and easy to clean between tests to prevent contamination. The beach is made from 6.4 mm acrylic sheet that can be submerge in the tank during isotherm measurements. Due to the range of frequencies and space limitation in the tank, the angle of the beach varies with depth. The slope of the upper region, 4.4 degrees, is as small as possible to effectively dampen higher frequency waves. The middle and lower regions have a larger slope that reduces reflection for lower frequencies, 3 - 6 Hz and keeps the length of the beach to a minimum.

Initial tests of the beach showed considerable reflection for high frequency waves($f > 10$ Hz.). The smooth finish of the acrylic sheet resulted in the surface "beading" where the beach pierced the surface. In an effort to correct the situation the upper portion of the beach was scuffed with 400 grit sandpaper. When water contacts the scuffed area, surface tension pulls the water surface up the beach, keeping it wet and improving decay.

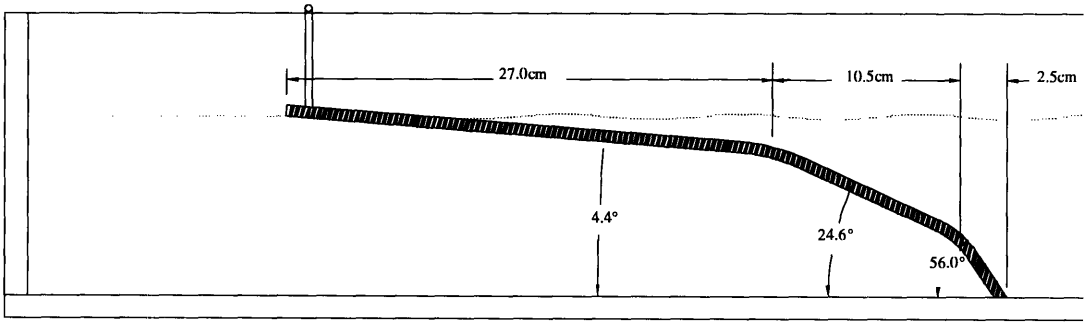

Figure B.4 Beach Design

The beach rests on the bottom of the tank and is suspended by wire clips from the tank walls; releasing the clips allows the beach to sink during surface compression measurements.

Appendix B.4. Surface Compression - Surfactant Skimming.

Prior to dynamic testing it is crucial to discern the elastic properties of the surface film present. The theoretical explanation is given in section 2.2. The practical aspect requires

the ability to move a barrier trapping surface film without leaking. Two film barriers, also referred to as skimmers, were built for the wave decay tank. The skimmers are equipped with slides that ride on the edge of the wave tank and a 2 mm thick acrylic barrier that pierces the surface and extends into the fluid 1 mm. The barrier is molded with a 90^0 bend at each end. The bend allows the barrier to approach the tank wall tangentially. The barrier contact points with the wall have been filed to ensure a smooth fit with the tank walls that prevents film leakage. The walls are indexed in 5 cm increments allowing accurate positioning of the barriers.

Appendix B.5. Surface Tension Measurement - Electronic Balance.

Measurement of the pressure-area isotherm, used to determine the quasi-static elasticity, requires monitoring film pressure while film area is varied. The barriers compress the surface film changing the area the film occupies. Monitoring pressure requires the ability to differentiate changes in surface pressure. A Wilhelmy Plate was used to discern changes in surface tension. As mentioned in Section 2.2, changes in film pressure are equal to changes in surface tension. The Wilhelmy Plate renders surface tension into a point force. The force, or change in force, becomes the first quantity of interest when measuring a pressure-area isotherm. An electronic balance equipped with an external center drop is used to measure the downward force exerted on the Wilhelmy Plate by the fluid.

To ensure accurate measurement of surface tension, the plate's vertical position is adjusted to a location where the water meniscus pulling on the plate is near breaking. The plate must be raised and lowered in small increments without vibration. An adjustable platform suspends the balance above the fluid. Screw adjustment raise and lower the balance and plate smoothly while keeping the balance level.

The balance, model FX-40, was manufactured by A&D Engineering. An RS-232 interface allows the balance output to be monitored by a computer using serial port communications. A subroutine in the program *TABLE* prompts the users for skimmer position then records electronic balance force measurement. The program reduces the time to measure a pressure area-isotherm and calculate the elastic properties to approximately 10 minutes. The efficiency is noteworthy because it allows several isotherm measurements in a short time, a necessity when evaluating the work hardening characteristics of a film.

The balance height adjustment platform is suspended from an overhead beam allowing film barriers to pass underneath. Prior to evaluation of spread films, such as oleyl alcohol, it is imperative to skim the surface of any potential contaminates that might be present on the surface. An acrylic shelf suspends the balance and height adjustment from the overhead beam. The shelf could slide on the overhead beam allowing its position with respect to the wavemaker to be adjusted. Suspending the force balance allows easy cleaning of the surface. A barrier is inserted at one end of the tank and moved to the opposite end pushing any contaminates before it and leaving the surface behind clean.

Figure B.5 shows a profile sketch of the electronic balance and Wilhelmy Plate used to measure film pressure during pressure-area isotherms and to monitor film pressure during wave decay experiments.

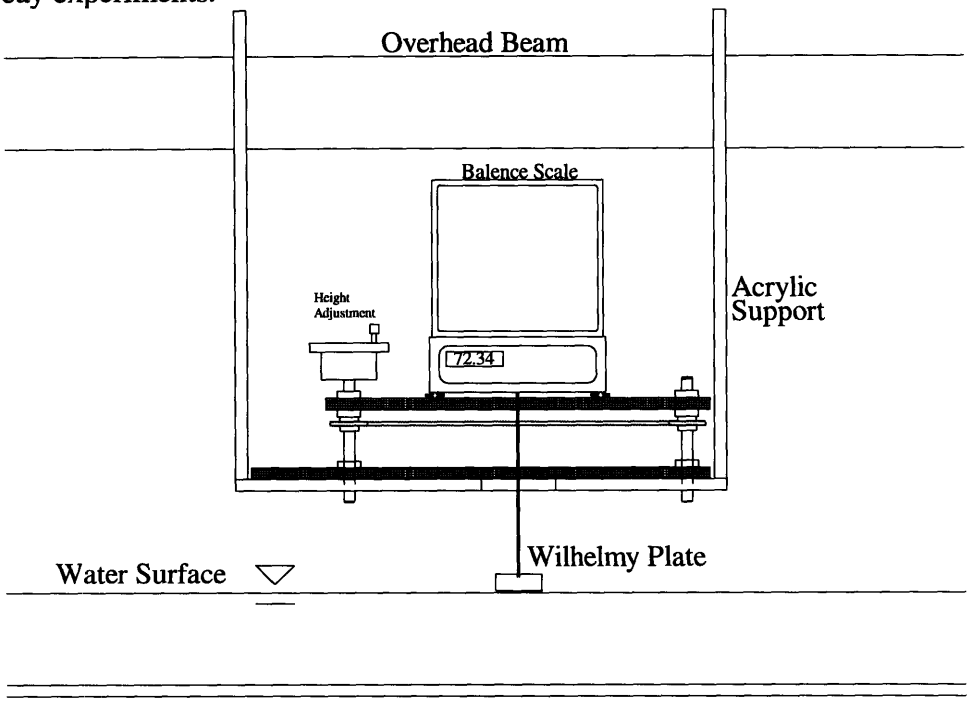

Figure B.5 Electronic Balance and Height Adjustment

Appendix B.6. Laser Carriage.

When the wave decay tank was built wave amplitudes were going to be measured at 4 location. Data was going to be collected for several seconds; the average amplitudes calculated and an exponential decay fit to the four average amplitudes. Due to the large variations in decay rates, O(30), changing the location of the wave gauges would be crucial. In order to adjust the location of the wave gauges an aluminum beam 3.4 meter in length was positioned above the tank so gauges could be clamped at various locations.

The method of data collection changed. The null points created by poorly aligned wavemakers (see Section B.2) made the error in measuring wave amplitudes at 4 locations and calculating decay rates unacceptable. In an effort to minimize the error it was necessary to measure the null point accurately. Sliding a gauge from the beach to wavemaker while taking data allows the decay envelope and null points to be mapped. Once the null points are mapped, a new wavemaker can be built with better alignment, effectively removing the null points.

A carriage was built capable of sliding four laser slope gauges. Sliding the gauges and resolving the amplitude versus position yields the decay rate along four lines between the beach and wavemaker. Sliding the laser carriage along the data window for 30 seconds results in hundreds of amplitude measurements on each line. With the carriage, decay rates

are based on hundreds of amplitude measurements spaced along the data window rather than 4 fixed points. Furthermore, the length of the data window can be varied to accommodate the large variation in decay rates. The data collection and reduction to decay rates are covered in Appendix B.8.2.

Moving the gauges requires collection accurate measurement of the laser position while the carriage is moving. Carriage position is obtained by using a 10 turn potentiometer, cogwheel pulley, and belt. The system is calibrated by moving the carriage to fixed locations and recording the potentiometer's output voltage. Fitting the output voltage verse position with a first order polynomial yielded a calibration coefficient of 0.0636 volts per centimeter. Figure B.6 shows the potentiometer output verse carriage position and a least squares fit of the data.

The calibration is checked prior to all amplitude decay tests. Variations were negligible.

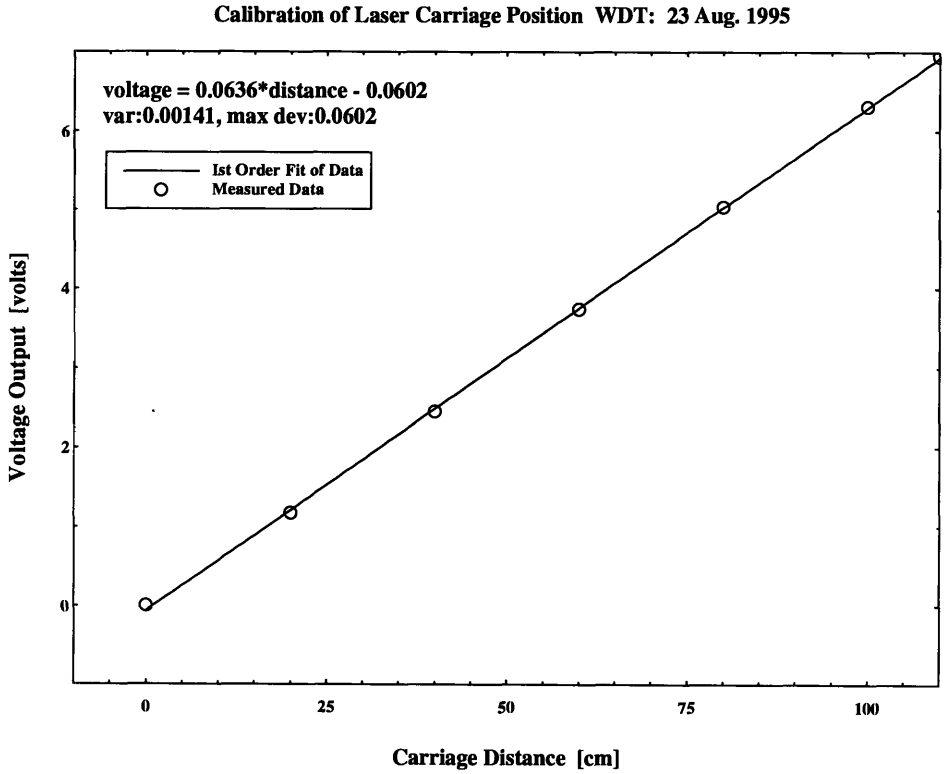

Figure B.6 Laser Carriage Position Calibration

Appendix B.7.Laser Slope Gauges.

Resolving variations in water elevation is the primary task in estimating wave amplitude. Traditional laboratory methods use wires penetrating the fluid, relying on fluid characteristics to alter an electronic signal, to measure changes in fluid height. Unfortunately, gauge performance often becomes dependent on properties other than those of interest. Common problems include ground noise, changes in temperature, cleanliness of

the wire, meniscus (surface tension) and salinity. The author's past experience with wire gauges lead to the development of a non-interference method of measuring variations in water elevation.

The air-water interface has excellent reflective characteristics; shining a laser directly at the surface will result in measurable reflection. From The Law of Reflection that states the incident and reflected angles are equal, one can acquire information regarding the slope of the interface. Positioning a beam with an incident angle close to 90 degrees results in reflected light shining up near the source. Using a beam position detector, the incident and reflection angles are determined and the direction of the surface normal vector calculated.

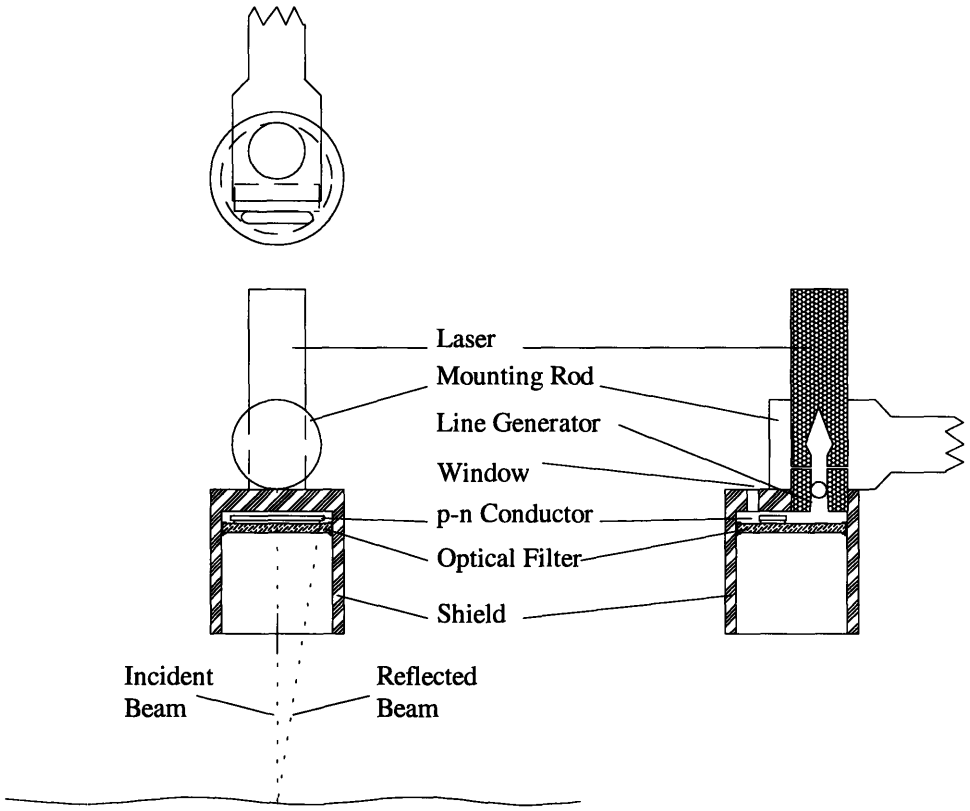

Figure B.7 Laser Slope Gauge Design

The incident beam is generated by a 19 mw 670 nm laser equipped with a 5 degree line generator, manufactured by LASERMAX. The laser line is oriented orthogonal to the propagation direction of the wave field (across the tank). The reflected beam passed into a shielded cone through an optical filter and onto a position detector. The optical filter, made by MELLS GRIOT (MN 03FIV048), has a center frequency of 650 nm. The black nylon shield was added because optical filters have poor blockage for high incident angles, measured from surface normal.

The position sensing detector, model IL-30SP manufactured by SiTek, is a p-n semiconductor with one anode and two cathodes. The anode is connected to ground. The

cathodes are located on opposite ends of the p-n material and biased with constant voltage. When the p-n material is excited by incoming light, resistance changes across the p-n junction altered the current flow through each cathode. Comparing the current flow through each cathode one can locate the point of excitation on the p-n material; i.e. equal current flow and the beam is centered on the p-n material.

Companion circuitry, model OT-300 manufactured by On-Trak Photonics, converts changes in current flow into voltage changes; then compares the relative values at each cathode and outputs a signal, -10 *v* to 10 *v*, that is a function of beam position. With slight modifications the OT-300 is able to process signals from two separate laser slope gauges. The output signals are filtered using a 2 pole low pass Butterworth filter with gain; model 3384 built by built by Krohn-Hite. The cutoff frequency was digitally set at 50 Hz with a typical gain value of 10 dB.

Four identical laser slope gauges were built for the wave decay tank. The laser slope gauge design is given in Figure B.7.

Appendix B.7.1. Laser Slope Gauge Calibration

In order to measure slopes the laser slope gauge output voltage must be calibrated against measured angles of incline. Inclinometers are mounted on the shield of each slope gauge. With a "calm" surface the gauges are rotated about the mounting rod axis while voltage and angle are recorded. First order polynomial fits of the data yield calibration coefficients for each gauge. The gauges proved to be linear and repeatable with calibration coefficient variations less than 1% over a 6 degree range.

Once data collection switched to sliding the four lasers on the carriage, calibration coefficients were no longer needed. The data analysis normalized the amplitude recorded while sliding the lasers with the final amplitude measured near the wavemaker. The inclinometers were left on the gauges in the event future slope measurements were needed.

Appendix B.8.Data Collection and Evaluation.

The author has found that the best experimental results come when data can be reduced in near real time. Knowing when you have bad data due to equipment problem is 90% of the battle toward building a good apparatus and carrying out successful experiments.

Appendix B.8.1.Pressure-Area Isotherm and Elastic Properties.

The method of measuring pressure-area isotherms in the wave decay tank is similar to those used in the longitudinal wave trough discussed in section A.6. Several programs carry out the tasks. The main program *TABLE* has several operating modes. One of which, User Input Quasi-Static data collection, prompts the user for barrier location then collects a surface tension measurement via the electronic force balance and Wilhelmy Plate. The program writes surface film area and force to a file. The program *QS_FIT2* analyzes the pressure-area isotherm to determine the pressure-elasticity relationship. The program *QS_FIT2* determines the coefficients of a 5^{th} order polynomial having a minimum mean

squared error relative to the pressure-area data, and calculates the first derivative with respect to film pressure.

Appendix B.8.2.Wave Amplitude Decay Rates.

Wave amplitude data is recorded using the program *DATA* and an analog to digital converter, model CIO-DAS1600 manufactured by Computer Boards. Prior to data collection the wavemaker frequency and amplitude are set to generate the desired waves. The laser carriage is moved away from the stop near the wavemaker, the program is started and the laser carriage is moved toward the wavemaker. Data is collected for 32 seconds, with a minimum of 2 seconds at the carriage stop without motion. Data is sampled on 5 channels providing position and four laser slopes verse time. Figure B.8 shows a plot of slope amplitude verse time for one channel of raw data. Data collection started at time 0. The carriage was moved toward the wavemaker between 4 and 24.5 seconds and the carriage was at rest near the wavemaker for 7.5 seconds. The record contains 6400 samples.

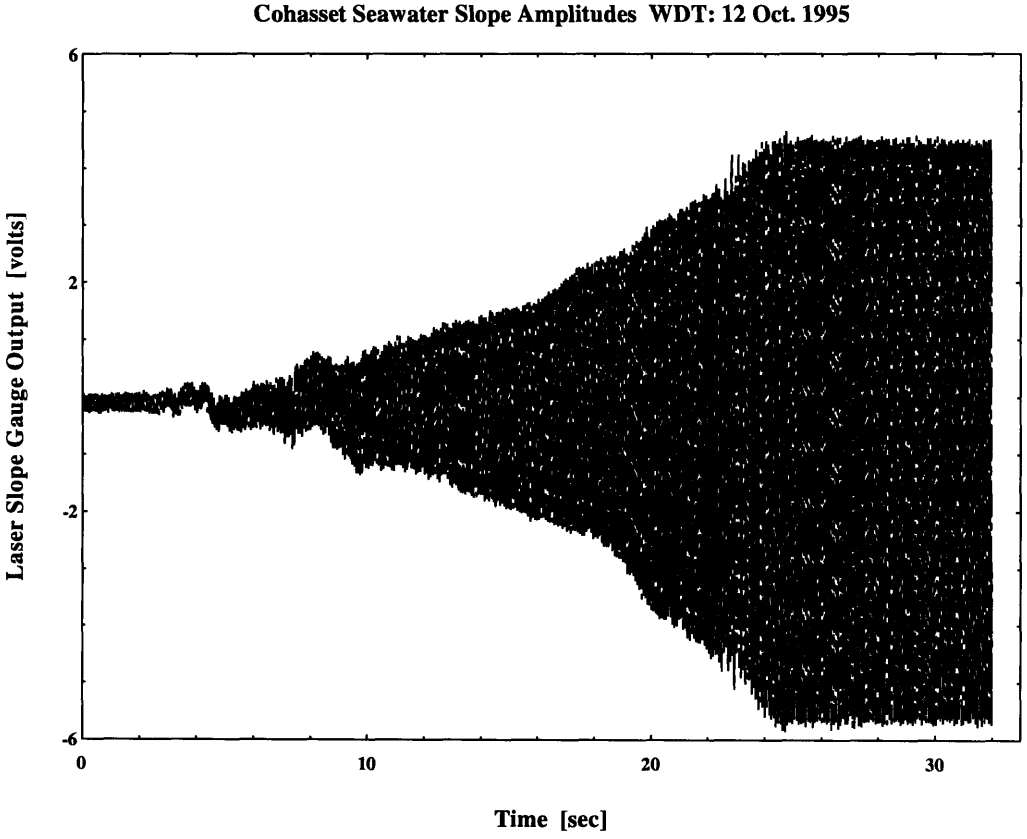

Figure B.8 Sample of Raw Wave Decay Data File

Once slope decay data is collected, the frequency and decay rate are calculated using the program *AMP4*. The frequency is calculated by analyzing using zero crossings in the final seconds of the data record. The frequency calculation takes place in two parts. The first part consists of calculating the mean value of the last 400 samples and subtracting it from

the data record. The second part consists of calculating wave periods from each zero crossing. The periods are then averaged to calculate the mean period and frequency.

After the wave frequency is determined for the 4 laser channels, the slope peak-to-peak values are calculated. The data is scanned for signal maximums, when a signal maximum is found the peak-to-peak value is determined by subtracting the next occurring signal minimum. The peak-to peak amplitude and location in the tank it occurred are written to a storage array. Figure B.9 shows the peak-to-peak voltage verse distance from the carriage stop near the wave maker calculated from the data in figure B.8.

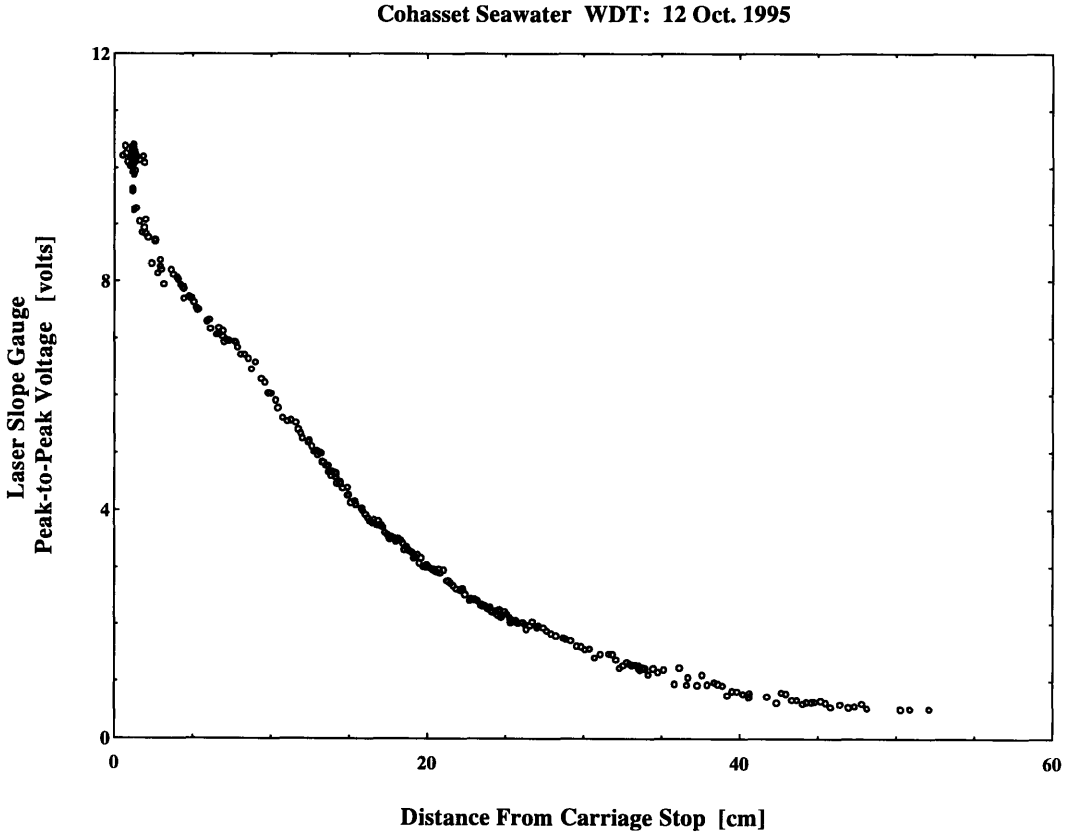

Figure B.9 Sample Peak-to-Peak Slope Amplitude Decay

The peak-to-peak data is normalized by dividing the data set with the average peak-to-peak amplitude from the final seconds of the data record.

The decay rate is calculated by finding a least squares fit to the linearized data set. Once the data was normalized the decay rate is calculated by minimizing the square of the error between the measured data and the expression:

$$\ln(V_{PP}) = -\alpha x \tag{B.1}$$

where α is the decay rate.

Figure B.10 shows the normalized slope data and the least squares fit of the data. The cluster of data points at 1 cm should fall on the y axis, sliding the data to the left. The discrepancy is due to an error in the carriage stop position indicator. The error was corrected before analysis of film data.

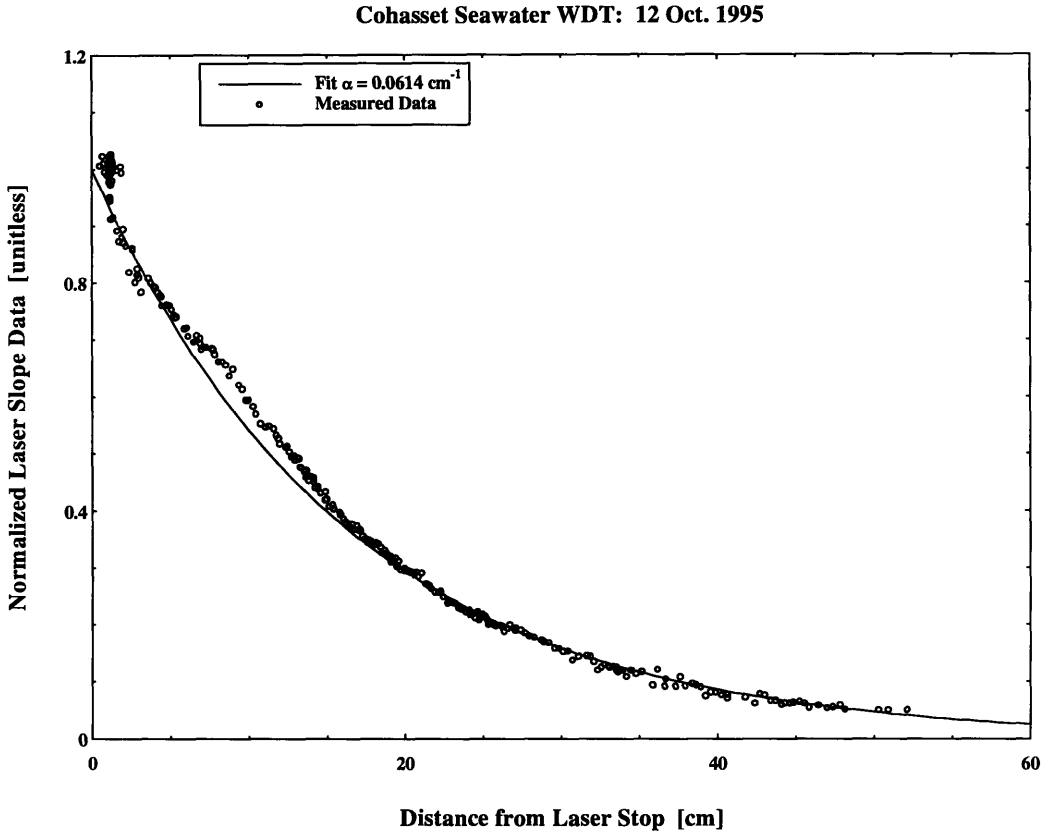

Figure B.10 Fit of Normalized Laser Slope Data

Using four laser wave gauges, four traces of the amplitude decay are measured as the waves move through the fluid. The four decay rates are then averaged giving a single decay rate for the frequency calculated.

Appendix C. Transverse Wave Phase Velocity and Surfactants.

It was brought to the author's attention that research was being done by others in the field regarding gravity-capillary wave phase velocities for surfactant covered water. Tentative conclusions suggest that measured gravity-capillary wave phase velocities for surfactant covered tap water ($\omega > 20 rad/sec$) do not agree with theoretical predictions and that the phase velocity's dependence on frequency goes through a transition at approximately 12 Hz. The Wave Decay Tank is an excellent apparatus to measure gravity-capillary phase velocities. The wavemaker produces 2D gravity capillary waves for frequencies between 3 - 25 Hz. The laser slope gauges measure surface slopes and several programs existed to calculate wavelength from phase angle data. Minor software changes to the data reduction programs used with the Wave Decay Tank enabled us to evaluate phase velocities over a range of frequencies on clean and surfactant covered water.

Appendix C.1. Theoretical Wave Speeds

Two types of velocities are associated with gravity-capillary water waves. The first, group velocity represents the speed at which the wave packet moves. In a wave tank it represents the time distance relationship for a group of waves to travel from the wavemaker to the beach. Newman [1977] defines group velocity by:

$$V_g = \frac{\partial \omega}{\partial k}. \tag{C.1}$$

In the case where surface tension contributes to the dispersion relationship, $\omega > 20\ rad / \sec$, equation 2.5 gives a dispersion relationship of $\omega^2 = gk + \gamma k^3 / \rho$ and the group velocity is simply

$$V_g = \frac{1}{2}\frac{g + \frac{3\gamma k^2}{\rho}}{\omega} \tag{C.2}$$

The second type of wave velocity, phase velocity, represents the speed at which the individual wave characteristics travel. The phase speed represents the time distance relationship for wave characteristics (e.g., trough, peak or zero crossing) to travel a fixed distance. The phase speed is greater than the group speed. A packet of waves consisting of a few wavelengths of transverse waves will travel at the group speed, but the peaks will travel at the phase speed. An observer will see peaks appear out of the back of the group move forward in the group and disappear at the front of the group. In a laboratory wave tank the phase velocity represents the time for a wave peak to travel the length of the tank. Phase speed is given by:

$$V_p = \frac{\omega}{k} \tag{C.3}$$

One can calculate theoretical phase speeds for transverse surface waves after measuring fluid and surfactant properties and using the relationships in equations 2.5 and 2.9.

Appendix C.2. Measurement of Phase Speeds

One can calculate wavenumbers and phase speeds using the wave decay tank. The wavemaker generates waves at known frequencies and the laser slope gauges can measure slopes at two points separated by a fixed distance. In a 2D sinusoidal wave field the signal phase angle at each wave gauge can be represented by phase shifting the signal phase of any other wave gauge by a factor not greater than 2π. Resolving the phase angle and using the fact that in the presence of a constant frequency wave field two wave gauges separated by a fixed distance, l, have a constant phase angle given by:

$$k\,l = \theta + 2\pi n \tag{C.4}$$

where the measured phase, θ, is between 0 and 2π and the correction, $2\pi n$ accounts for the whole number of wavelengths separating the gauges. Figure App C.1 illustrates the relationship between the distance and phase.

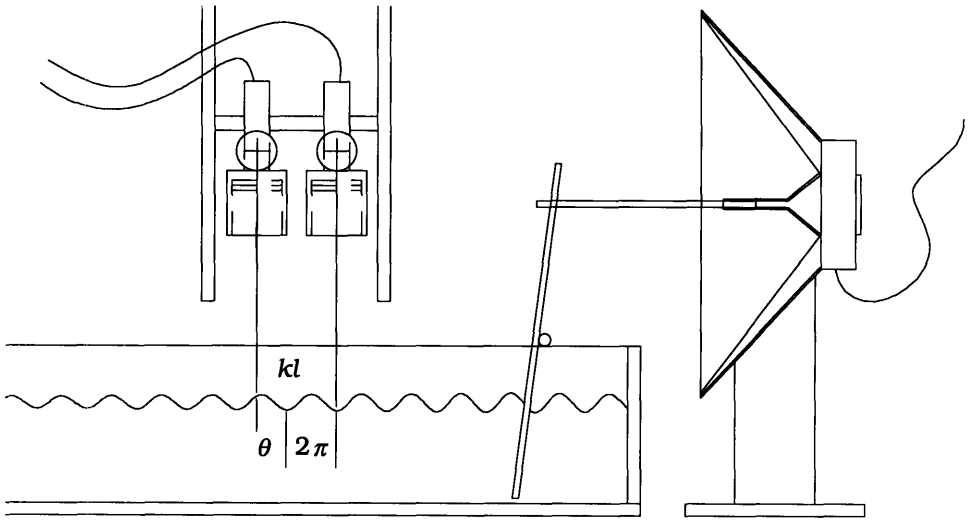

Figure C.1 Relationship between Phase and kl.

Solving equation App C.4 for k, and substituting into equation C.3 one gets a phase speed relationship of the form:

$$V_p = \frac{\omega l}{\theta + 2\pi n} \tag{C.5}$$

Experimental determination of phase velocity is accomplished by measuring the phase angle difference between the two lasers slope gauge signals and measuring the frequency of the 2D gravity-capillary waves. Using the fact that the wave gauges are separated by a fixed

distance, one can determine the number of whole wavelengths separating the two laser slope gauges. The frequency, separation distance, phase angle and number of whole wavelengths separating the wave gauges are used in equation C.5 to determine the waves' phase speed.

Appendix C.2.1. Resolving Signal Frequency and Phase Angle

Two commonly used methods to resolve frequency and phase information are spectral and time domain analysis. Spectral analysis uses Fourier transforms to convert the time domain data signal into frequency domain. In the frequency domain the signal is reduced to sinusoidal components with a magnitude and phase angle. Following is the Fourier Transform.

$$x(t) = \frac{1}{2\pi} \int_{-\infty}^{\infty} e^{i\omega t} X(\omega) \partial\omega \tag{C.6}$$

$$X(\omega) = \int_{-\infty}^{\infty} e^{-i\omega t} x(t) \partial t \tag{C.7}$$

In the case of discretely sampled data with $2^{1,2,3,4...}$ samples the Fast Fourier Transform (FFT) provides a quick conversion from the time domain to the frequency domain. For a given record length of T(sec), consisting of N samples the smallest incremental change in frequency that can be resolved is $1/T$.

After the time based signal is transformed to the frequency domain; the fundamental frequency is found by scanning over all the frequencies for the frequency with the largest magnitude. The phase shift, θ, between two signals is simply the difference between the phase of each signal at the corresponding frequency.

Once the phase shift is calculated for the maximum magnitude the wavenumber can be calculated using an iterative loop that minimizes the following expression:

$$\omega^2_{meas.} - \left[g k_{est.} + \frac{\gamma k_{est.}^3}{\rho} \right] \tag{C.8}$$

where

$$k_{est.} = \frac{\theta + 2\pi n}{l}; \quad n = 0,1,2,3.... \tag{C.9}$$

The measured phase velocity is calculated by dividing measured frequency by the measured wavenumber in equation C.3.

Appendix C.2.2. Experimental Setup and Data Acquisition

The wave decay tank was used with four laser wave gauges fixed in location. The four gauges were arranged in a rectangular fashion, provided a parallel measurement of signal phase angle that was converted into two wave phase speeds. The two speeds were averaged together providing one data point.

The laser slope gauges were connected to current amplifiers and low pass filtered with a cutoff frequency of 50 Hz.. Data was sampled for 32 seconds on four channels of an analog to digital converter sampling at 1000 samples per second. The data was zero padded and a 8192 FFT was used calculate the transform.

The tank was washed and vacuumed prior to being filled with City of Cambridge tap water. The Wave Decay Tank was filled to a depth of 10 cm. Three phase speed experiments were carried out on the water, the first, measured the phase velocity of "clean" tap water. Skimmers were used to push any surfactant present in the tap water out of the data acquisition area. Phase velocities were measured for transverse waves with frequencies between 6 and 19 Hz. The second test used the same water after it was left in the tank overnight to let surfactants come out of solution. The following morning the surface film area was compressed 50% and phase speed measurements were made on the surfactant covered water. The film pressure was adjusted to 2.5 mN/m representing a surface tension of 70.0 mN/m, and phase velocities were measured for frequencies between 6 and 19 Hz

After the completion of the surfactant covered data collection, a pressure-area isotherm was measured to calculate the quasi-static elasticity of the film.

Appendix C.3. Data Analysis

The measured wave phase speed data and theoretical predictions were graphed. Figures C.2 and C.3 show the results of the wave phase speed measurements. Figures C.4 and C.5 show the pressure-area isotherm and quasi-static elastic properties of the film that formed on the tap water.

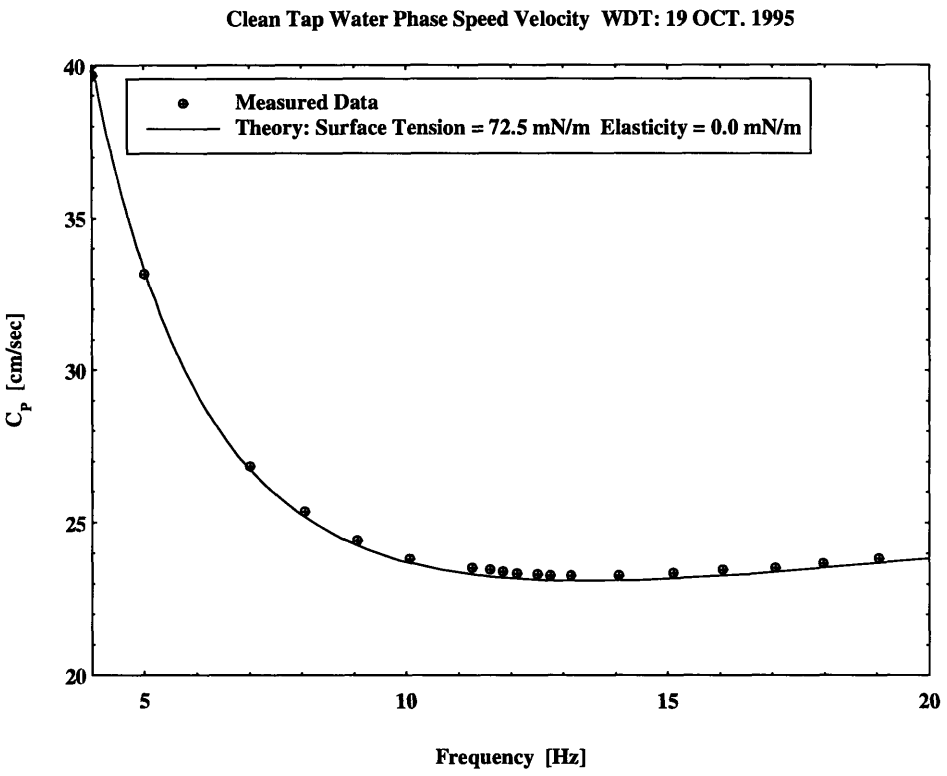

Figure C.2 Clean Water Phase Velocity

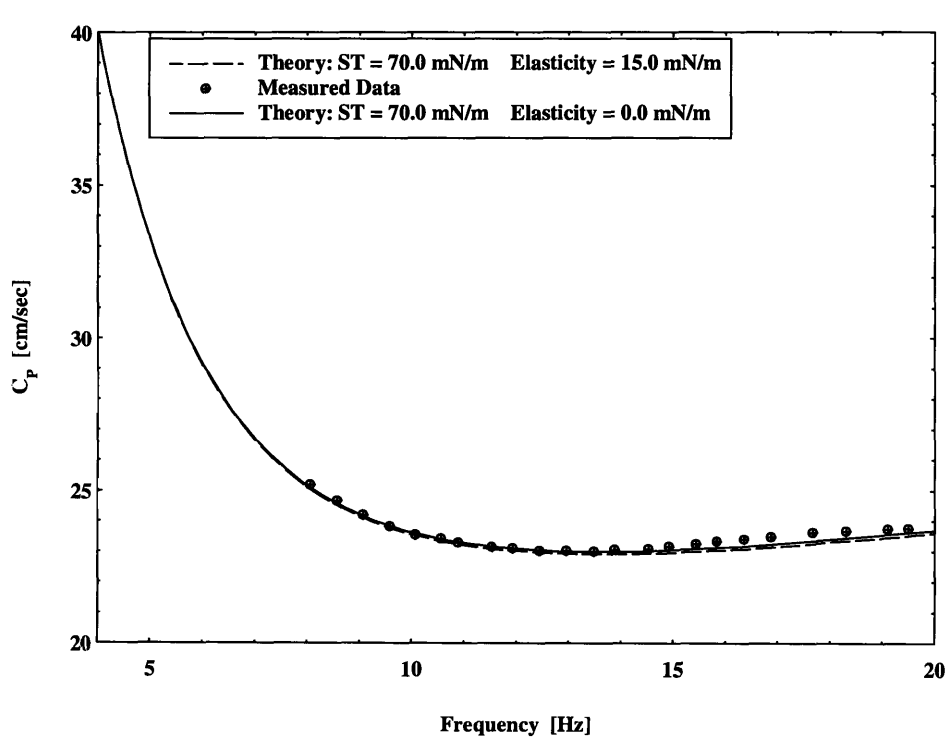

Figure C.3 Surfactant Water Phase Velocity

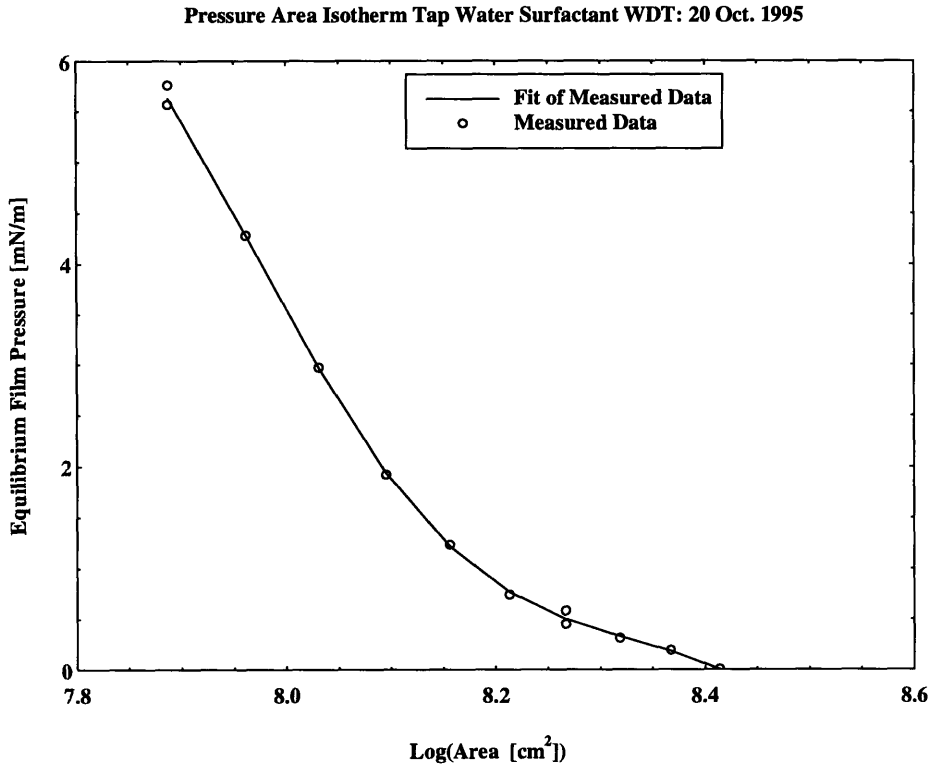

Figure C.4 Surfactant Water Pressure-Area Isotherm

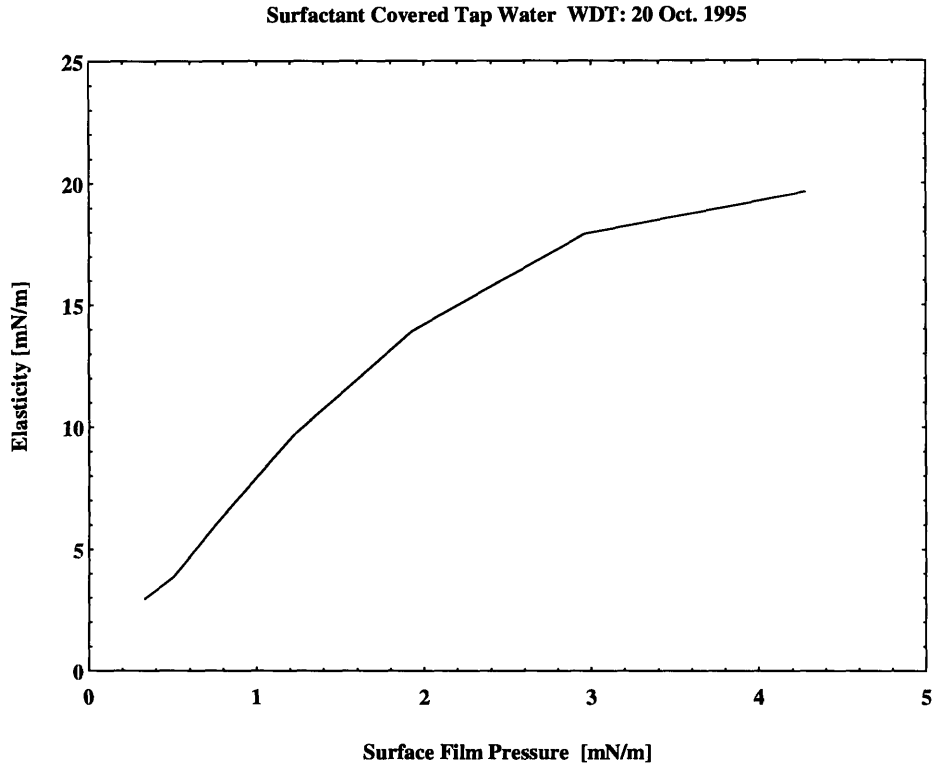

Figure C.5 Surfactant Water Elasticity Calculation

Appendix C.4. Conclusion

In both the clean and surfactant covered tests, the measured phase velocity is close to theoretical predictions. In both tests the phase speed is free of shifts or transitions. The measured phase data agrees with theoretical predictions with an error less than 3%. Possible explanations for the errors in phase speed include errors in length measurement and sampling clock error producing phase speed and frequency errors respectively.

REFERENCES

Adamson, A., *Physical Chemistry of Surfaces*, 3rd Ed. Wiley & Sons, 1976.

Alpers, W., and H Huhnerfuss, The damping of ocean waves by surface films: A new look at an old problem, Journal of Geophysical Research, Vol. 94, No. C2, pages 6251-6265, 1989.

Bock, E., and N. Frew, Static and dynamic response of natural multicomponent oceanic surface films to compression and dilation: laboratory and field observations, Journal of Geophysical Research, Vol. 98, No. C8, pages 14,599-14,617, 1993.

Barger, W., Naturally-occurring surface-active material concentrated at the air-water interface, Ph.D. dissertation, Univ. of Md., College Park, 1985

Dorrestein, R., General linearized theory of the effect of surface films on water ripples, Proc. K. Ned. Akad. Wet. Ser. B, Vol. 54, pages 260-272 and 350-356, 1951

Frew, N., and R. Nelson, Isolation of marine microlayer film surfactants for ex situ study of their chemical and physical properties, Journal of Geophysical Research, Vol. 97, pages 5281-5290, 1992.

Hansen, R., and J. Ahmed, in *Progress in Surface and Membrane Science*, Edited by J. Daniell, M. Rosenburg and D. Cadenhead, Vol 4, Academic Press, New York, 1971.

Lucassen, J., and R. Hansen, Damping of waves on monolayer-covered surfaces, II, Influence of bulk to surface diffusional interchange on ripple characteristics, J. Colloid Interface Sci., Vol 23, pages 319-328, 1967

Newman, J., *Marine Hydrodynamics,* The MIT Press, 1977.

Sohl, C., K. Miyano, and J. Ketterson, Novel technique for dynamic surface tension and viscosity measurements at liquid-gas interfaces, Rev. Sci. Instrum., Vol 49, No. 10, pages 1464-1469, 1978.

Wang, S., Plunger-Type Wavemakers: Theory and Experiment, Journal of Hydraulic Research, Vol 12, No. 3, pages 357-388, 1974

This page intentionally left blank